Title

Modulation of presynaptic function: The role of protein ubiquitination and the effects of environmental toxins

Permalink

https://escholarship.org/uc/item/8qg5g89k

Author

Myers, Katherine

Publication Date

2016

Peer reviewed|Thesis/dissertation

UNIVERSITY OF CALIFORNIA

Los Angeles

Modulation of presynaptic function:

The role of protein ubiquitination and the effects of environmental toxins

A dissertation submitted in partial satisfaction of the

requirements for the degree of Doctor of Philosophy

in Neuroscience

by

Katherine Myers

2016

ABSTRACT OF THE DISSERTATION

Modulation of presynaptic function: The role of protein ubiquitination and the effects of

environmental toxins

by

Katherine Myers

Doctor of Philosophy in Neuroscience

University of California, Los Angeles, 2016

Professor Felix Erich Schweizer, Chair

The nervous system rapidly integrates sensory modalities with higher order cognition to generate a seamless and appropriate output in the form of motor activity, behavior and cognitive functions. In order to do so, modification within neural circuits, individual cells and unique synapses is constantly occurring. In this dissertation, I focused on the problem of rapid modifications at pre-synaptic sites, and how those modifications generate information transfer in the form of synaptic vesicle release. In the first section of this dissertation, I examined the role of synaptic protein ubiquitination in modulating pre-synaptic release properties. In the second and third sections of the dissertation, I characterized the effects of agricultural pesticides, in particular ziram, on synaptic transmission. Electrophysiological recordings of mammalian neurons acutely exposed to inhibitors of ubiquitination indicate that disrupting the pathway

at various points in the ubiquitin cycle leads to enhanced spontaneous release in a matter of minutes. Imaging with fluorescent reporters of exo and endocytosis further suggest a role for synaptic protein ubiquitination in modulating evoked release within the same time frame; inhibitors rapidly reduced the amount of stimulated exocytosis, possibly through or in parallel to disruption of endocytosis and synaptic vesicle recycling. Similar techniques were employed to examine the effects of ziram and other pesticides which are linked to an increased risk of Parkinson's disease (PD) at mammalian and invertebrate synapses. *Drosophila melanogaster* larvae expressing either fluorescent sensors of exo and endocytosis, calcium, or voltage were used to measure changes in release at glutamatergic and aminergic neurons of the neuromuscular junction (NMJ) exposed to ziram. Combined, data from the NMJ and mammalian neurons demonstrated that ziram and other dithiocarbamate chemicals enhance spontaneous synaptic vesicle fusion and lead to spontaneous neural activity in aminergic neurons. Ziram leads to a depolarization of membranes, and differences in the outcome following exposure at different neurons may be related to pre-synaptic ion channel composition. These data offer insight into the dynamic modulation of release properties via ubiquitination, and offer insight into pre-synaptic changes in excitability that may occur in the onset and during the development of PD linked to environmental toxins.

The dissertation for Katherine Myers is approved.

Cameron B. Gundersen

David E. Krantz

Thomas J. O'Dell

Felix Erich Schweizer, Committee Chair

University of California, Los Angeles

2016

DEDICATION

This dissertation is dedicated in loving memory of:

S. Joan Myers and Krystal Birdsong

TABLE OF CONTENTS

LIST OF FIGURES AND TABLES

ACKNOWLEDGEMENTS

Finally, I owe a tremendous debt to my fiancé, Eric Gschweng. He has patiently supported me through every moment of graduate school. In addition to being an amazing confident, scientist, role model, and lover of adventure, he is my best and favorite friend.

Chapter 4 is a version of:

Martin CA, Myers KM, Chen A, Martin NT, Barajas A, Schweizer FE, Krantz DE. (2016) Ziram, a pesticide associated with increased risk for Parkinson's disease, differentially affects the presynaptic function of aminergic and glutamatergic nerve terminals at the Drosophila neuromuscular junction. *Exp Neurol*. 275(1):232-41

Chapter 4 acknowledgements:

Chapter 4 author contributions:

Doctoral Candidate, UCLA; Los Angeles, CA   2010 – 2016

      Laboratory of Dr. Felix Schweizer

M.A. in Biotechnology, Columbia University; New York City, NY   2008 – 2010

Research Employee, Columbia University; New York City, NY   2008 – 2010

      Laboratory of Dr. Ai Yamamoto

Research Employee, Columbia University; New York City, NY   2006 – 2008

      Laboratory of Dr. James Rothman

B.S. in Microbiology, University of Maryland; College Park, MD   2002 – 2005

Student Researcher, Food and Drug Administration; College Park, MD   2003 – 2005

      Laboratory of Dr. Sufian Al-Khaldi

Selected Publications

Martin CA, **Myers KM**, Chen A, Martin NT, Barajas A, Schweizer FE, Krantz DE. (2016) Ziram, a pesticide associated with increased risk for Parkinson's disease, differentially affects the presynaptic function of aminergic and glutamatergic nerve terminals at the Drosophila neuromuscular junction. *Exp Neurol*. 275(1):232-41

Schweizer FE, **Myers KM**, Caputo A. (2012) In the zone: presynaptic function at high res. *Nat Neurosci* 15(7):928-9.

Filimonenko M, Isakson P, Finley KD, Anderson M, Jeong H, Melia TJ, Bartlett BJ, **Myers KM**, Birkeland HC, Lamark T, Krainc D, Brech A, Stenmark H, Simonsen A, Yamamoto A. (2010) The selective macroautophagic degradation of aggregated proteins requires the PI3P-binding protein Alfy. *Molecular Cell*. 38(2):265-79.

Selected Presentations

Myers, K., Martin, C., Aamodt, C., Krantz, D.E., Schweizer, F.E. Effects of agricultural pesticides on synaptic function. *Society for Neuroscience, Poster presentation.* October 2015, Chicago, IL.

Myers, K.M., Caputo, A., Shamash, P.N., Schweizer, F.E. Bistable effect of Ubiquitination on Synaptic Function and Plasticity. *Gordon Conference on Synaptic Transmission, Poster presentation.* August 2014, Waterville Valley, NH.

Myers, K.M. Bistable effect of Ubiquitination on Synaptic Function and Plasticity. *Neural Microcircuits Annual Symposium, Oral presentation.* May 2014, UCLA.

Myers KM, Caputo A, Schweizer FE. The ubiquitin proteasome system differentially affects spontaneous and evoked synaptic transmission. *Society for Neuroscience, Poster presentation.* October 2012, New Orleans, LA.

Academic and Professional Honors

Achievement Rewards for College Scientists (ARCS) Fellowship	2014 – 2016
AAAS sponsored position in Catalyzing Advocacy in Science and Engineering workshop	2015
Neural Microcircuits Training Grant, UCLA	2012 – 2013
Neurobiology Course at the Marine Biological Laboratory in Woods Hole, MA	2012
Parkinson's Disease Foundation Summer Student Fellowship	2009 – 2010
Bursary winner, Human Pluripotent Stem Cell Conference, Dublin, Ireland	2009

Other Professional Activities

AAAS, student member	2012 – present
Society for Neuroscience, student member	2012 – present
Biological Sciences Council at UCLA, President	2014 – 2015
Biological Sciences Council at UCLA, Secretary	2013 – 2014
Biological Sciences Council at UCLA, Neurobiology Dept. Representative	2012 – 2013

Chapter 1: Introduction

Modulation of pre-synaptic release in neurotransmission

Membrane fusion is a fundamental process for information transfer and enables cellular communication between compartmentalized organelles. Examples of fusion events include endosome to lysosome trafficking, endoplasmic reticulum to Golgi transport (and the reverse), as well as mitochondrial fusion/fission events. In the nervous system the best characterized example of membrane fusion occurs during chemical neurotransmission where membrane enclosed 'packets' of neurotransmitter fuse with the cell membrane at synaptic junctions. These packets or 'synaptic vesicles' are able to fuse rapidly in response to an action potential – less than 150µs following depolarization in the mammalian central nervous system (CNS) (Sabatini and Regehr 1996). Fusion at the synapse is tightly controlled so as to convey the appropriate amount and timing of information.

The first indications that vesicles were the unit of information transfer in neurons came among electron microscope (EM) images and physiological studies of the frog neuromuscular junction (NMJ) in the mid-twentieth century. De Robertis and Bennett described the presence of what they coined 'synaptic vesicles' at synapses of earthworms and frog in 1955, while Palay and Palade described similar findings in an abstract published in 1954 and summarized in a later paper (De Robertis and Bennett 1955, Palay 1956). In conjunction with these findings the quantal theory of neurotransmitter release was being developed by Bernard Katz and colleagues based upon studies of transmission at the frog neuromuscular junction (Del Castillo and Katz 1956). Fatt and Katz had initially described the properties of spontaneous 'discharges' at the NMJ which appeared to them as miniature end plate potentials (mini EPPs) (Fatt and Katz 1952). Upon reduction of the external Ca^{2+} concentration, Katz and Del Castillo could then demonstrate that the mini EPP was the "*smallest quantum of action,*" with the EPP being a statistical summation of those quanta (Del Castillo and Katz 1954). Critical support that the synaptic vesicle was the

1

'quantum of neurotransmitter' further came from Heuser, Reese and colleagues, using a rapid freezing technique that could produce EM images of synapses within 2ms of stimulation, thus capturing the act of vesicle fusion in progress (Heuser, Reese et al. 1979). The classical form of synaptic transmission thus dictates that as an action potential travels down an axon and enters an axonal bouton (pre-synaptic site), depolarization opens voltage-gated calcium channels (VGCCs) that are strategically placed in proximity to docked synaptic vesicles. Calcium influx leads to a supralinear increase in the release probability of synaptic vesicles via calcium sensors in conjunction with fusion-control proteins called SNAREs; these fusion events unload neurotransmitters into the synaptic cleft where they can come into direct contact with post synaptic receptors. Information transfer thus continues on into the post synaptic neuron.

Precise control over the amount of release leading to a post-synaptic response, R, can be thought of in terms of the variables contained in the equation $R = Npq$. The variable N can represent either the number of release sites or the readily releasable pool (RRP), while p is the probability of release and q represents quantal size. The quantal size, q, is thought to be predominantly controlled by the number of post-synaptic receptors, although evidence indicates that experimentally manipulating the vesicular content of glutamate can alter the amplitude of the post-synaptic response (Ishikawa, Sahara et al. 2002). Examples of modulation to N and p, on the other hand, indicate that these factors underlie pre-synaptic control of synaptic strength and efficacy.

The subset of synaptic vesicles that readily fuse upon stimulation (N), may be dictated by both physical location as well as molecular determinants (Alabi and Tsien 2012, Crawford and Kavalali 2015). The number and availability of synaptic vesicles are typically subdivided into three categories: in addition to the RRP, a large portion of synaptic vesicles compose the recycling pool (RP) as well as the resting pool (RtP; also referred to as the reserve pool). The few synaptic vesicles that make up the RRP rapidly fuse with the plasma membrane following an action potential, while upon greater stimulation, vesicles of the RP become recruited. While the RtP may contribute to the RP under some circumstances, its role remains

2

less clear (Alabi and Tsien 2012). Interestingly, the reserve pool can be controlled in part by the balance of cyclin-dependent kinase 5 (CDK5) and calcineurin. Inhibition of CDK5 leads to a transfer of vesicles from the RtP to the active RP, and removing calcineurin can alter this ratio in the opposite direction. Further, CDK5 inhibition occurs in response to reduced neural activity, which unmasks previously 'silent' synapses (Kim and Ryan 2010). Other studies have similarly found that neural inactivity can lead to an enhancement in the size of the presynaptic site and the number of synaptic vesicles available for release (Murthy, Schikorski et al. 2001, Thiagarajan, Lindskog et al. 2005).

The probability of synaptic vesicle fusion, p, is a common target of pre-synaptic modulation. Intrinsic excitability is a key contributor to vesicle fusion probability. The Ca_V2 family of VGCCs are the primary pre-synaptic Ca^{2+} channels, and alterations in the expression or properties of these channels directly influence the properties of release. $Ca_V2.1$ (P/Q-type) channels, importantly contribute to facilitation at synapses by way of Ca^{2+}, calmodulin (Lee, Wong et al. 1999, Lee, Scheuer et al. 2000) and the neuronal calcium sensor 1 (NCS-1) (Tsujimoto, Jeromin et al. 2002). During development, there is a shift from $Ca_V2.2$ (N-type) channels, to $Ca_V2.1$ channels (Scholz and Miller 1995); the change in expression is modified by alteration in activity levels (Miki, Hirai et al. 2013) and importantly alters release properties and short term plasticity. Perhaps unsurprisingly, the *Drosophila* homologue of Ca_V2, cacophony (cac), is a common target of intrinsic homeostatic scaling (Davis and Müller 2015). Modification or expression of VGCCs is also critical in long term plasticity at pre-synaptic sites. In the mossy fibers of the hippocampus for instance, potentiation relies on Ca^{2+} influx through $Ca_V2.3$ (R-type) channels, but not $Ca_V2.1$ or 2.2 (Castillo, Weisskopf et al. 1994, Breustedt, Vogt et al. 2003, Dietrich, Kirschstein et al. 2003). On the other hand, 'depolarization-induced suppression of inhibition' (DSI) mediated by endocannabinoids at hippocampal synapses requires $Ca_V2.2$ channels (Wilson, Kunos et al. 2001).

VGCCs are a fundamental component in the modulation of vesicle release probability, however there are a number of molecular players at the active zone which also play an important role in release

properties. Perhaps the most obvious targets are SNARE (soluble NSF-attachment protein receptor) and SM (Sec1/Munc18-like) proteins, both of which are crucial for synaptic vesicle exocytosis to occur in neurons. SNARE proteins include the vesicle SNARE synaptobrevin 2/VAMP2 and the target membrane SNAREs syntaxin-1 and SNAP-25. These three proteins form a tight α-helical coil-coiled structure that is thought to bring the two membranes into close apposition, with fusion proceeding in an energetically favorable manner. There are a number of synaptic proteins that function in conjunction with SNAREs and/or in the modification of their properties. These include, but are not limited to, cysteine string protein α (CSPα), the absence of which strongly reduces evoked release (Umbach, Zinsmaier et al. 1994). This protein has been found to bind to and regulate ubiquitination and degradation of SNAP-25, and thus promote proper SNARE assembly (Sharma, Burré et al. 2011). Complexin is another protein that interacts with and modulates SNARE mediated fusion; at the *Drosophila* NMJ complexin mutants show increased spontaneous release, while in wild-type larvae phosphorylation of complexin similarly leads to enhanced spontaneous vesicle fusion (Huntwork and Littleton 2007, Cho, Buhl et al. 2015). Another modulator of release properties is RIM-1α, a scaffolding protein that tethers Ca^{2+} channels and activates priming of vesicles through Munc-13 (Deng, Kaeser et al. 2011, Han, Kaeser et al. 2011, Kaeser, Deng et al. 2011). RIM-1α importantly mediates changes at synapses that enable pre-synaptic LTP at mossy fibers, as well as homeostatic scaling and changes to the RRP at *Drosophila* NMJ (Castillo, Schoch et al. 2002, Müller, Liu et al. 2012). These examples highlight complex roles for synaptic proteins in altering vesicle release properties, many of which may occur via post-translation modifications.

Finally, endocytosis and the recycling of vesicles is crucial in maintaining the releasable vesicle pool as well as the functional integrity of the active zone for future release. There are several versions of the endocytosis pathway that have been described, including clathrin mediated, kiss and run, activity-dependent bulk endocytosis, and the recently characterized ultrafast endocytosis (Watanabe, Rost et al. 2013, Soykan, Maritzen et al. 2016). Each of these may be induced by a different pattern of activity, and

appear to be controlled by some common proteins (e.g., dynamin) but not others (e.g., clathrin). Endocytosis is known to be modified by the presence of Ca^{2+} in response to synaptic activity, the effects of which are mediated in part by calcineurin. Calcineurin dephosphorylates several critical endocytic proteins, including dynamin, synaptojanin, amphiphysin 1 and amphiphysin 2 (Marks and McMahon 1998). Additional calcium-binding proteins regulate endocytosis, as calcineurin-independent endocytosis is still Ca^{2+} dependent, and calcineurin control of endocytosis is determined by developmental age as well as patterns of pre-synaptic activity (Kumashiro, Lu et al. 2005, Smillie, Evans et al. 2005). Another protein recently implicated in the phosphorylation of endocytic proteins is LRRK2, a kinase associated with Parkinson's disease and which phosphorylates EndophillinA. Either too much or too little phosphorylation of EndoA by LRRK2 leads to a slowing of endocytosis at *Drosophila* NMJ (Matta, Van Kolen et al. 2012). Endocytic proteins are thus regulated by activity, and post-translational modifications including phosphorylation; a role for ubiquitination has also been implicated, although it is not clear whether this functions primarily in the degradation of endocytic proteins or if this modification would alter activity in a similar manner as phosphorylation (Chen, Polo et al. 2003, Uytterhoeven, Kuenen et al. 2011).

Despite tremendous advances in our understanding of the modulation of release at pre-synaptic sites, there is much still to learn. We have identified the amount and identities of proteins present at pre-synaptic sites, and very often their specific locations (Takamori, Holt et al. 2006, Wilhelm, Mandad et al. 2014). What remains is to uncover the complexities of synaptic protein modifications and their outcomes. For instance, the various synaptic vesicle pools may be distinguished in part by different molecular signatures. Defining the binding partners and post-translational modifications of different molecularly defined pools will be important to understand how they may be differentially released and endocytosed. Further, understanding the complexities of post-translational modification of synaptic proteins may help uncover seemingly disparate findings; certain functions of complexin and synaptotagmin have been a contentious subject, and this may be due to differences in post-translational modifications and the

context of the experimental environment. Additionally, the milieu of post-translational modifications is expanding; in addition to phosphorylation, ubiquitination and SUMOylation are being appreciated as modulators of activity at pre-synaptic sites. The outcome of these modifications, in addition to the timing over which they occur will likely be important in our understanding of the dynamic nature of synaptic transmission, and very likely the breakdown that occurs under neuropathological states.

References

Alabi, A. A. and R. W. Tsien (2012). "Synaptic vesicle pools and dynamics." <u>Cold Spring Harb Perspect Biol</u> **4**(8): a013680.

Breustedt, J., K. E. Vogt, R. J. Miller, R. A. Nicoll and D. Schmitz (2003). "Alpha1E-containing Ca2+ channels are involved in synaptic plasticity." <u>Proc Natl Acad Sci U S A</u> **100**(21): 12450-12455.

Castillo, P. E., S. Schoch, F. Schmitz, T. C. Südhof and R. C. Malenka (2002). "RIM1alpha is required for presynaptic long-term potentiation." <u>Nature</u> **415**(6869): 327-330.

Castillo, P. E., M. G. Weisskopf and R. A. Nicoll (1994). "The role of Ca2+ channels in hippocampal mossy fiber synaptic transmission and long-term potentiation." <u>Neuron</u> **12**(2): 261-269.

Chen, H., S. Polo, P. P. Di Fiore and P. V. De Camilli (2003). "Rapid Ca2+-dependent decrease of protein ubiquitination at synapses." <u>Proc Natl Acad Sci U S A</u> **100**(25): 14908-14913.

Cho, R. W., L. K. Buhl, D. Volfson, A. Tran, F. Li, Y. Akbergenova and J. T. Littleton (2015). "Phosphorylation of Complexin by PKA Regulates Activity-Dependent Spontaneous Neurotransmitter Release and Structural Synaptic Plasticity." <u>Neuron</u> **88**(4): 749-761.

Crawford, D. C. and E. T. Kavalali (2015). "Molecular underpinnings of synaptic vesicle pool heterogeneity." <u>Traffic</u> **16**(4): 338-364.

Davis, G. W. and M. Müller (2015). "Homeostatic control of presynaptic neurotransmitter release." <u>Annu Rev Physiol</u> **77**: 251-270.

De Robertis, E. D. and H. S. Bennett (1955). "Some features of the submicroscopic morphology of synapses in frog and earthworm." <u>J Biophys Biochem Cytol</u> **1**(1): 47-58.

Del Castillo, J. and B. Katz (1954). "Quantal components of the end-plate potential." <u>J Physiol</u> **124**(3): 560-573.

Del Castillo, J. and B. Katz (1956). "Biophysical aspects of neuro-muscular transmission." <u>Prog Biophys Biophys Chem</u> **6**: 121-170.

Deng, L., P. S. Kaeser, W. Xu and T. C. Südhof (2011). "RIM proteins activate vesicle priming by reversing autoinhibitory homodimerization of Munc13." <u>Neuron</u> **69**(2): 317-331.

Dietrich, D., T. Kirschstein, M. Kukley, A. Pereverzev, C. von der Brelie, T. Schneider and H. Beck (2003). "Functional specialization of presynaptic Cav2.3 Ca2+ channels." <u>Neuron</u> **39**(3): 483-496.

Fatt, P. and B. Katz (1952). "Spontaneous subthreshold activity at motor nerve endings." <u>J Physiol</u> **117**(1): 109-128.

Han, Y., P. S. Kaeser, T. C. Südhof and R. Schneggenburger (2011). "RIM determines Ca²+ channel density and vesicle docking at the presynaptic active zone." <u>Neuron</u> **69**(2): 304-316.

Heuser, J. E., T. S. Reese, M. J. Dennis, Y. Jan, L. Jan and L. Evans (1979). "Synaptic vesicle exocytosis captured by quick freezing and correlated with quantal transmitter release." <u>J Cell Biol</u> **81**(2): 275-300.

Huntwork, S. and J. T. Littleton (2007). "A complexin fusion clamp regulates spontaneous neurotransmitter release and synaptic growth." Nat Neurosci **10**(10): 1235-1237.

Ishikawa, T., Y. Sahara and T. Takahashi (2002). "A single packet of transmitter does not saturate postsynaptic glutamate receptors." Neuron **34**(4): 613-621.

Kaeser, P. S., L. Deng, Y. Wang, I. Dulubova, X. Liu, J. Rizo and T. C. Südhof (2011). "RIM proteins tether Ca2+ channels to presynaptic active zones via a direct PDZ-domain interaction." Cell **144**(2): 282-295.

Kim, S. H. and T. A. Ryan (2010). "CDK5 serves as a major control point in neurotransmitter release." Neuron **67**(5): 797-809.

Kumashiro, S., Y. F. Lu, K. Tomizawa, M. Matsushita, F. Y. Wei and H. Matsui (2005). "Regulation of synaptic vesicle recycling by calcineurin in different vesicle pools." Neurosci Res **51**(4): 435-443.

Lee, A., T. Scheuer and W. A. Catterall (2000). "Ca2+/calmodulin-dependent facilitation and inactivation of P/Q-type Ca2+ channels." J Neurosci **20**(18): 6830-6838.

Lee, A., S. T. Wong, D. Gallagher, B. Li, D. R. Storm, T. Scheuer and W. A. Catterall (1999). "Ca2+/calmodulin binds to and modulates P/Q-type calcium channels." Nature **399**(6732): 155-159.

Marks, B. and H. T. McMahon (1998). "Calcium triggers calcineurin-dependent synaptic vesicle recycling in mammalian nerve terminals." Curr Biol **8**(13): 740-749.

Matta, S., K. Van Kolen, R. da Cunha, G. van den Bogaart, W. Mandemakers, K. Miskiewicz, P. J. De Bock, V. A. Morais, S. Vilain, D. Haddad, L. Delbroek, J. Swerts, L. Chávez-Gutiérrez, G. Esposito, G. Daneels, E. Karran, M. Holt, K. Gevaert, D. W. Moechars, B. De Strooper and P. Verstreken (2012). "LRRK2 controls an EndoA phosphorylation cycle in synaptic endocytosis." Neuron **75**(6): 1008-1021.

Miki, T., H. Hirai and T. Takahashi (2013). "Activity-dependent neurotrophin signaling underlies developmental switch of Ca2+ channel subtypes mediating neurotransmitter release." J Neurosci **33**(48): 18755-18763.

Müller, M., K. S. Liu, S. J. Sigrist and G. W. Davis (2012). "RIM controls homeostatic plasticity through modulation of the readily-releasable vesicle pool." J Neurosci **32**(47): 16574-16585.

Murthy, V. N., T. Schikorski, C. F. Stevens and Y. Zhu (2001). "Inactivity produces increases in neurotransmitter release and synapse size." Neuron **32**(4): 673-682.

Palay, S. L. (1956). "Synapses in the central nervous system." J Biophys Biochem Cytol **2**(4 Suppl): 193-202.

Sabatini, B. L. and W. G. Regehr (1996). "Timing of neurotransmission at fast synapses in the mammalian brain." Nature **384**(6605): 170-172.

Scholz, K. P. and R. J. Miller (1995). "Developmental changes in presynaptic calcium channels coupled to glutamate release in cultured rat hippocampal neurons." J Neurosci **15**(6): 4612-4617.

Sharma, M., J. Burré and T. C. Südhof (2011). "CSPα promotes SNARE-complex assembly by chaperoning SNAP-25 during synaptic activity." Nat Cell Biol **13**(1): 30-39.

Smillie, K. J., G. J. Evans and M. A. Cousin (2005). "Developmental change in the calcium sensor for synaptic vesicle endocytosis in central nerve terminals." J Neurochem **94**(2): 452-458.

Soykan, T., T. Maritzen and V. Haucke (2016). "Modes and mechanisms of synaptic vesicle recycling." Curr Opin Neurobiol **39**: 17-23.

Takamori, S., M. Holt, K. Stenius, E. A. Lemke, M. Grønborg, D. Riedel, H. Urlaub, S. Schenck, B. Brügger, P. Ringler, S. A. Müller, B. Rammner, F. Gräter, J. S. Hub, B. L. De Groot, G. Mieskes, Y. Moriyama, J. Klingauf, H. Grubmüller, J. Heuser, F. Wieland and R. Jahn (2006). "Molecular anatomy of a trafficking organelle." Cell **127**(4): 831-846.

Thiagarajan, T. C., M. Lindskog and R. W. Tsien (2005). "Adaptation to synaptic inactivity in hippocampal neurons." Neuron **47**(5): 725-737.

Tsujimoto, T., A. Jeromin, N. Saitoh, J. C. Roder and T. Takahashi (2002). "Neuronal calcium sensor 1 and activity-dependent facilitation of P/Q-type calcium currents at presynaptic nerve terminals." Science **295**(5563): 2276-2279.

Umbach, J. A., K. E. Zinsmaier, K. K. Eberle, E. Buchner, S. Benzer and C. B. Gundersen (1994). "Presynaptic dysfunction in Drosophila csp mutants." Neuron **13**(4): 899-907.

Uytterhoeven, V., S. Kuenen, J. Kasprowicz, K. Miskiewicz and P. Verstreken (2011). "Loss of skywalker reveals synaptic endosomes as sorting stations for synaptic vesicle proteins." Cell **145**(1): 117-132.

Watanabe, S., B. R. Rost, M. Camacho-Pérez, M. W. Davis, B. Söhl-Kielczynski, C. Rosenmund and E. M. Jorgensen (2013). "Ultrafast endocytosis at mouse hippocampal synapses." Nature **504**(7479): 242-247.

Wilhelm, B. G., S. Mandad, S. Truckenbrodt, K. Kröhnert, C. Schäfer, B. Rammner, S. J. Koo, G. A. Claßen, M. Krauss, V. Haucke, H. Urlaub and S. O. Rizzoli (2014). "Composition of isolated synaptic boutons reveals the amounts of vesicle trafficking proteins." Science **344**(6187): 1023-1028.

Wilson, R. I., G. Kunos and R. A. Nicoll (2001). "Presynaptic specificity of endocannabinoid signaling in the hippocampus." Neuron **31**(3): 453-462.

Chapter 2: Dynamic ubiquitination regulates presynaptic release

Abstract

The nervous system is regulated at many levels while constantly integrating a variety of input stimuli with biological demands and generating an appropriate output. Modulation occurs at the level of circuits, cells, and even individual synapses. Synaptic sites undergo forms of plasticity in response to changes in activity, which can be important for learning and memory. Changes to synapses include the synthesis and degradation of proteins in addition to post-translational modifications which may alter a protein's activity, localization or turnover. One pathway which regulates proteins involved in synaptic transmission is the ubiquitin proteasome system (UPS). Critically, disruption of the enzymes in the UPS leads to neurological disorders including neurodegeneration, ataxia and autism. While a number of studies have examined the role of the UPS in protein turnover, the role of non-degradative ubiquitination in modifying synaptic release is relatively unknown. My hypothesis is that protein ubiquitination acts to dynamically modulate synaptic release. Using electrophysiological recording and imaging of activity in neurons, I found that acute pharmacological inhibition of enzymes in the UPS enhanced spontaneous synaptic activity and diminished synchronous, evoked responses. It is possible that the decrease in evoked responses is related to a deficit in vesicle recycling. Our lab has uncovered numerous synaptic targets of dynamic ubiquitination using a proteomics approach, one of which is the SNARE protein VAMP2, a critical component of vesicle fusion. I developed genetic constructs to investigate the impact of VAMP2 ubiquitination and results of those experiments suggest a role in the trafficking between the plasma membrane and vesicles. These data highlight the feasibility of this approach to study other targets of ubiquitination and shed light on a novel pathway for modulation of synaptic transmission.

Introduction

Within a circuit, individual neurons adjust the physiological response to local conditions and to meet system demands. At synapses, trafficking of mRNA and local protein synthesis are important mediators of plasticity, structural change, and maintenance of synaptic function (Cajigas, Will et al. 2010, Lai and Ip 2013). These changes may occur over the course of hours to days. Rapid modification of proteins, e.g. within seconds to minutes, often occurs through post-translational modifications, including phosphorylation or the conjugation of small proteins such as ubiquitin, NEDD8, SUMO or other ubiquitin-like modifiers (UBLs) to targets. Addition of ubiquitin to a protein can lead to changes in activity, binding partners, localization or degradation by the proteasome. Ubiquitination plays an important role in numerous cellular pathways including DNA repair, the immune response, and inflammation (Komander 2010). Additionally, ubiquitination has an important role at synapses, regulating the outgrowth of neurites and the addition, elimination, and maintenance of synapses (Yi and Ehlers 2005). Protein ubiquitination and degradation are integral to post-synaptic remodeling in response to neural activity (Ehlers 2003). More recently, a role for ubiquitination in modifying the activity of pre-synaptic proteins has been appreciated, although questions remain as to what the targets are and what the impact of modification on those targets may be.

Ubiquitin is a 76 amino acid protein that is conjugated to substrate proteins through formation of a covalent bond at lysine residues. The addition of ubiquitin requires three enzymes to modify targets: E1 ubiquitin activating enzyme, E2 ubiquitin conjugating enzyme, and E3 ubiquitin ligase. One to two E1, tens of E2, and hundreds of E3 enzymes exist. Diversity in this cascade imparts a level of specificity in the modification of proteins. Differences also exist in the ubiquitin chain structure, e.g. mono- or polyubiquitination, which can specify changes in protein trafficking or degradation, respectively. The pattern of branching and the location of lysine conjugation within a chain of poly-ubiquitin plays an additional role in the fate of substrates (Glickman and Ciechanover 2002). De-ubiquitinating enzymes

(DUBs), of which approximately 100 are known in humans, are important for the dynamic nature of ubiquitination and for maintaining a pool of free ubiquitin within the cell (Figure 1). A large diversity in ubiquitin-chain modifications, as well as the compartmental localization and other-protein interacting motifs are used for specificity in DUBs. Cells and cellular compartments actively work to maintain the appropriate balance in these pathways, and disturbance of the system can lead to neurodegeneration, cancer and other pathologies (Komander 2010).

Mutations in ubiquitinating and de-ubiquitinating enzymes have been associated with neurological disorders, including neurodegeneration, autism, and ataxia. Changes in the expression – either up or down – of the E3 enzyme Ube3a lead to behavioral, learning, and motor deficits. Angelman syndrome, part of the autism spectrum (ASD), is due to loss of an allelic region that includes Ube3a enzyme, and manifests as motor dysfunction, seizures, and context dependent learning difficulties (Jiang, Armstrong et al. 1998). Increased dosage of Ube3a is also implicated in autism, and models of duplication or triplication of the protein display behavior characteristic of ASD with significant disruptions in excitatory synaptic transmission (Smith, Zhou et al. 2011). Of the DUBs, variations in UCH-L1, a protein specific to neurons, are correlated with Parkinson's disease (PD) (Maraganore, Lesnick et al. 2004); interestingly, this enzyme is down-regulated in idiopathic PD and Alzheimer's disease (Choi, Levey et al. 2004). Mutations in either UCH-L1 or another DUB, Usp14, have been found to cause ataxia in mice (Wilson, Bhattacharyya et al. 2002, Sakurai, Sekiguchi et al. 2008) and both display altered properties of plasticity. In the UCH-L1 ataxic mouse, LTP occurs following tetanus induced stimulation but not following theta-burst stimulation (Sakurai, Sekiguchi et al. 2008) a property which is suggestive of a deficit in GABAergic transmission (Pacelli, Su et al. 1989, Davies, Starkey et al. 1991). Further, Usp14 mice are deficient in short-term facilitation at hippocampal synapses and at the neuromuscular junction (Bhattacharyya, Wilson et al. 2012, Walters, Hallengren et al. 2014).

Stable genetic modifications demonstrate the importance of UPS enzymes to the normal functioning of the nervous system. However, they do not inform us on the dynamic or acute effects of disrupting the pathway on synaptic function. A few studies to date have found an acute role for the UPS in neural activity. In *Drosophila* and mammalian cultured neurons, pharmacological inhibitors of the proteasome increase synaptic vesicle recruitment within 15 to 45 min (Speese, Trotta et al. 2003, Willeumier, Pulst et al. 2006). In Speese et al. the authors found that proteasome inhibition in this time led to a two fold increase in levels of DUNC-13, a protein involved in vesicle priming (Speese, Trotta et al. 2003). In another study by Chen and colleagues, stimulation of synaptosomes with high K^+ led to a global decrease of poly-ubiquitination in samples within just 15s of treatment, including a decrease in mono-ubiquitination of the endocytic protein epsin1 (Chen, Polo et al. 2003). Our lab previously found that pharmacological inhibitors of the proteasome or E1 enzyme led to an enhancement of spontaneous synaptic vesicle fusion, as seen by an increase in mini EPSC and mini IPSC frequency in hippocampal neurons within minutes (Rinetti and Schweizer 2010). These studies suggest that synaptic proteins are actively regulated by ubiquitination, although the synaptic mechanisms and targets remain unknown.

In order to follow up on the previous finding of alteration in spontaneous vesicle fusion, I examined the effect of inhibitors of various enzymes in the ubiquitin pathway including E1 and DUBs. Initially measuring the properties of mini EPSCs, I found that inhibitors of both UPS targets led to a rapid increase in frequency, similar to the previously published findings with E1 or proteasome inhibition (Rinetti and Schweizer 2010). Next, I examined the effect of each these inhibitors on evoked release, using vGlut1-pHluorin (Voglmaier, Kam et al. 2006, Balaji and Ryan 2007) to image exo and endocytosis in neurons. In spite of an increase in mini frequency, which might suggest an increase in release probability, the same inhibitors led to a decline in evoked responses over the a time course parallel to the changes in mini frequency. The decrease in evoked release was accompanied by an increase in localization of protein at the plasma membrane and a decrease in endocytic rate, which may indicate a disruption in vesicle

recycling. These data demonstrate that inhibition of either E1 or DUBs – the addition or removal of ubiquitin – lead to disruptions in synaptic transmission.

Finally, I examined the effects of ubiquitination on the SNARE protein VAMP2/synaptobrevin 2. VAMP2 is a major component of synaptic vesicles and part of the core machinery needed for fusion of vesicles with the plasma membrane. It is also one of a number of synaptic targets of both E1 and DUB inhibition that came out of a proteomic screen performed by our lab in collaboration with the Wolhschlegel lab at UCLA (unpublished). The screen identified two lysine residues to be targets of ubiquitination in VAMP2, and each of these was mutated in the fluorescent reporter, VAMP2-pHluorin. Expression of the mutant probes in cortical neurons indicated that they are localized to synaptic vesicles as well as the plasma membrane and participate in exo and endocytosis. Intriguingly, the double mutant probe appears to reside more often in synaptic vesicles than at plasma membrane compared to VAMP2-pHluorin distribution. These results suggest that VAMP2 ubiquitination may determine the subcellular localization of the protein, and may be in line with the finding that pharmacological inhibition at synapses alters the synaptic vesicle cycle. These results suggest the feasibility of this approach to further investigate other substrates of ubiquitination at the synapse.
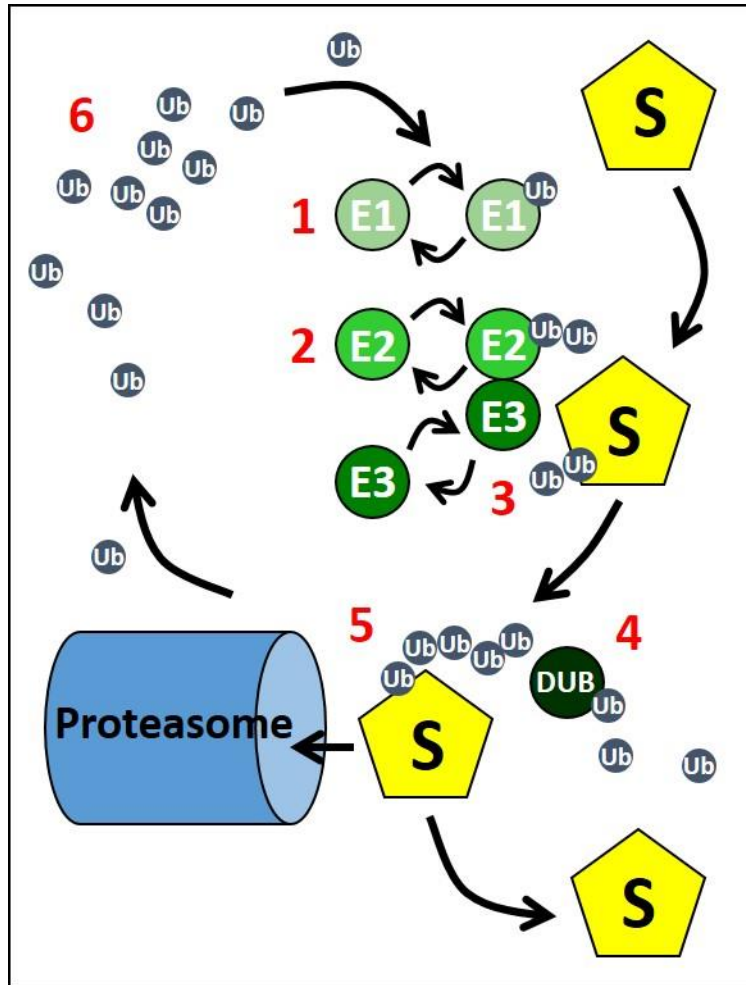
Figure 1. The Ubiquitin-Proteasome pathway. Addition of ubiquitin (Ub) to substrate proteins (S) leads to changes in protein trafficking, activity, binding partners and half-life. Critical steps in the ubiquitin pathway include (1) the activation and binding of ubiquitin by the E1 enzyme. Following which, (2) activated ubiquitin is transferred to E2-conjugating enzyme. (3) E3-ligating enzymes recruits E2 and catalyzes the transfer of ubiquitin to the substrate. This process may occur iteratively to create poly-ubiquitin chains, or alternatively stop after mono-ubiquitination. (4) Ubiquitin is removed from proteins by de-ubiquitinating enzymes (DUBs) either prior to (5) degradation or in a cell-signaling capacity. (6) DUBs maintain the free pool ubiquitin for further downstream modification.

Materials and Methods

Preparation of primary cortical neuron cultures

Animal procedures were conducted in accordance with the UCLA Institutional Animal Care and Use Committee's regulations. Dissociated cortical neurons were prepared from P0 to P2 Sprague Dawley male and female rat pups. Pups were decapitated, the whole brain removed, and the cortices isolated in L-15 media (USBio). Tissue was dissociated in 1μg/mL papain dissolved in L-15 for 10min at 37°C. Neurons were plated in media containing: Eagle's Minimum Essential Media without L-glutamine and phenol red (EMEM, MediaTech Inc) supplemented with 5% fetal bovine serum (Life Technologies), 2% B27 supplement (Life Technologies), 5mg/mL glucose, Glutamax (Life Technologies) and 0.1mg/mL transferrin (EMD Millipore). Poly-D-Lysine coated glass coverslips were used with neurons plated at a density of 60,000 cells/cm^2; cells were maintained in a humidified incubator with 95% air and 5% CO2 at 37°C. Glial cell division was inhibited using addition of 2μM cytosine arabinoside to cultures at DIV 5. Alternatively, E18 rat whole brain was purchased from BrainBits, LLC. Brains were processed as described above, except that dissociation was performed in 1μg/mL papain dissolved in Hibernate E media (BrainBits) for 15min at 37°C. Electrophysiological and imaging experiments were performed on primary neurons maintained from two and three weeks in culture.

Chemical reagents

Ziram was purchased from Chem Service, Inc and G5 was purchased from Santa Cruz Biotechnology. Tetrodotoxin (TTX), picrotoxin (PTX), LDN57444, DNQX, DL-AP5 and NSC 624206 were purchased from Tocris/R&D Systems. Unless indicated all other drugs and reagents were obtained from Sigma-Aldrich.

Electrophysiological Recordings

Neurons were mounted in a perfusion chamber (WPI) and viewed with a Zeiss Axiovert 200. Cells were constantly perfused in external solution (in mM): NaCl 134, KCl 2.5, CaCl2 3, MgCl2 1, NaH2PO4 0.34, NaHCO3 1, glucose 20, HEPES 10; 0.1% DMSO was added and the solution was adjusted to pH 7.3 and 310 mOsm. Thick-walled borosilicate glass (Sutter Instruments) was used at a resistance of $3 - 6$ MΩ. Miniature excitatory post-synaptic currents (EPSCs) recordings were made with a Cairn Optopatch patch-clamp amplifier and currents were low pass filtered at 10kHz using an 8-pole Bessel filter. Recordings were acquired at a rate of 50kHz with a computer interface (6502E, National Instruments) and using custom programs in LabView 2013 (National Instruments). The series resistance was monitored during each recording and those experiments with Rs ≤ 10% of total membrane resistance, and where Rs did not increase to >15% during 30min, were used for analysis.

During whole cell patch clamp, neurons were perfused in external solution with 0.5µM TTX and 100µM PTX to inhibit either action potentials or inhibitory currents. The internal solution contained the following (in mM): Na2ATP 5, Na3GTP 0.3, Na2-phosphocreatine 10, Cs-methansulfonate 100, MgCl2 5, EGTA 0.6, HEPES 30; solutions were adjusted to pH 7.2 and 295 mOsm. For mini EPSCs, neurons were clamped at -75mV. After five minutes of baseline recording, the perfusion was switched to either drug or vehicle in external solution. Analysis was initially performed with custom written programming in LabView. Mini events properties were measured by aligning at the event midpoint and measurements were binned at 30s with the median.

pHluorin imaging and stimulation

Cortical neurons were transfected with vGlut1-pHluorin, vGlut1-pHluorin R-GECO, or VAMP2-pHuorins between DIV 7 and 9. Transfection was performed using the Ca^{2+}-phosphate method; 0.8µg of

DNA was prepared in 0.2M $CaCl_2$ and added dropwise to equal volume 2x HEPES-buffered saline (HBS). The solution was allowed to precipitate for 20 min in the dark and added to neurons in serum-free media for 10 min. Following incubation, neurons were rinsed two times in serum free media and replaced with conditioned media. Imaging with stimulation of pHluorins was performed between 14 to 21 DIV.

For experiments with either vGlut1-pHluorin or vGlut1-pHluorin R-GECO cells were placed in a custom built closed stimulation chamber using a Warner Precision Instruments (WPI) base made for a 12mm coverslip, hand cut gasket, plastic cover and electrodes made of recycled platinum filament from a Sutter Instruments micropipette puller. Neurons were perfused with external solution containing 40μM DL-AP5 and 10μM DNQX, and stimulated with 100 pulses for 1ms each, at 20Hz frequency with 20V using a Grass Instruments SD9 Stimulator. Imaging was performed using a Zeiss LSM 5 with PASCAL software and using a Plan-Apochromat 63x oil immersion 1.4NA objective (Zeiss); the rate of acquisition was 1 frame per 2s. The stimulation protocol was repeated every five minutes for a total of 30 min. Perfusion was switched to external containing drug or DMSO vehicle 1 min prior to the second stimulus, such that the drug would reach cells just following the second round of release. To reveal the total pHluorin pool at the end of experiments, perfusion was switched to external solution containing 50mM NH_4Cl with equivalent subtraction of NaCl (84mM instead of 134mM). Experiments with neurons expressing VAMP2-pHluorin and lysine mutants were performed in the same manner except using 600 pulse stimulation three times with five minute intervals.

For analysis of the pHluorin experiments, 20 individual boutons were selected per neuron (the same boutons were use across all time trials of a single experiment) using ImageJ (NIH) and the Time Series Analyzer plugin. The individual boutons were background subtracted and then averaged per frame. Following which, the value of fluorescence (max or min) or the ΔF/F was reported. Endocytosis was measured as a percentage of the peak ΔF/F at 30s post stimulus.

VAMP2-pHluorin mutation

Using peptide sequences identified in mass spectrometry experiments (A. Caputo and J. Wohlschlegel), two lysine residues in VAMP2 were targeted for mutation to arginine. We used the VAMP2-pHluorin construct for introduction of mutations. Primers were custom designed to overlap with lysine residues and make point mutations by mismatched base pairing (see Table 1 for sequences; oligos purchased from ValueGene). The primers were used in conjunction with QuikChange II Site-Directed Mutagenesis Kit per the manufacturers' instructions (Agilent Technologies). Single mutations were performed with individual primer sets and a double mutation made using the same kit with verified single mutant constructs. All mutations were verified by sequencing (UCLA GenoSeq Core).

Data Analysis

In mini EPSC the mean of the median binned values during the first 5 minutes was used for normalization. For multiple experiments, the mean ± SEM was reported. For pHluorins, the F values prior to stimulus were averaged to use as the baseline and to calculate ΔF/F. In most experiments, n represents the number of cells per data set, with the exception of certain VAMP2 plots using individual ROIs (boutons). As the individual data points per experiment was between 3 and 20, no assumption was made about the normality and non-parametric tests were used. Two sample comparisons were performed with the Mann-Whitney rank-based test while group comparison was done with Krustal-Wallis ANOVA testing followed by Mann-Whitney. Results were considered statistically significant when the p value was < 0.05. Analysis was performed with Excel (Microsoft) and OriginPro 2016 (OriginLab Corp).

Primer target	5' to 3' sequence	5' to 3' antisense sequence
K52R (A54G)	atgagggtgaatgtggacagggtcctggagc	gctccaggaccctgtccacattcaccctcat
K59R (A75G)	gagcgggaccagaggttgtcggagctg	cagctccgacaacctctggtcccgctc

Table 1. Primer sequences for VAMP2 lysine to arginine mutations. Primers were designed using Agilent's QuickChange primer design to cover two regions encompassing lysine 52 and lysine 59 in VAMP2. Point mutations were introduced via primer mismatch to alter the codon AAG (lysine) to AGG (arginine). In the table, the primer target indicates the target lysine residue and adenine to guanine change, along with the sense and anti-sense primers.

Results

Inhibitors of E1 enzyme and deubiquitinase rapidly increase mini EPSC frequency

Published work from our lab has demonstrated that inhibition of either the proteasome or E1 ubiquitin activating enzyme leads to an increase in mini EPSC or mini IPSC frequency in hippocampal cultures (Rinetti and Schweizer 2010). These experiments were performed during whole cell recordings in which either MG-132, an inhibitor of the 26s proteasome, or ziram, a dithiocarbamate pesticide which inhibits E1 (Chou, Maidment et al. 2008), were perfused onto cells and the immediate response recorded. This work demonstrated that a non-degradative form of ubiquitination could control synaptic release in a time course of minutes.

As either E1 or the proteasome leads to an increase in mini frequency, I wanted to next test the effect of inhibition of deubiquitinase (DUB), another important enzyme in the ubiquitin pathway (Figure 1). Although DUBs act alongside the proteasome to recycle ubiquitin, they also function in non-degradative roles, and the simplest prediction was that inhibition would lead to a decrease in mini

20

frequency by directly antagonizing an ubiquitinated substrate of E1 (in coordination with E2 and 3). In order to test this hypothesis, I recorded from cortical neurons in the presence of tetrodotoxin (TTX) and picrotoxin (PTX) to block both action potentials and IPSPs, respectively, and to isolate mini EPSCs. Following a baseline recording of five minutes, I bath applied a general inhibitor of DUBs, G5 (5µM) (Aleo, Henderson et al. 2006) onto cells and continued measurement of minis. Unexpectedly, and within a matter of a few minutes of its application, the frequency of mini EPSCs began to increase and continued in this manner until the end of the recording at 30 minutes where the frequency was approximately 10 fold higher than at the start (Figure 2C). As a control, and as the previous experiments had been performed in hippocampal neurons and not cortical neurons, I performed recordings using 10µM ziram; again I recorded a rapid increase in mini frequency that began within 5 minutes of application, however in these experiments the effect peaked approximately 10min following drug application and the frequency subsequently declined (Figure 2A). These results indicate that as had been reported before, ziram induced a rapid increase in mini frequency in cortical neurons, and that in addition to blocking E1, blocking DUBs with G5 had a similar effect within the same time frame (at ten minutes in drug, ziram frequency increased 11.47 ± 1.38 fold; G5 increased frequency 5.21 ± 0.91 fold; n = 3-6 cells per condition; KWANOVA followed by Mann-Whitney, $p < 0.0001$ for ziram and $p = 0.007$ for G5). The two results were however, distinguished by the constant increase over 30 minutes in G5, compared to the ziram effect which peaked and then declined.

In order to verify the effects of E1 and DUB inhibition, two additional pharmacological agents were tested: NSC624206 (20µM), which is an E1 inhibitor (Ungermannova, Parker et al. 2012), and LDN57444 (10µM), an inhibitor of UCH-L1 (Liu, Lashuel et al. 2003), a DUB that is specific to neurons (Osaka, Wang et al. 2003). Application of either drug led to enhanced mini EPSC frequency within the time of recording (Figure 2E, G). However, NSC624206 led to an increase within ten minutes of application (6.18 ± 1.24 fold change, n = 5; KWANOVA followed by Mann-Whitney, $p = 0.001$), as ziram and G5 did,

and the increase continued to approximately 10 fold change by the end of recording; it was noted that bursts of higher frequency occurred at various points in three of five cells (see Figure 2E arrow). LDN57444 application led a more modest increase in mini frequency, which was significant after 20 min in drug (2.15 ± 0.55 fold increase; n = 3; KWANOVA followed by Mann-Whitney, p = 0.016) and similarly peaked at the end of the recording. This was intriguing, as both E1 inhibitors and G5 would be expected to target all ubiquitinated proteins while UCH-L1 may only target a subset. That the general inhibitors had similarly large increases of approximately 10-fold to the occurrence of mini EPSCs, while inhibition of UCH-L1 alone led to a change of two-fold, may indicate that inhibition of multiple ubiquitinated substrates result in mini increase, or alternatively that there is redundancy in the DUB enzymes which modulate the same target(s). It also possible, however, that the differences are due simply to variation in pharmacological affinity or kinetics.

When examining the effects of E1 and DUB inhibitors on mini EPSC amplitude, both ziram and NSC624206 led to a small but significant increase in size at 15min (Figure 2B, F; 1.16 ± 0.07 fold increase with ziram, and 1.05 ± 0.03 fold increase with NSC624206; n = 5-6 cells per condition; KWANOVA followed by Mann-Whitney, p = 0.008 for ziram and p = 0.04 for NSC624206) which then declined back towards baseline by 25 min (1.01 ± 0.08 fold change in ziram, 0.97 ± 0.05 fold change in NSC624206; p = 0.55). Neither DUB inhibitor led to a significant change in mini EPSC amplitude, although there was a small trend to increase with G5 (Figure 2D, H; n = 3 cells per condition; KWANOVA followed by Mann-Whitney, p = 0.55 at 25 min).
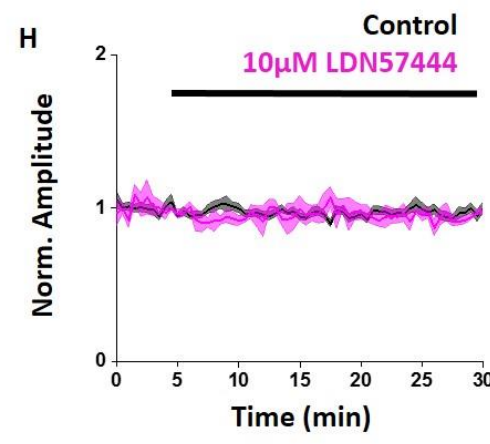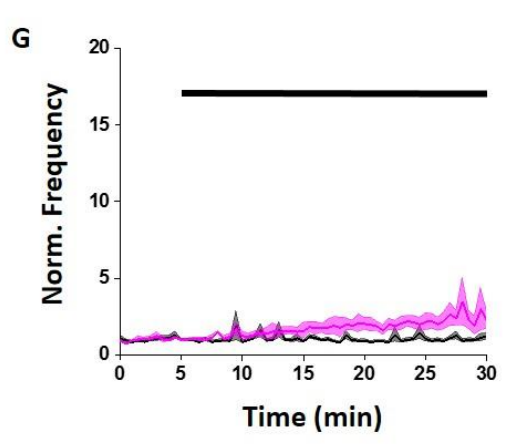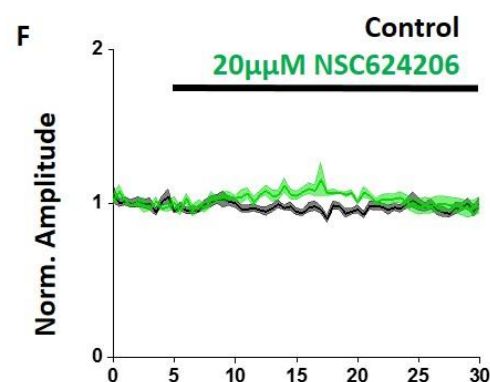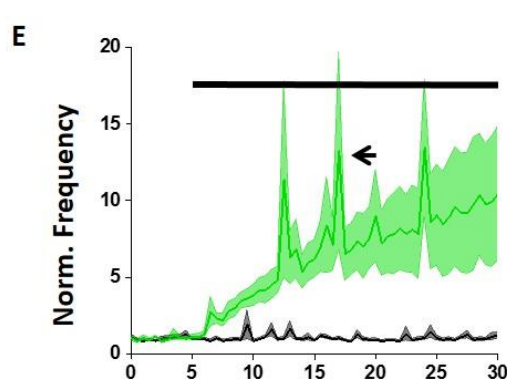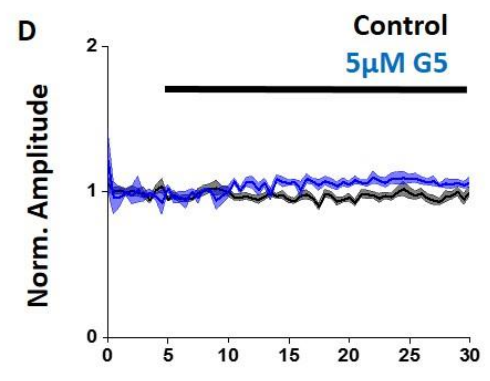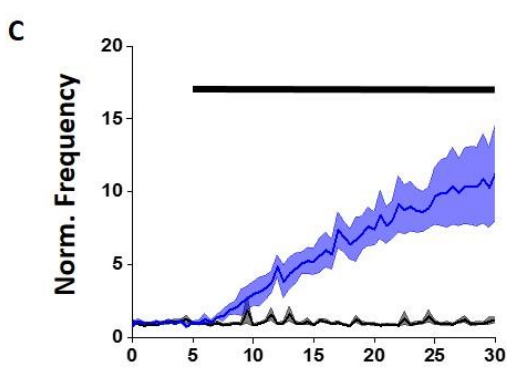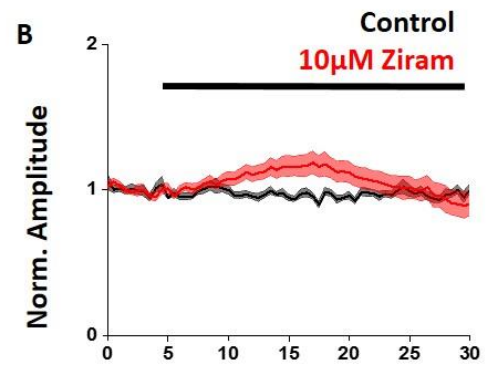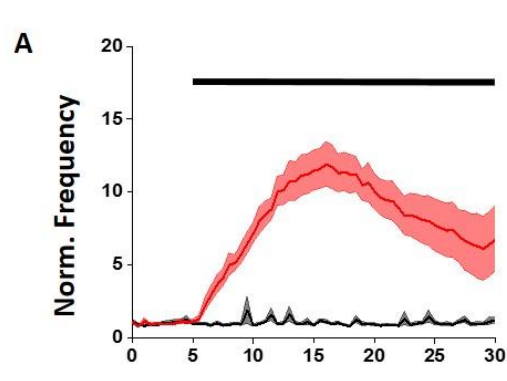
Figure 2. E1 enzyme and DUB inhibition increase mini EPSC frequency. Cortical neurons were voltage-clamped at -75mV in TTX and picrotoxin. A baseline recording of 5min was followed by perfusion with (A-B) 10μM ziram, (C-D) 5μM G5, (E-F) 20μM NSC624206 or (G-H) 10μM LDN57444. (A) Ziram rapidly increases, and then decreases, mini EPSC frequency (KWANOVA, p <0.0001). (B) Ziram leads to a small, but significant increase in mini amplitude followed by decline (KWANOVA, p = 0.008). (C) G5 increases mini frequency (KWANOVA, p = 0.007), but does not significantly affect amplitude (D). (E) NSC624206 enhances mini frequency, occasionally leading to high-frequency bursting (arrow) (KWANOVA, p = 0.001). (F) NSC624206 causes a small but significant increase in mini amplitude (KWANOVA, p = 0.04). (G) The UCH-L1 specific inhibitor LDN57444 causes a modest increase in mini EPSC frequency (KWANOVA, p = 0.02). (H) No change in mini EPSC amplitude was detected with LDN57444. For these experiments, n represents a different cell from multiple coverslips and multiple cultures when possible; for ziram n = 7, G5 n = 3, NSC624206 n = 5, LDN57444 n = 3, control n = 19.

The robust increase in mini EPSC frequency with acute application of inhibitors of both E1 and DUB enzymes is suggestive of a change in pre-synaptic release properties. What is unclear is how blocking two enzymes with presumably antagonistic activity – addition of ubiquitin and removal of ubiquitin – may lead to the same effect. Further, while there were subtle effects on the size of mini EPSCs, these varied between the different inhibitors. Both ziram and NSC624206 changed the amplitude only transiently, while G5 appeared to have a small but non-significant effect that lasted throughout the 30 min. These data suggest that in addition to pre-synaptic targets there are likely post-synaptic targets of dynamic ubiquitination which modulate the amplitude of minis.

Inhibitors of E1 enzyme and deubiquitinase decrease evoked exocytosis

The most striking effect of E1 and DUB inhibition on mini EPSCs was the frequency change, which is generally an indication that pre-synaptic release properties have been altered. An increase in frequency might be due to an increase in release probability, but since recording of minis is an indirect measure from the post-synaptic neuron, I next chose an assay that would allow measurement directly from the pre-synaptic neuron.

In order to visualize pre-synaptic boutons, cortical neurons were transfected with a fluorescent marker of exo and endocytosis, vGlut1-pHluorin (Voglmaier, Kam et al. 2006, Balaji and Ryan 2007). vGlut1-pHluorin is a fusion protein of the glutamate transporter with pH-shifted GFP added to the luminal portion of the transporter. When the protein is localized to synaptic vesicles, the fluorescence of GFP is quenched in the acidic lumen environment. However, upon stimulation and fusion of a synaptic vesicle with the plasma membrane, the GFP moves from acidic to a more neutral (~pH 7.4) extracellular environment, and increases rapidly in fluorescence. Additionally, when the cells are perfused with solution containing NH_4Cl, ammonia permeates membranes and acts to collapse the pH gradient in

25
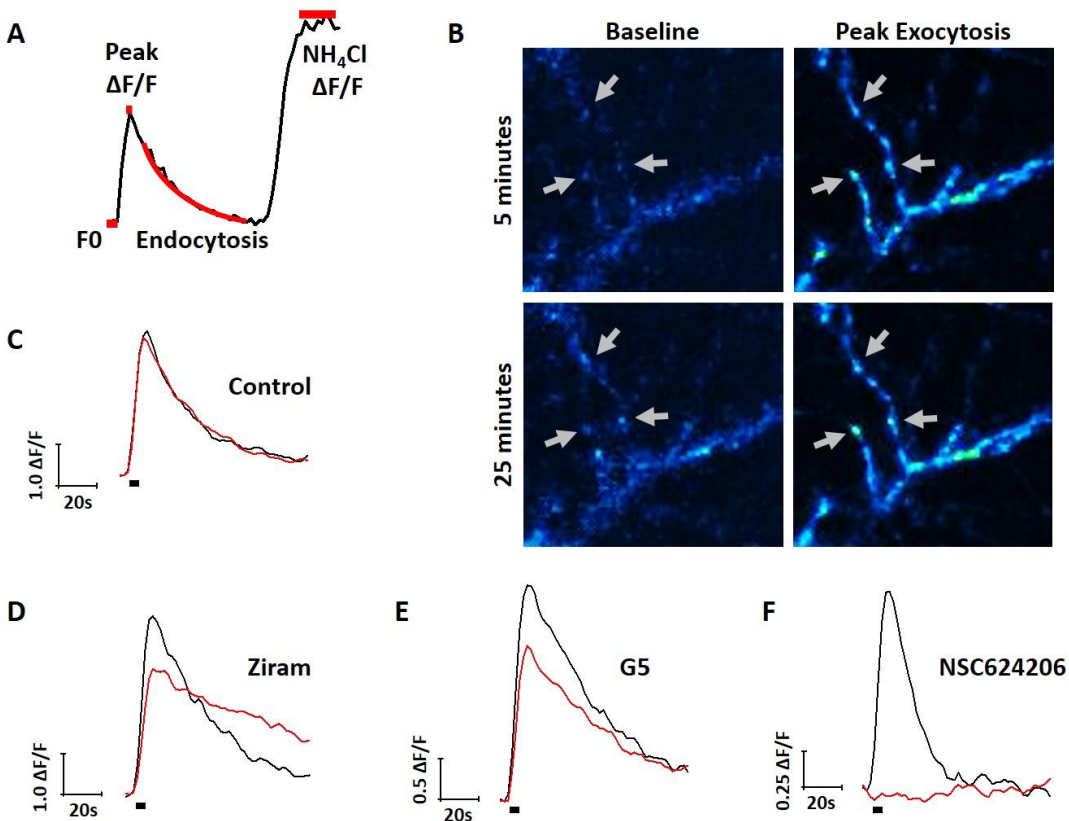
Figure 3. vGlut1-pHluorin expression and properties in cortical neurons. Neurons transfected with vGlut1-pHluorin were field stimulated with 100 action potentials at 20Hz, and this procedure was repeated every five minutes for 30 minutes. Following stimulation during the last trial at 30min, solution containing NH_4Cl was applied to reveal the entire synaptic pool. (A) Sample trace with the various measurements identified: F0 is the baseline just prior to stimulation. Peak ΔF/F is the peak change from baseline in response to stimulation. The subsequent decline from peak ΔF/F provides measurement of endocytosis. Finally, NH_4Cl collapses the pH gradient in acidic compartments, leading to a large change in ΔF/F that can be related to the entire synaptic pool at a synapse. (B) A typical control experiment: early in the time trial, little to no surface expression is detected prior to stimulus; following 100 APs a large increase in fluorescence is seen. By 25min, there is a slight increase in baseline F0, but still a large change in fluorescence in response to stimulus. Arrows point to boutons. (C-F) Representative sample peaks from

26

experiments using E1 and DUB inhibitors. Black traces represent the 'five minute' response, immediately following which the drug is added. Red traces represent the response to stimulus five minutes later. Black bar under traces represents the duration of stimulus.

synaptic vesicles, which rapidly enhances fluorescence and thus reveals the entire pHluorin-containing synaptic pool of vesicles (Miesenböck, De Angelis et al. 1998).

Cortical neurons expressing vglut1-pHluorin were field stimulated with 100 action potentials at 20Hz in the presence of DNQX and DL-AP5 to measure evoked exocytosis while blocking synaptic responses. This pattern of stimulation was repeated in five minute intervals, such that the response in control or in the presence of inhibitors could be monitored over time. In control conditions, there was always a decline in the peak $\Delta F/F$ during exocytosis between the first stimulus and the second stimulus five minutes later (Figure 4A; 0.73 ± 0.03 fold decrease at 5 min). From the second stimulus on, the peak $\Delta F/F$ decreased but to a lesser extent, and at 30 min was 0.59 ± 0.05 of the first response. Likely an amount of vGlut1-pHluorin remained on the plasma membrane surface following release, as there was concurrently a gradual increase in the baseline fluorescence, F0, over the same time (Figure 4B). Additionally, examining the peak absolute fluorescence during stimulation (F_{max}) revealed that this value remained stable and even increased slightly over the duration of the experiment (Figure 4C; F_{max} during stimulation at 30 minutes was 1.21 ± 0.12 fold higher than the first response); thus while there was a decrease in the $\Delta F/F$ during exocytosis, it was likely not due to movement of the probe out of the bouton, but an incomplete recycling of protein from the plasma membrane.

The same time series was performed with either E1 or DUB inhibitors perfused onto cells at the five minute mark (the second round of stimulation); thus from 10 minutes on the effect of drug is observed on exo and endocytosis. E1 inhibitors appeared to have the strongest effect on $\Delta F/F$, with ziram and NSC624206 reducing the peak value during exocytosis to virtually zero (Figure 4A). Within five minutes of exposure to NSC624206, $\Delta F/F$ during stimulation was drastically reduced to 0.13 ± 0.04 fold of the first response (Figure 4A; n = 5 cells; KWANOVA followed by Mann-Whitney, p = 0.008), and by ten minutes the $\Delta F/F$ stimulus peak was nearly abolished to only 4% of the original response (p = 0.008). Treatment with ziram lead to a strong decline by 15 minutes of exposure with 0.12 ± 0.05 of the first response (Figure

28

4A; n = 5 cells; KWANOVA followed by Mann-Whitney, p = 0.008), followed by a decline to only 4% of the first peak at 20 min of exposure (p = 0.008). In G5, on the other hand, there was a decline in peak $\Delta F/F$ during stimulation, but not to the same extent as E1 inhibition. By 15min in G5, the $\Delta F/F$ for exocytosis was 0.37 ± 0.07 of the baseline (Figure 4A; n = 5 cells; KWANOVA followed by Mann-Whitney p = 0.008) and by 25 min it was down to 0.26 ± 0.06 of the baseline (p = 0.014). These data indicated that the amount of evoked release decreased in the presence of ubiquitin inhibitors over time, which was in striking contrast to the increase in spontaneous release detected by the rise in mini frequency over the same time.

In the control condition the peak $\Delta F/F$ declined somewhat over the course of each stimulus trial, but appeared to be conserved in the total amount of fluorescence as some of the probe likely remained on the plasma membrane while another portion was effectively recycled and re-released upon stimulation. As E1 and DUB inhibitors had led to a strong decline in $\Delta F/F$, I next examined both the baseline and F_{max} during stimulation to determine if these values could compensate for the loss of fluorescence change over time. In all three conditions, the baseline F0 could be seen to increase in value at each time point (Figure 4B). By the end of the 30 min experiment, cells treated with ziram displayed the largest baseline change in fluorescence, increasing 2.76 ± 0.43 fold compared to the control which had increased 1.89 ± 0.23 over the same time course. NSC624206 and G5 also led to a gradual increase in F0, up to a 2.34 ± 0.31 and 2.06 ± 0.43 fold change at 30 min, respectively. Although the mean F0 of each experimental condition was greater than that of control, the changes in baseline F0 were not statistically significant (n = 5-6 cells per condition; KWANOVA, p = 0.34 at 30 min).

The $\Delta F/F$ during stimulation takes into account the change in fluorescence over baseline, and the baseline increased under each condition; as such, I wanted examine the F_{max} during stimulation to determine whether there was any loss in *total* fluorescence during exocytosis. In cells treated with NSC624206, the F_{max} at 10min was reduced to 0.58 ± 0.07 of the first response (Figure 4C; n = 5 cells; KWANOVA followed by Mann-Whitney, p = 0.02), however this value subsequently increased from this

time on, and at 30 min the F_{max} during stimulation was 0.94 ± 0.12 of the first response, and not significantly different from control (p = 0.11). Ziram-treated cells were significantly reduced in the F_{max} during stimulation at 15min (Figure 5C; 0.68 ± 0.08 fold decrease, n = 5 cells; KWANOVA followed by Mann-Whitney, p = 0.02), one time point further than a significant effect measured in NSC624206-treated cells. Similarly to NSC624206, the F_{max} increased from this time point until the end of recording at 30min in ziram, where the value was 0.74 ± 0.10 of the first measurement, and not significantly different from control (p = 0.11). In experiments with G5, where there was a more modest decline in ΔF/F compared to the E1 inhibitors, the F_{max} during stimulation remained stable throughout the recordings, and at 30min had only decreased from the start by about 4% (Figure 5C; 0.96 ± 0.07 of the first response, n = 5 cells; KWANOVA, p = 0.11).

In all of the drugs, there was a tendency to increase in baseline fluorescence. While this did not reach significance, each was on average greater than control, and this would be reflected in a reduced change from baseline during stimulation, ΔF/F. Importantly, both NSC624206 and ziram-treated cells showed a significant decrease in F_{max} during the five and ten minute time points in drug, followed by an increase back towards the initial value of F_{max} prior to drug. As the F0 continuously increases, and the F_{max} decreases initially in NSC624206 and ziram, this suggests that in the early time points the available vesicle pool was not yet depleted and that there was a deficit in the ability of synaptic vesicles to fuse with the membrane during stimulation. In G5, however, there was no significant decrease in F_{max}, despite there being a significant decline in ΔF/F at later time points. While this does not demonstrate an inability to release vesicles during fusion, it is possible that this did occur but to a degree below the detection threshold. Another important consideration in the decrease of ΔF/F and the increase in F0 is whether there was a deficit in endocytosis; this might also account for the late increase in F_{max} with NSC624206 and ziram.
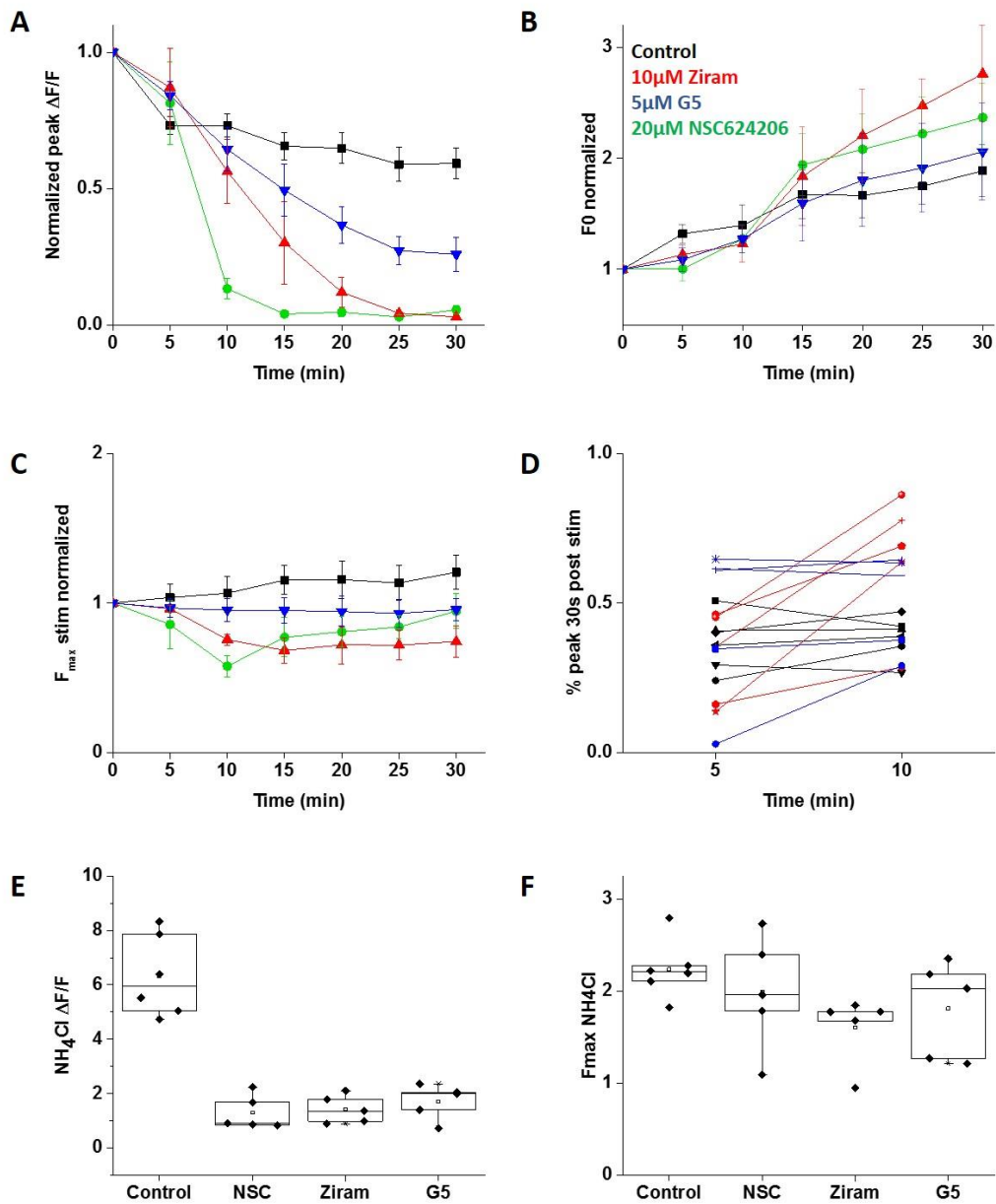
Figure 4. E1 and DUB inhibitors reduce evoked exocytosis and decrease synaptic vesicle pool size. Cortical neurons expressing vGlut1-pHluorin were stimulated with 100APs at 20Hz every five minutes. Inhibitors were applied at the 5minute mark. (A) Peak DF/F in response to stimulation reduces somewhat in control (black trace) over time. A rapid and strong decrease is seen in 20µM NSC624206 (green trace) by 10min (KWANOVA, p = 0.008). 10uM ziram (red trace) leads to a robust decrease in exocytosis (KWANOVA, p = 0.008) with slower onset compared to NSC624206, and 5µM G5 (blue trace) decreases

31

evoked exocytosis with the slowest onset (KWANOVA, p = 0.01). (B) In each condition, a gradual increase in baseline F0 was detected, indicating the probe was not fully retrieved from the plasma membrane. (C) Measurement of F_{max} during stimulus indicates that controls increase slightly while G5 remains constant in value. Ziram and NSC624206 both drop early on in F_{max} value (p = 0.02), but increase with later time points. (D) For each control (black), ziram (red) and G5 (blue) experiment the %peak at 30s post-stimulus was measured at 5min (just prior to drug) and compared to 10min (5min incubation in drug). Ziram lead to an increase in value (slowing of exocytosis) in each experiment (KWANOVA, p = 0.008) while control and G5 over all did not change. (E) Compared to control cells, each drug led to a strong decline in synaptic pool size revealed by NH_4Cl (KWANOVA, p = 0.008) (F) however there was no significant change in F_{max} during NH_4Cl indicating that the loss of internal pool was likely present on the surface of the plasma membrane. For these experiments, n represents a different cell from a different coverslip and multiple cultures when possible; for ziram n = 5, G5 n = 5, NSC624206 n = 5, control n = 6.

Ziram reduces synaptic vesicle recycling

As the rise to peak ΔF/F in response to stimulation relates to properties of exocytosis, the decay in fluorescence can be directly related to the properties of endocytosis as vesicle reacidification occurs at synapses. Throughout my recordings, I noted a large variability in the time to decay (distribution shown in Figure 4D), which led to variable results in successful fitting of curves to the endocytic rate. Similar variability with endocytic rates has been described with other pHluorins, for instance VAMP2-pHluorin is retrieved from the plasma membrane between 4 and 90s (Sankaranarayanan and Ryan 2000). In order to consistently measure endocytosis, I calculated the % of the ΔF/F peak 30s following stimulation as indication of pHluorin retrieval. Then, in control and in drug-treated conditions, I compared the first recording in drug (10min) to the previous recording (5min). Without any inhibitors present, the % peak at 30s post-stimulus increased an average of 2% from 5 to 10 min (individual traces in Figure 4D). In ziram, however, the % peak increased at 10min by 34% compared to five min (Figure 4D; n = 5; KWANOVA followed by Mann-Whitney, p = 0.008), indicating an overall slowing of pHluorin retrieval. In NSC624206 there was virtually no exocytosis at 10min (Figure 4A) and so the % peak at 30s post stim could not be measured. Finally, in G5, the % peak at 30s post stimulus did not change greatly at 10min compared to the earlier time point (Figure 4A; mean increase of 6%, n = 5 cells; KWANOVA followed by Mann-Whitney, p = 0.78). Of all of the inhibitors, only ziram demonstrated a clear slowing of endocytosis; interestingly this was also reported with ziram using VMAT-pHluorin at the *Drosophila* neuromuscular junction (Martin, Myers et al. 2016) (chapter 3 of this dissertation).

Another important measure to determine whether vesicle recycling has been disrupted is the change in fluorescence upon addition of NH_4Cl to reveal the remaining synaptic vesicle pool. This was performed at the 30 min time point during recording, 25 min after application of drug. In the control cells, the ΔF/F upon application of NH_4Cl solution ranged between approximately 5 and 8, with an average response of 6.31 ± 0.61. When cells were treated with any of the inhibitors, the remaining vesicle pool

precipitously decreased (Figure 4E). In cells exposed to ziram the peak $\Delta F/F$ following NH_4Cl was $1.42 \pm$ 0.23 (Figure 4E; n = 5 cells; KWANOVA followed by Mann-Whitney, p = 0.008), while NSC624206 had on average a change of 1.30 ± 0.28 in NH_4Cl (Figure 4E; n = 5 cells; KWANOVA followed by Mann-Whitney, p = 0.008) and in G5-treated cells the $\Delta F/F$ was 1.70 ± 0.29 (Figure 4E; n = 5 cells; KWANOVA followed by Mann-Whitney, p = 0.008). The decrease in pool size was not due to an overall loss of pHluorin or fluorescence, as measurement of the F_{max} during NH_4Cl application indicated these values were similar between conditions (Figure 4F; n = 5-6 cells per condition; KWANOVA, p = 0.09).

Taken together, the decrease in exocytosis, along with an increase in baseline fluorescence and a decrease in synaptic pool size – but not total fluorescence – could be due to incomplete vesicle recycling from the plasma membrane back to the internal pool of synaptic vesicles. Another possibility is that while spontaneous fusion is occurring, the synaptic vesicle pool is being depleted faster than it can be recycled, leading to the reduction in evoked exocytosis. A third alternative is that spontaneous and evoked synaptic vesicle release are independently regulated and that E1 or DUB inhibition had the same effect of inhibiting evoked exocytosis while simultaneously enhancing spontaneous release. One of the simplest explanations for a decrease in evoked amplitude would be a decrease in calcium influx, and importantly, spontaneous fusion can still occur in the absence of calcium. In order to test this possibility, in the next set of experiments I used a fluorescent calcium probe to measure whether calcium handing changed at synapses exposed to either E1 or DUB inhibitors.

Calcium levels at boutons does not decrease with E1 or DUB inhibition

Synaptic vesicle release during an action potential is intrinsically linked to calcium. Increases in calcium lead to supralinear changes in release probability; however, at low calcium levels or in the presence of the fast calcium chelator BAPTA, docked and primed vesicles will still undergo spontaneous

34

fusion at synapses (Schneggenburger and Rosenmund 2015). Measuring properties of calcium handling during stimulation of neurons would thus provide mechanistic insight into the regulation of evoked versus spontaneous release deficits in the presence of either E1 or DUB inhibitors.

As the experiments with pHluorins directly examined the pre-synaptic sites of exocytosis, I wanted to use a tool that would allow direct measurement of calcium in the same region. To do so, I transfected cortical neurons with a construct expressing the fluorescent calcium indicator R-GECO (Zhao, Araki et al. 2011) fused to vGlut1-pHluorin so that it localizes directly to synaptic vesicles (gift from Dr. M Hoppa). R-GECO is a red-shifted fluorescent probe developed by directed evolution of GCaMP3, and with the replacement of mApple for circularly-permutated GFP. Although this particular construct was initially developed to take advantage of dual measurements at synapses, it has since been found that R-GECO can photoactivate at 488nm, making dual recordings unreliable when this wavelength is excited (Akerboom, Carreras Calderón et al. 2013), and thus the probe was only used with laser excitation at 561nm for calcium measurements in these experiments.

Timed stimulations with R-GECO were set up in a similar manner to those performed with vGlut1-pHluorin. Every five minutes, field stimulation at 20Hz for 5s was applied (100 action potentials), and following the five min recording, either ziram or G5 was perfused onto cells. In the control condition, the peak $\Delta F/F$ during stimulation decreased gradually with each time trial, and from 5min to 25min this was seen as total decline of 33% (Figure 5B). The two time points were chosen for comparison as drug was added just after 5 min, and at 25min both drugs had reached significant declines in evoked exocytosis. In cells treated with ziram, calcium peaks occurred throughout the trials, including during times in which virtually no exocytosis was measured; at 25min the peak $\Delta F/F$ with R-GECO during stimulation was reduced by 27% compared to 5min (Figure 5B; n = 3 cells; KWANOVA, p = 0.23). G5 application, on the other hand, led to a small but not significant increase in calcium $\Delta F/F$ peaks – a mean 6% increase from 5 to 25min (Figure 5B; n = 3 cells; KWANOVA, p = 0.23). Neither ziram nor G5 decreased calcium relative to
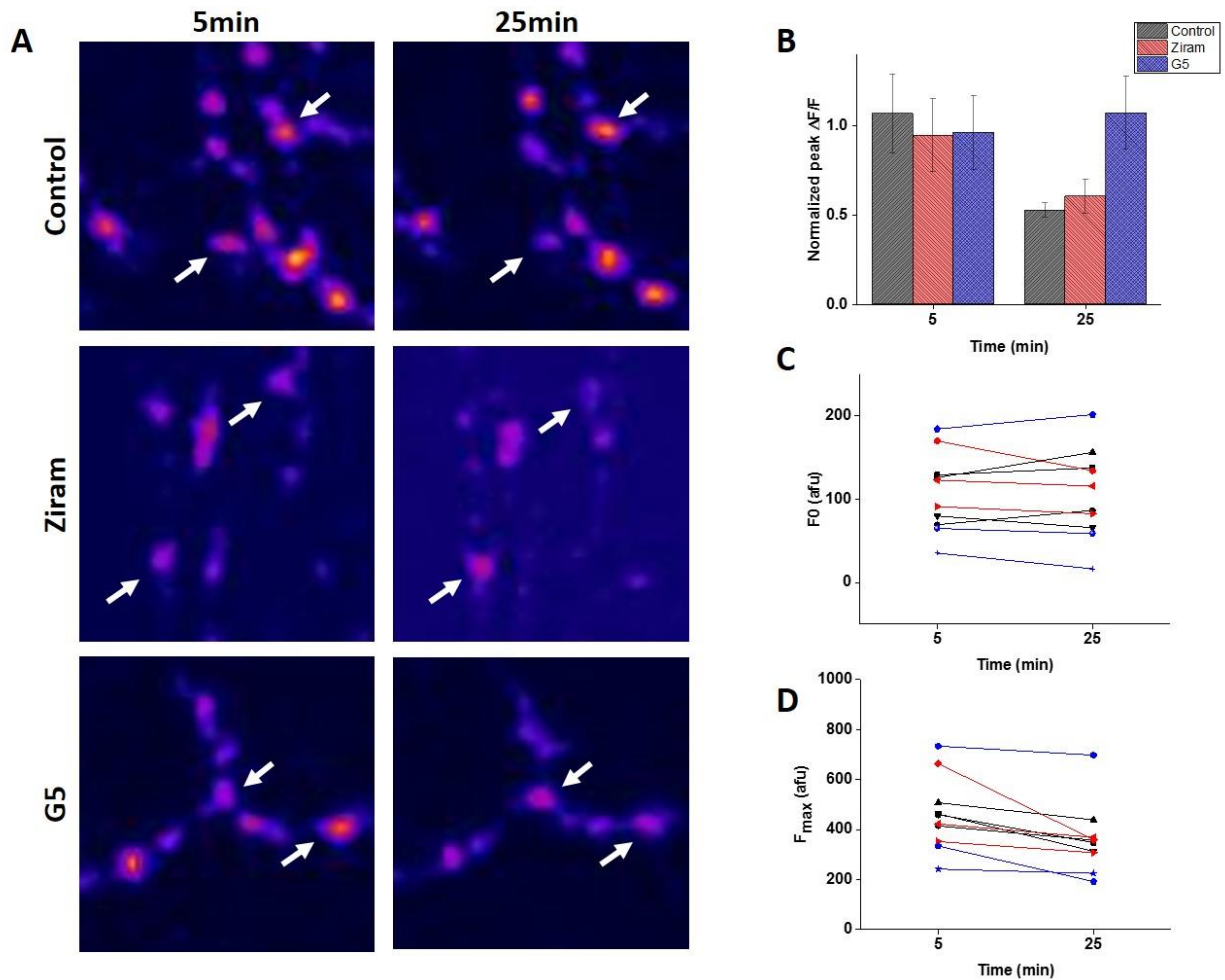
Figure 5. E1 and DUB inhibitors do not reduce calcium handling at synapses relative to control. Neurons were transfected with the calcium probe R-GECO fused to vGlut1-pHluorin, and the same stimuli were applied as in experiments with vGlut1-pHluorin only (100APs every 5 min). (A) Sample images from control, 10µM ziram and 5µM G5 during the peak of stimulus at 5 and 25min. Arrows point to boutons. (B) Peak ΔF/F corresponding to calcium influx in control (black) decreases between the 5 and 25min trials. Ziram (red) leads to a similar decline while calcium influx in G5 (blue) remains stable between the time points. (C) No overall change was observed in baseline F0 between conditions, and (D) a small decline was seen in F_{max} during stimulation between 5 and 25min for each condition. For these experiments, n represents a different cell from a different coverslip and multiple cultures when possible; for ziram n = 3, G5 n = 3, control n = 4.

the controls; if anything there was a slight, but not significant stabilization or increase in calcium. Importantly, during this same time period, there was overall no change in either the baseline F0 calcium level or the F_{max} of calcium during stimulation (Figure 5C, D; n = 3-4 cells per condition; KWANOVA, p = 0.28 for F0 and p = 0.41 for F_{max}).

The experiments with R-GECO indicate that in the presence of ziram or G5, neither a reduction in calcium influx nor a change in baseline calcium occurred at pre-synaptic sites of release. It is possible, however, that various other changes in neuronal excitability occur, and relevant experiments with ziram are discussed in Chapter 2 of this dissertation.

VAMP2 ubiquitination and characterization of mutations

Pharmacological inhibitors of enzymes in the ubiquitin pathway consistently led to disruption of evoked and spontaneous vesicle fusion within 5 to 25 min. These data suggest that the targets of the inhibitors are likely rapidly ubiquitinated and deubiquitinated, and that the targets include proteins directly involved in vesicle fusion or recycling. To identify these proteins, our lab used a mass-spectrometry based approach to isolate synaptic substrates from cortical neurons treated with either ziram or G5 and compared them to untreated neurons. In those samples, proteins were identified which were differentially ubiquitinated between conditions. One target was the SNARE protein VAMP2/synaptobrevin 2 (unpublished). VAMP2 is not absolutely required for fusion at synapses, but in its absence virtually no calcium-dependent evoked exocytosis occurs, although some spontaneous vesicle fusion events can still be detected (Deitcher, Ueda et al. 1998, Nonet, Saifee et al. 1998, Schoch, Deák et al. 2001). Based on these properties, I developed a probe to study the ubiquitination of VAMP2 at synapses.

Two lysine residues were identified as sites of ubiquitination: K52 and K59. Both of these residues lie in a region just between two predicted alpha helices that are important for both SNARE protein interactions and endocytosis of VAMP2 (Grote, Hao et al. 1995, Grote and Kelly 1996, Sutton, Fasshauer et al. 1998). Examining this region between isoforms of VAMP indicated that these residues are conserved between VAMP1, 2, 3 and 5 (Figure 6A). Of these, VAMP1 and 2 are expressed in neurons, with VAMP2 as the primary v-SNARE in the CNS although VAMP1 is still expressed to a lesser extent (Liu, Sugiura et al. 2011). Further, these residues were conserved among multiple species, with the exception that K59 was replaced by arginine in yeast and *Legionella* bacterium (Figure 6A). That the lysine residues 52 and 59 are common among species and isoforms, and are situated in a region known to be important for fusion and endocytosis in neurons, makes them particularly interesting as a region of modulation by ubiquitin.

In order to examine the effects of these two sites of ubiquitination on VAMP2, a construct of the protein fused to pHluorin was chosen as starting material as its properties of exo and endocytosis have been characterized (Sankaranarayanan and Ryan 2000). Either and both lysine residues were mutated to arginine, as arginine cannot be ubiquitinated and is similar to lysine in charge and structure, thus ideally making minimal change to protein's tertiary structure. VAMP2-pHluorin and VAMP2 K52R K59R pHluorin were both expressed in cortical neurons (Figure 6B). The double mutant additionally was able to be followed upon stimulation by an increase in fluorescence and a decay in fluorescence representing endocytosis. In order to measure the properties of release, I used a strong stimulus (compared to vGlut-pHluorin experiments) of 600 APs at 20Hz. The VAMP2-pHluorin construct reaches a plateau in fluorescence change at greater than 600 APs (Sankaranarayanan and Ryan 2000), and so this number was chosen to maximize response but still accurately compare release properties between the double mutant and the non-mutant probe. The stimulus was given three times in 5 min intervals, and at the end of the third stimulus the external solution was switched to one containing NH_4Cl to reveal the total synaptic pool of pHluorin.
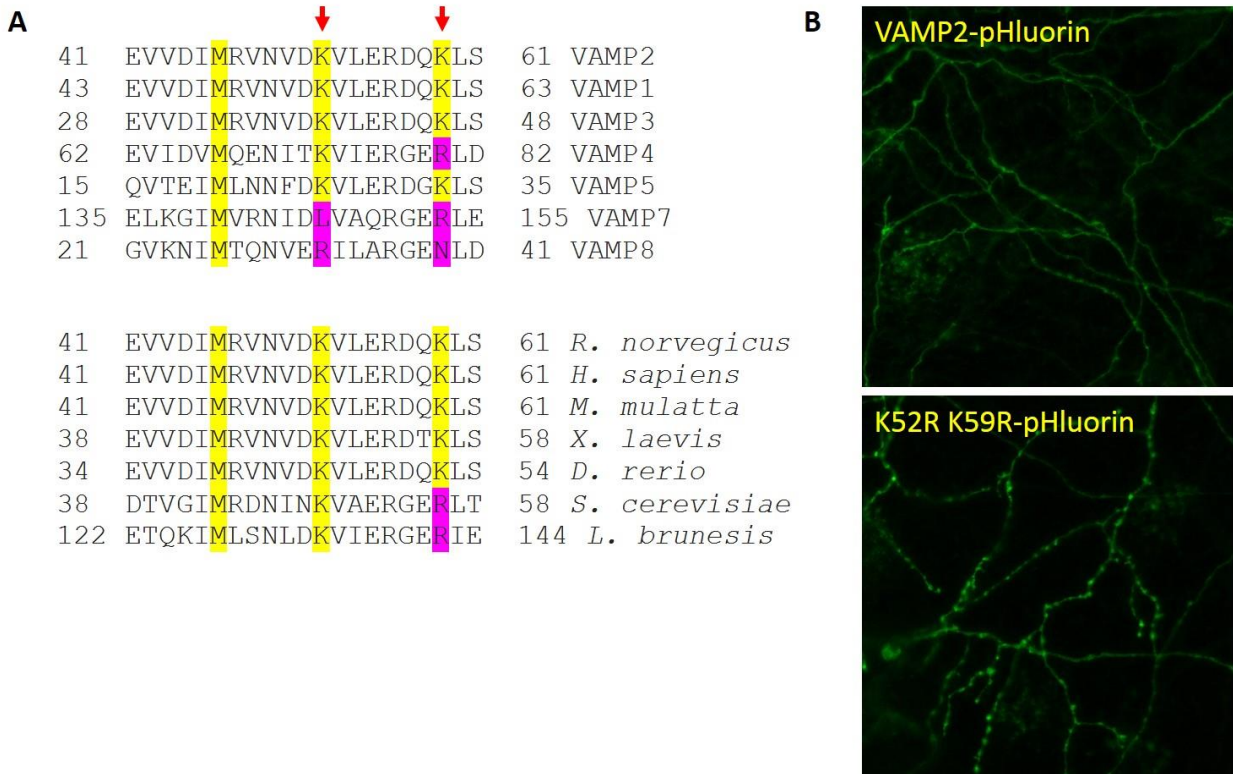
Figure 6. VAMP2 is ubiquitinated at two conserved lysine residues. VAMP2 was identified as a substrate of ubiquitination at two lysine residues: K52 and K59, both of which were mutated in VAMP2-pHluorin to arginine residues. (A) VAMP2 ubiquitination occurs at a junction between two predicted amphipathic alpha-helices, a highly conserved region important for SNARE binding, endocytosis and synaptic vesicle targeting. Top: red arrows point to K52 and K59. The common lysine residues between VAMP isoforms are highlighted in yellow in addition to M46, a residue which is critical for endocytosis. Bottom: K52 and K59 are conserved between various species; K59 is not conserved in yeast nor bacteria. (B) Both VAMP2-pHluorin and the double mutant, K52R K59R-pHluorin are expressed in cortical neurons.

In the control condition, VAMP2-pHluorin increased in fluorescence upon the first stimulation at an amount of 1.03 ± 0.14 ΔF/F. There was a decline in the ΔF/F between trials in the control cells, and at the third trial the value was 39% of the first value; however, on examining the F_{max} during stimulation with VAMP2-pHluorin, this value was only reduced to 97% of the first stimulus (Figure 7A, B, D). This indicates that the decrease observed in ΔF/F over each trial was due to the probe not being completely retrieved from the plasma membrane, and not necessarily less exocytosis. When the same stimulus was applied to the K52R K59R pHluorin-expressing neurons, the total change in fluorescence upon first stimulation was 1.89 ± 0.32 ΔF/F, and this was significantly larger than the control pHluorin (Figure 7A; n = 11-13 cells per condition; Mann-Whitney, p = 0.048). By the third trial however, ΔF/F with K52R K59R pHluorin was down to 49% of the first stimulus, which was larger but not significantly different from that of control (Figure 7B; n = 11-13 cells per condition; Mann-Whitney, p = 0.35). The normalized F_{max} during stimulation was unchanged relative to controls indicating a similar proportion of probe was stuck on the plasma membrane (Figure 7D; 92% of the first F_{max} stim; n = 11-13 cells per condition; Mann-Whitney, p = 0.18). Further, the absolute value of F_{max} during stimulation was not significantly different between the double mutant and the control, although the double mutant was somewhat brighter (Figure 7C; 108.96 ± 18.50 afu in control compared to 133.98 ± 0.38 afu in K52R K59R pHluorin; n = 11-13 cells; Mann-Whitney, p = 0.38). This indicates that the total expression of probe was not different at synapses between the two conditions, just the amount of change relative to baseline in K52R K59R pHluorin (as measured by ΔF/F).

The ΔF/F is importantly related to both the surface expression and the change in that expression upon stimulation. I next examined other properties of distribution of the K52R K59R pHluorin to determine what was responsible for this difference. First, comparing the absolute values of the baseline F0, there was no difference between the two probes (Figure 7E; 59.33 ± 11.56 afu for VAMP2 and 54.03 ± 8.17 afu for K52R K59R pHluorin; n = 11-13 cells per condition; Mann-Whitney, p = 0.77). Additionally, there was no relative change over 3 trials in F0 between control and the double mutant (Figure 7F; 1.41 ±

0.05 fold change for VAMP2 and 1.47 ± 0.11 fold change for K52R K59R pHluorin at trial 3 relative to trial 1; n = 11-13 cells per condition; Mann-Whitney, p = 0.97). Although the values of baseline did not appear different between the two, it is still possible that there was a difference in the relative distribution of protein between the surface and the intravesicular pool. Next, I compared the change in fluorescence upon addition of NH_4Cl to the pHluorin-expressing cells. For the control pHluorin, the $\Delta F/F$ in NH_4Cl was 1.2 ± 0.17, which was less but not significantly so than the synaptic pool in the double mutant, at 1.68 ± 0.21 $\Delta F/F$ (Figure 7G; n = 11-13 cells per condition; Mann-Whitney, p = 0.08). This was similar to the trend towards increased F_{max} during stimulation with the double mutant. Finally, I compared the ratio of the baseline F0 to the F_{max} during NH_4Cl to determine if there was a change in the ratio. The ratio F0/ F_{max} NH_4Cl was reduced, as expected in the double mutant K52R K59R pHluorin, as F0 was relatively similar while NH_4Cl pools were slightly brighter compared to control (Figure 7H; ratio of 0.45 ± 0.03 in control, 0.37 ± 0.03 in K52R K59R pHluorin; n = 11-13 cells per condition; Mann-Whitney, p = 0.09). Upon examining the cumulative distribution of surface to pool ratio for all boutons individually across the experiments, however, a more precise distribution emerged with the double mutant still displaying a ratio of 0.37 ± 0.01 and the control ratio being 0.44 ± 0.01 (Figure 7I; n = 199-235 boutons per condition; Kolmogorov–Smirnov, p < 0.0001). Thus, it appears that there are subtle but clear differences in the distribution of VAMP2 K52R K59R pHluorin wherein the probe resides less often on the surface relative to the total internal pool.

The difference in the distribution between the plasma membrane surface and the vesicular pool may be due to a regulatory property of VAMP2 ubiquitination relative to synaptic vesicle recycling; e.g. the protein may be more likely to be taken up from the membrane when no ubiquitin residue(s) are present at the K52 and K59 sites. As this may directly relate to the endocytic rate following stimulation, these values were next compared between the mutant and control probes. Similar to vGlut1-pHluorin, I
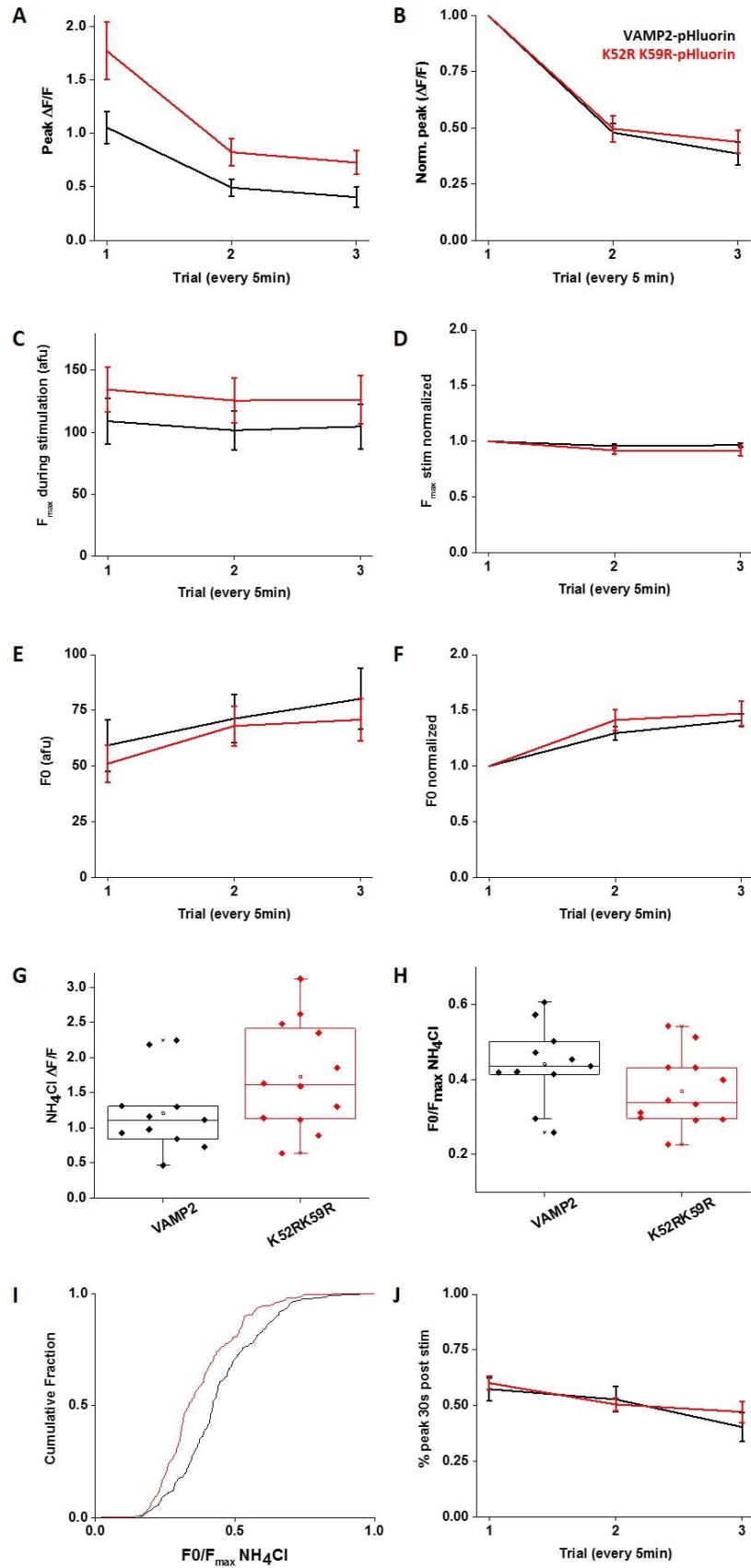
Figure 7. K52R K59R-pHluorin preferentially localizes to synaptic vesicles. Either VAMP2-pHluorin or K52R K59R-pHlourin expressing neurons were stimulated with 600 APs at 20Hz. The stimulus was applied three times, with five minute intervals, and NH_4Cl applied at the end of the third trial. (A) Peak $\Delta F/F$ in response to stimulation was larger with K52R K59R-pHlourin (red) compared to VAMP2-pHlourin (black) (Mann-Whitney test, $p = 0.048$), and each exhibited a decline over the trials in the peak. (B) Normalizing these values indicates that the decline in $\Delta F/F$ between trials for the two probes was nearly identical. (C-D) F_{max} during stimulation was not significantly different in value or in the relative change over trials. (E-F) The baseline F0 was similarly not different in absolute value or relative change over trials. (G) The $\Delta F/F$ in response to NH_4Cl tends to be larger in the mutant, K52R K59R-pHlourin, although not significantly so. (H) Comparing the surface expression F0 to the F_{max} during NH_4Cl shows a non-significant trend towards lower values in K52R K59R-pHlourin, indicating a lower ratio of surface to synaptic-pool expression of the probe. (I) Examining this ratio for all individual boutons across experiments indicates that K52R K59R-pHlourin is significantly shifted in expression from the plasma membrane to the synaptic vesicle pool (Kolmogorov–Smirnov test, $p < 0.0001$). (J) Endocytosis of VAMP2 or K52R K59R pHluorin, as measured by % peak 30s post stimulus, was not different between conditions. For experiments, n represents a different cell from a different coverslip and multiple cultures when possible; for VAMP2-pHluorin n = 11 cells, 199 boutons, K52R K59R-pHlourin n = 13 cells, 235 boutons.

used the %peak at 30s post stimulation as a point of comparison for endocytosis. At each of the three stimulus trials, there was no significant difference measured between VAMP2 and K52R K59R pHluorin (Figure 7J; n = 11-12 cells per condition; Mann-Whitney; p = 0.88 for trial 1, p = 0.52 for trial 2 and p = 0.56 for trial 3). Thus, while the distribution was different, the amount and rate of endocytosis immediately following stimulation did not appear to vary between the two conditions.

Discussion

E1 and DUB inhibitors disrupt synaptic function

Our lab has previously demonstrated that ziram, an E1 inhibitor, and MG-132, an inhibitor of the proteasome, can increase mini EPSC frequency in hippocampal neurons (Rinetti and Schweizer 2010). Following on these findings, I demonstrated here that two different E1 inhibitors (ziram and NSC624206) as well as two different DUB inhibitors (G5 and LDN57444) similarly led to a rapid enhancement of mini EPSC frequency in cortical neurons within 5 to 25 min. Rather surprisingly, these combined data indicate that inhibition of the ubiquitin proteasome system (UPS) at any one of three points – addition, removal or degradation – leads to the same outcome of enhancing spontaneous release. Precisely why this would be is not known, however one implication is that the normal function of the ubiquitin pathway occurs through the maintenance of the 'cycle;' that is the constant balance between ubiquitinated substrates, deubiquitinated substrates and the free ubiquitin pool. One indication that the 'balance' is necessary is that changes in the amount of free ubiquitin can also disrupt synaptic function (Hallengren, Chen et al. 2013). Interestingly, theoretical studies have proposed that the ubiquitin proteasome system acts as a 'biological oscillator' wherein levels of E3 and free ubiquitin lead to oscillations of ubiquitinated substrate and deubiquitinated substrate, and these dynamics are critical for downstream signaling outcome (Nguyen, Dobrzyński et al. 2014).

Although each of the E1 and DUB inhibitors tested led to an increase in spontaneous release, there were some differences. For instance, ziram led to an increase followed within the 30 min recording by a decline in mini frequency. None of the other inhibitors led to a similar decline in the same time frame. Ziram is a drug that is commonly employed as an herbicide and has other targets including ALDH, the $Na^+/Ca2^+$-exchanger and possibly one or more ion channels (see chapter 2 for further discussion). Thus it is possible that the decline in ziram is due to alternative targets. Interestingly, among the two E1 inhibitors there was a small but significant increase in mini EPSC amplitude that peaked and declined within the time of recording. It is unclear why this effect would be varied between E1 and DUB inhibitors, however it does suggest that a rapid change in post-synaptic receptors may be due to protein ubiquitination.

The increase in mini EPSC frequency observed is generally an indication of an increase in pre-synaptic release probability. In a simplistic manner, this would similarly be borne out as an increase in the amplitude of evoked release. However, using stimulation of cortical neurons expressing vGlut1-pHluorin, I found that this was not the case. Each of the inhibitors – ziram, NSC624206 and G5 – led to a progressive decline in the amount of evoked release, although there were subtle differences in the effects. For instance, although each of the chemicals tested led to a decrease in peak $\Delta F/F$ during stimulation, there was a concurrent increase in baseline fluorescence in each condition. As such, I compared the F_{max} during stimulation and found that this value only significantly declined in ziram and NSC624206 – and only in early time points. At the later time points F_{max} was at or near the pre-drug value. The combination of F0 increase and the late increase of F_{max} indicate that there was pHluorin stuck on the plasma membrane that was not available for release. That the $\Delta F/F$ for NH_4Cl was reduced in each condition further indicates that there were fewer synaptic vesicles available for release.

In considering the increased F0 and decreased synaptic pool, it is important to note that each of the drugs also enhanced spontaneous release; it is possible that the rate of spontaneous fusion could not be adequately balanced by endocytosis, or it is also possible that there was a deficit in the synaptic vesicle

recycling process (or both). Disruption of recycling likely occurred with ziram, where endocytosis could clearly be seen to decline; however as this could not be replicated with the other drugs it is possible the slowing of endocytosis was unrelated to ubiquitination. Based on the available data, it appears that E1 inhibition prohibits evoked release directly, and E1 as well as DUB inhibition may prohibit evoked release indirectly by disrupting vesicle recycling.

This raises another important question on the mechanism by which E1 inhibition enhanced spontaneous release yet prevented synchronized release. The first explanation that I considered was a disruption in calcium handling. A decrease in the amount of calcium available could lead to a decline in evoked exocytosis, while an independent mechanism may be responsible for mini release. However, using a calcium probe directed to synapses – vGlut pHluorin R-GECO – no decrease in calcium was detected with either ziram or G5. Another possible explanation for disparate effects on evoked and spontaneous release is that protein ubiquitination may act on molecularly distinct populations of synaptic vesicles (Crawford and Kavalali 2015). For instance, various isoforms of the SNARE protein VAMP preferentially label vesicles involved in evoked release, asynchronous release and spontaneous release (Schoch, Deák et al. 2001, Hua, Leal-Ortiz et al. 2011, Raingo, Khvotchev et al. 2012). Finally, it is possible that there are multiple targets of ubiquitination in different pathways involved in vesicle release, endocytosis and subsequent recycling, and that the effects that I see are the combination of disrupting substrates involved in each of these pathways. Targets of vesicle fusion came out of our mass spec screen – including the SNARE proteins SNAP-25, syntaxin and VAMP1/2 (unpublished). Previous studies have demonstrated that proteins involved in priming and endocytosis, Dunc 13 and epsin1, are ubiquitinated and/or degraded by the proteasome (Chen, Polo et al. 2003, Speese, Trotta et al. 2003). Although these last two targets may not have come out of our screen, this could be due to detection threshold. In the instance that multiple proteins at the synapse are dynamically ubiquitinated, this would likely explain the various effects on spontaneous and evoked release that I've observed. Importantly, follow up with individual targets from

our mass spec screen will be necessary to identify the various effects of ubiquitination at synapses. Further, identification of E3 or DUB enzymes with fewer specific targets as opposed to E1 or general DUB inhibition will also lead to a more complete understanding of the role of dynamic ubiquitination at the synapse.

VAMP2 ubiquitination alters distribution of the protein

In our efforts to find synaptic proteins that are ubiquitinated the SNARE protein VAMP2 was identified. I used point mutations in a VAMP2-pHluorin construct in order to create a probe that could not be ubiquitinated at lysine residues 52 and 59 in VAMP2, and could be used to track the properties of exo and endocytosis.

When expressed in cortical neurons, the mutant probe led to an enhancement in peak $\Delta F/F$ during stimulation compared to the control VAMP2-pHluorin. The absolute value of baseline $F0$ was similar between the two, although the F_{max} during stimulation was slightly higher in K52R K59R pHluorin but not significantly so. This indicates that the absolute values, while not different by direct comparison, must have still been different enough to lead to a greater change from baseline in response to stimulus. The same subtle changes could be noted in the synaptic vesicle pool, which tended to be higher in the mutant as opposed to VAMP2-pHluorin. Finally, comparing the baseline $F0$ to the Fmax during NH_4Cl for each of the boutons used for analysis made clear that there was indeed a preferential shift to internal vesicle pool as opposed to the plasma membrane in K52R K59R pHluorin compared to VAMP2-pHluorin. It's unclear exactly what this shift means. For instance, is there an equivalent pool size in both, but VAMP2-pHluorin does not express in all vesicles? Or is it possible that more K52R K59R pHluorin is expressed *per* vesicle? Of course, it may be that there are indeed more synaptic vesicles in the double mutant. I did note during the experiments that the synaptic boutons often appeared more 'bloated' in the double mutant compared

to VAMP2-pHluorin (representative images in Figure 6B). However, I used the same size ROI to analyze all data, so this wouldn't take into consideration an increase in bouton volume size.

Interestingly, two independent studies have described abnormally sized synaptic vesicles and boutons in VAMP2 knock out synapses (Deák, Schoch et al. 2004, Imig, Min et al. 2014). In these studies, the authors found that there was no change in the number of vesicles, but there were fewer docked vesicles and the vesicles present were larger (25-30% based on the study). Further, in Imig et al they found that the PSD and presynaptic terminals were on average larger, although not significantly so (Imig, Min et al. 2014). It is possible that preferential, or increased, expression of K52R K59R pHluorin in synaptic vesicles is related to the same physiological finding. This could mean that ubiquitination of K52 and K59 is important for proper synaptic vesicle recycling. Another study using tetanus toxin to acutely cleave VAMP2 found the protein to be important for endocytosis on a rapid time scale (Xu, Luo et al. 2013). However, in my experiments I found no indication that K52R K59R pHluorin altered the rate of endocytosis, simply the ratio between vesicles and the plasma membrane. Thus, it will be important to not only follow up on the findings here with VAMP2 ubiquitination, but to note there may be a distinction between endocytosis and any 'processing' of vesicles retrieved from the membrane. It may be worth noting that ubiquitination has been described in 'vesicle sorting' in other systems. In terms of synapses, this is best described in the recycling of post-synaptic receptors. Ubiquitination has been demonstrated as an important pathway for recycling and sorting of glutamate receptors and various metabotropic receptors (Marchese and Trejo 2013, Goo, Scudder et al. 2015).

In the context of my findings with VAMP2 ubiquitin mutants, my hypothesis is that ubiquitination is important for the sorting or processing of synaptic vesicles. This may be in line with the findings with pharmacological inhibitors as well. There seems to be either a lack of retrieval of membrane protein, or an inability to mobilize available synaptic vesicles for evoked release. Although these findings may not be related to VAMP2 specifically, the suggestion that ubiquitination of proteins modulates the synaptic

vesicle cycle seems to be a relevant and reasonable proposal. In order to test these hypotheses, I think that further examination of the VAMP2 mutant will be necessary, particularly in a knock out background. Further, I think that direct examination of other targets of ubiquitination in a similar manner is warranted.

In sum, this body of work demonstrates that synaptic protein ubiquitination rapidly alters pre-synaptic release properties, and that ubiquitination of a synaptic fusion protein, VAMP2, is important for the distribution or expression of the protein in synaptic vesicles. The use of other synaptic ubiquitin mutants, particularly in a knock out background and in the presence of pharmacology, should importantly help to further elucidate the role of ubiquitination in regulating synaptic transmission.

References

Akerboom, J., N. Carreras Calderón, L. Tian, S. Wabnig, M. Prigge, J. Tolö, A. Gordus, M. B. Orger, K. E. Severi, J. J. Macklin, R. Patel, S. R. Pulver, T. J. Wardill, E. Fischer, C. Schüler, T. W. Chen, K. S. Sarkisyan, J. S. Marvin, C. I. Bargmann, D. S. Kim, S. Kügler, L. Lagnado, P. Hegemann, A. Gottschalk, E. R. Schreiter and L. L. Looger (2013). "Genetically encoded calcium indicators for multi-color neural activity imaging and combination with optogenetics." Front Mol Neurosci **6**: 2.

Aleo, E., C. J. Henderson, A. Fontanini, B. Solazzo and C. Brancolini (2006). "Identification of new compounds that trigger apoptosome-independent caspase activation and apoptosis." Cancer Res **66**(18): 9235-9244.

Balaji, J. and T. A. Ryan (2007). "Single-vesicle imaging reveals that synaptic vesicle exocytosis and endocytosis are coupled by a single stochastic mode." Proc Natl Acad Sci U S A **104**(51): 20576-20581.

Bhattacharyya, B. J., S. M. Wilson, H. Jung and R. J. Miller (2012). "Altered neurotransmitter release machinery in mice deficient for the deubiquitinating enzyme Usp14." Am J Physiol Cell Physiol **302**(4): C698-708.

Cajigas, I. J., T. Will and E. M. Schuman (2010). "Protein homeostasis and synaptic plasticity." EMBO J **29**(16): 2746-2752.

Chen, H., S. Polo, P. P. Di Fiore and P. V. De Camilli (2003). "Rapid Ca2+-dependent decrease of protein ubiquitination at synapses." Proc Natl Acad Sci U S A **100**(25): 14908-14913.

Choi, J., A. I. Levey, S. T. Weintraub, H. D. Rees, M. Gearing, L. S. Chin and L. Li (2004). "Oxidative modifications and down-regulation of ubiquitin carboxyl-terminal hydrolase L1 associated with idiopathic Parkinson's and Alzheimer's diseases." J Biol Chem **279**(13): 13256-13264.

Chou, A. P., N. Maidment, R. Klintenberg, J. E. Casida, S. Li, A. G. Fitzmaurice, P. O. Fernagut, F. Mortazavi, M. F. Chesselet and J. M. Bronstein (2008). "Ziram causes dopaminergic cell damage by inhibiting E1 ligase of the proteasome." J Biol Chem **283**(50): 34696-34703.

Crawford, D. C. and E. T. Kavalali (2015). "Molecular underpinnings of synaptic vesicle pool heterogeneity." Traffic **16**(4): 338-364.

Davies, C. H., S. J. Starkey, M. F. Pozza and G. L. Collingridge (1991). "GABA autoreceptors regulate the induction of LTP." Nature **349**(6310): 609-611.

Deák, F., S. Schoch, X. Liu, T. C. Südhof and E. T. Kavalali (2004). "Synaptobrevin is essential for fast synaptic-vesicle endocytosis." Nat Cell Biol **6**(11): 1102-1108.

Deitcher, D. L., A. Ueda, B. A. Stewart, R. W. Burgess, Y. Kidokoro and T. L. Schwarz (1998). "Distinct requirements for evoked and spontaneous release of neurotransmitter are revealed by mutations in the Drosophila gene neuronal-synaptobrevin." J Neurosci **18**(6): 2028-2039.

Ehlers, M. D. (2003). "Activity level controls postsynaptic composition and signaling via the ubiquitin-proteasome system." Nat Neurosci **6**(3): 231-242.

Glickman, M. H. and A. Ciechanover (2002). "The ubiquitin-proteasome proteolytic pathway: destruction for the sake of construction." <u>Physiol Rev</u> **82**(2): 373-428.

Goo, M. S., S. L. Scudder and G. N. Patrick (2015). "Ubiquitin-dependent trafficking and turnover of ionotropic glutamate receptors." <u>Front Mol Neurosci</u> **8**: 60.

Grote, E., J. C. Hao, M. K. Bennett and R. B. Kelly (1995). "A targeting signal in VAMP regulating transport to synaptic vesicles." <u>Cell</u> **81**(4): 581-589.

Grote, E. and R. B. Kelly (1996). "Endocytosis of VAMP is facilitated by a synaptic vesicle targeting signal." <u>J Cell Biol</u> **132**(4): 537-547.

Hallengren, J., P. C. Chen and S. M. Wilson (2013). "Neuronal ubiquitin homeostasis." <u>Cell Biochem Biophys</u> **67**(1): 67-73.

Hua, Z., S. Leal-Ortiz, S. M. Foss, C. L. Waites, C. C. Garner, S. M. Voglmaier and R. H. Edwards (2011). "v-SNARE composition distinguishes synaptic vesicle pools." <u>Neuron</u> **71**(3): 474-487.

Imig, C., S. W. Min, S. Krinner, M. Arancillo, C. Rosenmund, T. C. Südhof, J. Rhee, N. Brose and B. H. Cooper (2014). "The morphological and molecular nature of synaptic vesicle priming at presynaptic active zones." <u>Neuron</u> **84**(2): 416-431.

Jiang, Y. H., D. Armstrong, U. Albrecht, C. M. Atkins, J. L. Noebels, G. Eichele, J. D. Sweatt and A. L. Beaudet (1998). "Mutation of the Angelman ubiquitin ligase in mice causes increased cytoplasmic p53 and deficits of contextual learning and long-term potentiation." <u>Neuron</u> **21**(4): 799-811.

Komander, D. (2010). "Mechanism, specificity and structure of the deubiquitinases." <u>Subcell Biochem</u> **54**: 69-87.

Lai, K. O. and N. Y. Ip (2013). "Structural plasticity of dendritic spines: the underlying mechanisms and its dysregulation in brain disorders." <u>Biochim Biophys Acta</u> **1832**(12): 2257-2263.

Liu, Y., H. A. Lashuel, S. Choi, X. Xing, A. Case, J. Ni, L. A. Yeh, G. D. Cuny, R. L. Stein and P. T. Lansbury (2003). "Discovery of inhibitors that elucidate the role of UCH-L1 activity in the H1299 lung cancer cell line." <u>Chem Biol</u> **10**(9): 837-846.

Liu, Y., Y. Sugiura and W. Lin (2011). "The role of synaptobrevin1/VAMP1 in Ca2+-triggered neurotransmitter release at the mouse neuromuscular junction." <u>J Physiol</u> **589**(Pt 7): 1603-1618.

Maraganore, D. M., T. G. Lesnick, A. Elbaz, M. C. Chartier-Harlin, T. Gasser, R. Krüger, N. Hattori, G. D. Mellick, A. Quattrone, J. Satoh, T. Toda, J. Wang, J. P. Ioannidis, M. de Andrade, W. A. Rocca and U. G. G. Consortium (2004). "UCHL1 is a Parkinson's disease susceptibility gene." <u>Ann Neurol</u> **55**(4): 512-521.

Marchese, A. and J. Trejo (2013). "Ubiquitin-dependent regulation of G protein-coupled receptor trafficking and signaling." <u>Cell Signal</u> **25**(3): 707-716.

Martin, C. A., K. M. Myers, A. Chen, N. T. Martin, A. Barajas, F. E. Schweizer and D. E. Krantz (2016). "Ziram, a pesticide associated with increased risk for Parkinson's disease, differentially affects the presynaptic function of aminergic and glutamatergic nerve terminals at the Drosophila neuromuscular junction." <u>Exp Neurol</u> **275 Pt 1**: 232-241.

Miesenböck, G., D. A. De Angelis and J. E. Rothman (1998). "Visualizing secretion and synaptic transmission with pH-sensitive green fluorescent proteins." Nature **394**(6689): 192-195.

Nguyen, L. K., M. Dobrzyński, D. Fey and B. N. Kholodenko (2014). "Polyubiquitin chain assembly and organization determine the dynamics of protein activation and degradation." Front Physiol **5**: 4.

Nonet, M. L., O. Saifee, H. Zhao, J. B. Rand and L. Wei (1998). "Synaptic transmission deficits in Caenorhabditis elegans synaptobrevin mutants." J Neurosci **18**(1): 70-80.

Osaka, H., Y. L. Wang, K. Takada, S. Takizawa, R. Setsuie, H. Li, Y. Sato, K. Nishikawa, Y. J. Sun, M. Sakurai, T. Harada, Y. Hara, I. Kimura, S. Chiba, K. Namikawa, H. Kiyama, M. Noda, S. Aoki and K. Wada (2003). "Ubiquitin carboxy-terminal hydrolase L1 binds to and stabilizes monoubiquitin in neuron." Hum Mol Genet **12**(16): 1945-1958.

Pacelli, G. J., W. Su and S. R. Kelso (1989). "Activity-induced depression of synaptic inhibition during LTP-inducing patterned stimulation." Brain Res **486**(1): 26-32.

Raingo, J., M. Khvotchev, P. Liu, F. Darios, Y. C. Li, D. M. Ramirez, M. Adachi, P. Lemieux, K. Toth, B. Davletov and E. T. Kavalali (2012). "VAMP4 directs synaptic vesicles to a pool that selectively maintains asynchronous neurotransmission." Nat Neurosci **15**(5): 738-745.

Rinetti, G. V. and F. E. Schweizer (2010). "Ubiquitination acutely regulates presynaptic neurotransmitter release in mammalian neurons." J Neurosci **30**(9): 3157-3166.

Sakurai, M., M. Sekiguchi, K. Zushida, K. Yamada, S. Nagamine, T. Kabuta and K. Wada (2008). "Reduction in memory in passive avoidance learning, exploratory behaviour and synaptic plasticity in mice with a spontaneous deletion in the ubiquitin C-terminal hydrolase L1 gene." Eur J Neurosci **27**(3): 691-701.

Sankaranarayanan, S. and T. A. Ryan (2000). "Real-time measurements of vesicle-SNARE recycling in synapses of the central nervous system." Nat Cell Biol **2**(4): 197-204.

Schneggenburger, R. and C. Rosenmund (2015). "Molecular mechanisms governing Ca(2+) regulation of evoked and spontaneous release." Nat Neurosci **18**(7): 935-941.

Schoch, S., F. Deák, A. Königstorfer, M. Mozhayeva, Y. Sara, T. C. Südhof and E. T. Kavalali (2001). "SNARE function analyzed in synaptobrevin/VAMP knockout mice." Science **294**(5544): 1117-1122.

Smith, S. E., Y. D. Zhou, G. Zhang, Z. Jin, D. C. Stoppel and M. P. Anderson (2011). "Increased gene dosage of Ube3a results in autism traits and decreased glutamate synaptic transmission in mice." Sci Transl Med **3**(103): 103ra197.

Speese, S. D., N. Trotta, C. K. Rodesch, B. Aravamudan and K. Broadie (2003). "The ubiquitin proteasome system acutely regulates presynaptic protein turnover and synaptic efficacy." Curr Biol **13**(11): 899-910.

Sutton, R. B., D. Fasshauer, R. Jahn and A. T. Brunger (1998). "Crystal structure of a SNARE complex involved in synaptic exocytosis at 2.4 A resolution." Nature **395**(6700): 347-353.

Ungermannova, D., S. J. Parker, C. G. Nasveschuk, D. A. Chapnick, A. J. Phillips, R. D. Kuchta and X. Liu (2012). "Identification and mechanistic studies of a novel ubiquitin E1 inhibitor." J Biomol Screen **17**(4): 421-434.

Voglmaier, S. M., K. Kam, H. Yang, D. L. Fortin, Z. Hua, R. A. Nicoll and R. H. Edwards (2006). "Distinct endocytic pathways control the rate and extent of synaptic vesicle protein recycling." Neuron **51**(1): 71-84.

Walters, B. J., J. J. Hallengren, C. S. Theile, H. L. Ploegh, S. M. Wilson and L. E. Dobrunz (2014). "A catalytic independent function of the deubiquitinating enzyme USP14 regulates hippocampal synaptic short-term plasticity and vesicle number." J Physiol **592**(4): 571-586.

Willeumier, K., S. M. Pulst and F. E. Schweizer (2006). "Proteasome inhibition triggers activity-dependent increase in the size of the recycling vesicle pool in cultured hippocampal neurons." J Neurosci **26**(44): 11333-11341.

Wilson, S. M., B. Bhattacharyya, R. A. Rachel, V. Coppola, L. Tessarollo, D. B. Householder, C. F. Fletcher, R. J. Miller, N. G. Copeland and N. A. Jenkins (2002). "Synaptic defects in ataxia mice result from a mutation in Usp14, encoding a ubiquitin-specific protease." Nat Genet **32**(3): 420-425.

Xu, J., F. Luo, Z. Zhang, L. Xue, X. S. Wu, H. C. Chiang, W. Shin and L. G. Wu (2013). "SNARE proteins synaptobrevin, SNAP-25, and syntaxin are involved in rapid and slow endocytosis at synapses." Cell Rep **3**(5): 1414-1421.

Yi, J. J. and M. D. Ehlers (2005). "Ubiquitin and protein turnover in synapse function." Neuron **47**(5): 629-632.

Zhao, Y., S. Araki, J. Wu, T. Teramoto, Y. F. Chang, M. Nakano, A. S. Abdelfattah, M. Fujiwara, T. Ishihara, T. Nagai and R. E. Campbell (2011). "An expanded palette of genetically encoded Ca^{2+} indicators." Science **333**(6051): 1888-1891.

Chapter 3: Dithiocarbamate pesticides dysregulate synaptic transmission

Abstract

Long term exposure to environmental toxins enhances the risk of developing Parkinson's disease (PD) including early onset PD. Toxins which have been associated with PD risk include ziram, a dithiocarbamate fungicide, among many others of varying chemical structure and classification. What is not known is whether and how these chemicals act to disrupt neuronal activity, and whether these properties are shared among different pesticides. In this study we characterized the physiological effects of ziram on cortical neurons from rats, and found that ziram increased spontaneous activity in a dose-dependent manner and led to enhanced excitability. We examined other pesticides and chemicals, finding that while several led to an increase in spontaneous activity, dithiocarbamates including maneb and disulfiram were most similar to ziram in their ability to rapidly enhance spontaneous release. While there are known molecular targets of these drugs, we found that the nature of modification varied among the dithiocarbamates. Finally, we demonstrated that dithiocarbamates can lead to spontaneous calcium transients in aminergic neurons, a cell type which may be selectively affected in PD. The results of this study indicate that pesticides which are linked to PD dysregulate synaptic activity, and that these effects are most similar among dithiocarbamates. Dithiocarbamates likely have shared targets that effect synaptic transmission, although with variability in the nature of target modification. These findings should help inform future studies of early PD-risk factors, and particularly neurophysiological targets.

Introduction

Parkinson's Disease (PD) is a common neurodegenerative disorder, second in prevalence only to Alzheimer's Disease (AD) (Dauer and Przedborski 2003). PD is perhaps best known for the motor dysfunction associated with a striking loss of dopaminergic (DA) neurons in the Substania Nigra pars compacta (SNc). However, the pathophysiology of the disorder is by no means restricted to these regions.

Proteinaceous inclusions, called Lewy bodies and Lewy neurites, are a defining hallmark of PD and are found in select glutamatergic, GABAergic, dopaminergic, cholinergic and noradrenergic neurons throughout the central and peripheral nervous system. While only subsets of neurons develop pathological inclusions, regional damage appears to be consistent across post-mortem cases of idiopathic PD (Braak, Del Tredici et al. 2003).

The majority of PD cases are of 'unknown' origin, with only about 5% of cases inherited. Environmental exposure, in combination with genetic background, is thought to play an important etiological role in PD. Strikingly, a number of epidemiological studies have been published which demonstrate a positive correlation between long-term pesticide exposure and PD, summarized in several meta-analyses (Priyadarshi, Khuder et al. 2000, Brown, Rumsby et al. 2006, Allen and Levy 2013).

A number of pesticides have been identified as candidate neurotoxins, including various fungicides, herbicides and insecticides (Hatcher, Pennell et al. 2008). Fungicides are typically metal and sulfur containing chemicals, including the dithiocarbamates maneb and ziram, which have been linked to increased PD risk (Meco, Bonifati et al. 1994, Wang, Costello et al. 2011). The herbicide and bipyridyl compound paraquat is structurally similar to MPP+, the active metabolite of MPTP, a drug discovered to cause Parkinsonian symptoms in IV drug users (Langston, Ballard et al. 1983). Epidemiological studies also support a causal relationship between paraquat and development of PD, particularly in combination with maneb, ziram or both (Hertzman, Wiens et al. 1990, Liou, Tsai et al. 1997, Wang, Costello et al. 2011). Insecticides, of which organochlorides are perhaps the most notorious, include dichlorodiphenyltrichloroethane (DDT) and the cyclodiene dieldrin. These substances cause acute toxicity at high doses, and have been found in post-mortem brains of persons with PD (Fleming, Mann et al. 1994).

What remains unknown is precisely how pesticides of differing class and structure may lead to the consistent and stereotyped pathology of PD. Several studies have revealed common cellular targets.

For instance, pesticides including ziram and dieldrin cause proteasomal dysfunction, which may be disrupted in PD (Wang, Li et al. 2006). Metabolism of aldehyde dehydrogenase (ALDH), an enzyme important for dopamine metabolism, has been found as a target of PD-linked toxins, ziram and dieldrin included (Fitzmaurice, Rhodes et al. 2014). Maneb and ziram have also been shown to disrupt mitochrondrial function, another potentially important PD pathway (Zhang, Fitsanakis et al. 2003, Domico, Zeevalk et al. 2006, Li, Kobayashi et al. 2012).

More compelling, however, may be whether and how these chemicals disrupt neurophysiological activity. Studies have previously found that dieldrin can inhibit GABA-A receptors (Cole and Casida 1986), which would presumably lead to enhanced excitability. Ziram alters the activity of the Na^+-Ca^{2+} exchanger (Jin, Lao et al. 2014), and enhances spontaneous neurotransmitter release (Rinetti and Schweizer 2010). Exposure to ziram has also been shown to initiate spontaneous activity selectively in aminergic synapses of the *Drosophila* NMJ (Martin, Myers et al. 2016). These studies report on acute effects of pesticides and may inform early, precipitating events that constitute risk factors and thus lead to development of clinically diagnosable PD.

In this study we set out to describe the neurophysiological impact of exposure to a subset of pesticides linked to increased PD risk. We focused especially on ziram as it is heavily used at present (EPA 2004) and exposure at the workplace and residence combined can lead to a three-fold increase in the risk of developing PD (Wang, Costello et al. 2011). We characterized the ability of ziram to increase spontaneous neurotransmitter release in mammalian cortical neurons, following the hypothesis that drugs linked to PD risk should alter the physiology of neurons besides those of the SNc. We next examined whether chemicals that have structural similarities (e.g., dithiocarbamates) or molecular targets (e.g., the proteasome), led to the same physiological outcome on cortical neurons as ziram. Finally, we examined an *in vivo* aminergic circuit that has been shown to be selectively sensitive to ziram, in the presence of

similar drugs. We found that ziram not only enhanced the excitability of neurons, but that many of these properties were shared among dithiocarbamates.

Materials and Methods

Preparation of primary cortical neuron cultures

All animal procedures were conducted in accordance with the UCLA Institutional Animal Care and Use Committee's regulations. Dissociated cortical neurons were prepared from P0 to P2 Sprague Dawley rat pups. Both male and female pups were used and chosen at random. Rats were decapitated and the whole brain removed and placed in chilled Leibovitz's L-15 medium (USBio). The brain was hemisected and separated from the midbrain, olfactory bulb and cerebellum. Hippocampi were trimmed from the cortices and the meninges removed. Separated cortices were placed in 1µg/mL papain dissolved in L-15 for 10min at 37°C. The tissue was rinsed twice in L-15 media before triturating by pipetting up and down. Cells were then resuspended in culture media containing: Eagle's Minimum Essential Media without L-glutamine and phenol red (EMEM, MediaTech Inc) supplemented with 5% fetal bovine serum (Life Technologies), 2% B27 supplement (Life Technologies), 5mg/mL glucose, Glutamax (Life Technologies) and 0.1mg/mL transferrin (EMD Millipore). Neurons for culture were plated at a density of 60,000 cells/cm^2 onto Poly-D-Lysine coated glass coverslips and maintained in a humidified incubator with 95% air and 5% CO_2 at 37°C. On the fifth day of culture 2µM cytosine arabinoside was added to inhibit glial cell division. Electrophysiological recordings and western blots were performed on primary neurons maintained from two and three weeks in culture.

Pesticides, Reagents and Drugs

Pesticides (ziram, maneb, benomyl, dieldrin and paraquat) were purchased from Chem Service, Inc and disulfiram was purchased from Santa Cruz Biotechnology. Tetrodotoxin (TTX), picrotoxin (PTX)

BAPTA-AM and NSC 624206 were purchased from Tocris/R&D Systems. Unless indicated all other drugs and reagents were obtained from Sigma-Aldrich.

Electrophysiological Recordings

Cortical neurons on coverslips were mounted onto a perfusion chamber (Warner Precision Instruments) and visualized on a Zeiss Axiovert 200 in external solution containing the following (in mM): NaCl 134, KCl 2.5, $CaCl_2$ 3, $MgCl_2$ 1, NaH_2PO_4 0.34, $NaHCO_3$ 1, glucose 20, HEPES 10; external solution included 0.1% DMSO and was adjusted to pH 7.3 and 310 mOsm. Recording electrodes made of thick-walled borosilicate glass (Sutter Instruments) were pulled on a Sutter Instrument Model P-97 puller to a resistance of 3 – 6 MΩ. Whole cell recordings were performed using either a Cairn Optopatch patch-clamp amplifier or an Axon Instruments MultiClamp 700A with currents low pass filtered at 10kHz using an 8-pole Bessel filter. Data was acquired at 50kHz using a computer interface (6502E, National Instruments) and custom-written programs in LabView 2013 (National Instruments). During intracellular recordings the series resistance was monitored to ensure it was not greater than 10% of total membrane resistance and did not increase to >15% over the course of the experiment.

For recording miniature EPSCs, cultures were constantly perfused in external solution containing 0.5µM TTX and 100µM PTX to inhibit action potentials and inhibitory currents, respectively. The internal solution contained the following (in mM): Na_2ATP 5, Na_3GTP 0.3, Na_2-phosphocreatine 10, Cs-methansulfonate 100, $MgCl_2$ 5, EGTA 0.6, HEPES 30; solutions were adjusted to pH 7.2 and 295 mOsm. Neurons were voltage-clamped at -75mV and miniature excitatory post-synaptic currents (EPSCs) were continuously recorded throughout the duration of experiment. The first five minutes of recording were considered the baseline, following which the perfusion was switched to external solution containing either drug or vehicle. In experiments where intracellular calcium was buffered, cells were perfused for at least 30 minutes with 10µM BAPTA-AM which remained in the external solution throughout the duration of

the recording. Mini recordings were analyzed using custom written programs in LabView; mini events were aligned by the midpoint and the data was binned in 30s intervals using the median. The instantaneous frequency was measured as the inverse of the inter-event interval.

For current clamp experiments, neurons were perfused with the same external solution as above but without inhibitors (e.g. TTX, PTX). The internal solution contained (in mM): Na_2ATP 5, Na_3GTP 0.3, Na_2-phosphocreatine 10, K-methylsulfonate 100, EGTA 0.6, HEPES 30; the solution pH was 7.2 with 295 mOsm. Following patch clamp of neurons, each was injected with 50pA of depolarizing current to bring the cell past threshold to fire an action potential; the current injection was given for a total of one second and repeated every ten seconds. Following five minutes of baseline recording the perfusion was switched to external solution containing either ziram or vehicle. These recordings were analyzed using custom script in LabView. The data was binned by median values measured over 5 minute intervals.

Western blots

For western blot analysis of E1 protein following treatment with pesticides and other reagents, whole cell lysis of neurons was performed using ice-cold RIPA buffer. Protein concentration was determined using a Pierce BCA Protein Assay kit (ThermoScientific), and lysates were maintained in a non-reducing condition. For each sample, of 5µg of protein was run on a 6% SDS-polyacrylamide gel followed by transfer onto nitrocellulose membrane (BioRad). Membranes were blocked with 5% milk in PBS/0.1%Tween20 (BioRad) and incubated in α-E1 Ub activating enzyme antibody (pAb, 1:1000, Enzo/Biomol) in blocking solution overnight at 4°C. The next day blots were washed in PBS/0.1% Tween20 and incubated with HRP-conjugated goat anti-rabbit secondary antibody (1:1000 in 5% milk/PBST) for 45 minutes, and developed using Pierce ECL Western Blotting kit (ThermoScientific) for imaging.

Drosophila experiments

Tdc2-GAL4 (Cole, Carney et al. 2005) and UAS-GCaMP6m(III) (Chen, Wardill et al. 2013) flies were maintained on standard molasses yeast agar at room temperature. Crosses were set up between the two strains and F1 progeny were collected for calcium imaging experiments.

For experiments with Tdc2 x GCaMP6 F1 flies, third instar larval filets were prepared in chilled HL3.1 without calcium (in mM: NaCl 70, KCl 5, MgCl2 4, NaHCO3 10, trehalose 5, sucrose 115, HEPES 5) and adjusted to pH 7.32 (Feng, Ueda et al. 2004). Dissection and recording were performed in the presence of 7mM L-glutamic acid to block post-synaptic responses. Following the dissection, filets were switched to HL3.1 containing 2mM calcium and the fluorescent nerve endings on segment A4 muscle 13 were located. A baseline recording lasting 50s was made. Afterwards, the solution was washed three times in HL3.1 including calcium and either 20μM ziram, 20μM disulfiram or 20μM NSC624206. The prep was then imaged at the same location 10, 15, 20 and 25 minutes following addition of drug. Images were taken on a Zeiss Axio Examiner Z1 microscope using a Zeiss Achroplan water-immersion objective (100x, 1.0 NA) and DG4 light source (Sutter). An electron-multiplying CCD camera (Andor iXon 897) captured images at 20 frames/second in the Andor IQ2 software. Post-hoc analysis was performed using ImageJ (NIH) and the Measure Stack plugin. Multiple ROIs (2-5 boutons) were selected for each experiment and then averaged, background subtracted, corrected for photobleaching and the ΔF/F was calculated for each.

Data Analysis

In an individual experiment, data was binned at either 30s (for mini EPSCs) or 5min (for current clamp) using the median. For mini recordings, the mean of the median values during the first 5 minutes was used for normalization and the median of the 5 minute baseline was used for normalization in current clamp recordings. Afterwards, multiple experiments were combined and the mean ± SEM was reported. As the n (cells) per data set was 5 to 20, no assumption was made about the normality of the population and non-parametric testing was used throughout. For two sample comparison, a Mann-Whitney rank-

based test was used, and for more than a two group comparison a Krustal-Wallis ANOVA was employed followed by Mann-Whitney. Results were judged as statistically significant if a p value was < 0.05. Curve fitting of mini EPSC frequency kinetics was performed in OriginPro 2016 (OriginLab Corp). Each data set was modeled using a linear, exponential growth and a polynomial fit. Each model was compared by the adjusted R^2 value (R^2 corrected for the degrees of freedom) and the second order Akaike Information Criterion (AIC) test that measures goodness-of-fit with consideration of the number of fitting parameters. For AIC, the preferred model is the one with the lowest value.

Results

Ziram increases mini EPSC frequency in a dose dependent manner

Ziram exposure leads to cell toxicity and death in cell lines (Wang, Li et al. 2006) and dopaminergic neurons in primary cultures (Chou, Maidment et al. 2008), but little is known about the drug's physiological effects on neurons prior to 'death'. In one study, acute application of ziram was found to increase the frequency of miniature EPSCs recorded in rat hippocampal neurons (Rinetti and Schweizer 2010). We decided to expand on these findings, but instead of hippocampal neurons, using cortical neurons to determine whether the effects of ziram on mini EPSCs would be replicated in a culture with more varied neuronal subtypes.

As we wanted to know the acute physiological effects of ziram, we recorded from cells and measured the changes in response to bath application of drug. Neurons were voltage clamped in the presence of 500nM tetrodotoxin (TTX) and 100µM picrotoxin (PTX) to block action potentials and IPSCs respectively. Baseline mini EPSCs were recorded for five minutes, followed by ziram in concentrations of either 1µM, 5µM or 10µM. In the two higher concentrations, we observed that mini frequency increased

in less than five minutes of exposure while neurons in 1µM ziram showed a more modest increase towards the end of the 30min recording (Fig 1B, C).

The strength of the change in frequency over time appeared to be dose-dependent, and we fit a curve to each dosage effect in order to directly compare. We found that the kinetics of the frequency increase per concentration could best be described by a second degree polynomial (quadratic) equation, $y = \alpha + \beta_1 x + \beta_2 x^2$ (Adj R^2 and AIC values [see methods] in Table 1). In this model, the absolute value of the β_2 coefficient describes how steep the curve is, and a negative or positive sign on β_2 indicates the curve is approaching a maximum vertex followed by decline, or is increasing towards infinity from a minimum vertex, respectively. From 1 to 10µM in ziram the value of β_2 was 7×10^{-4} (-4×10^{-4}, 0.001), -0.001 (-0.004, 0.001) and -0.05 (-0.06, -0.03); 95% CI in parentheses. The kinetics of the frequency increase thus increased in a concentration dependent manner, as per $|\beta_2|$. In 5 and 10µM ziram, the negative value of β_2 indicated the trend line was approaching a maxima, while in 1µM the trend was increasing away from a minimum. The CI of β_2 in 1 and 5µM were close to zero and so the direction of change may vary somewhat within the population. As predicted by the curve fit, a peak and subsequent decline in 10µM ziram was observed within the time of recording. In the control condition, without ziram, there was some fluctuation throughout the time of recording, but the frequency never followed a pattern of consistent increase or decrease. Some fluctuation in control cells is not surprising; there is inherent variability in these neurons and 30 minutes is a long period over which to patch clamp cultured cells. When fitting a line to the control frequency the best fit was a linear equation, $y = \alpha + \beta x$, where the slope β approached zero ($\beta = -5 \times 10^{-4}$; 95% CI: -0.003, 0.002).

The peak in mini frequency of neurons in 10µM ziram was reached approximately 10min after drug application with an 11.90 ± 1.53 fold increase over baseline (mean ± SEM). At the time in which neurons in 10µM ziram peaked in frequency, this was clearly a large change from the control cells which had a frequency of 1.10 ± 0.14 (Figure 1C; n = 7-19 cells per treatment; KWANOVA followed by Mann-
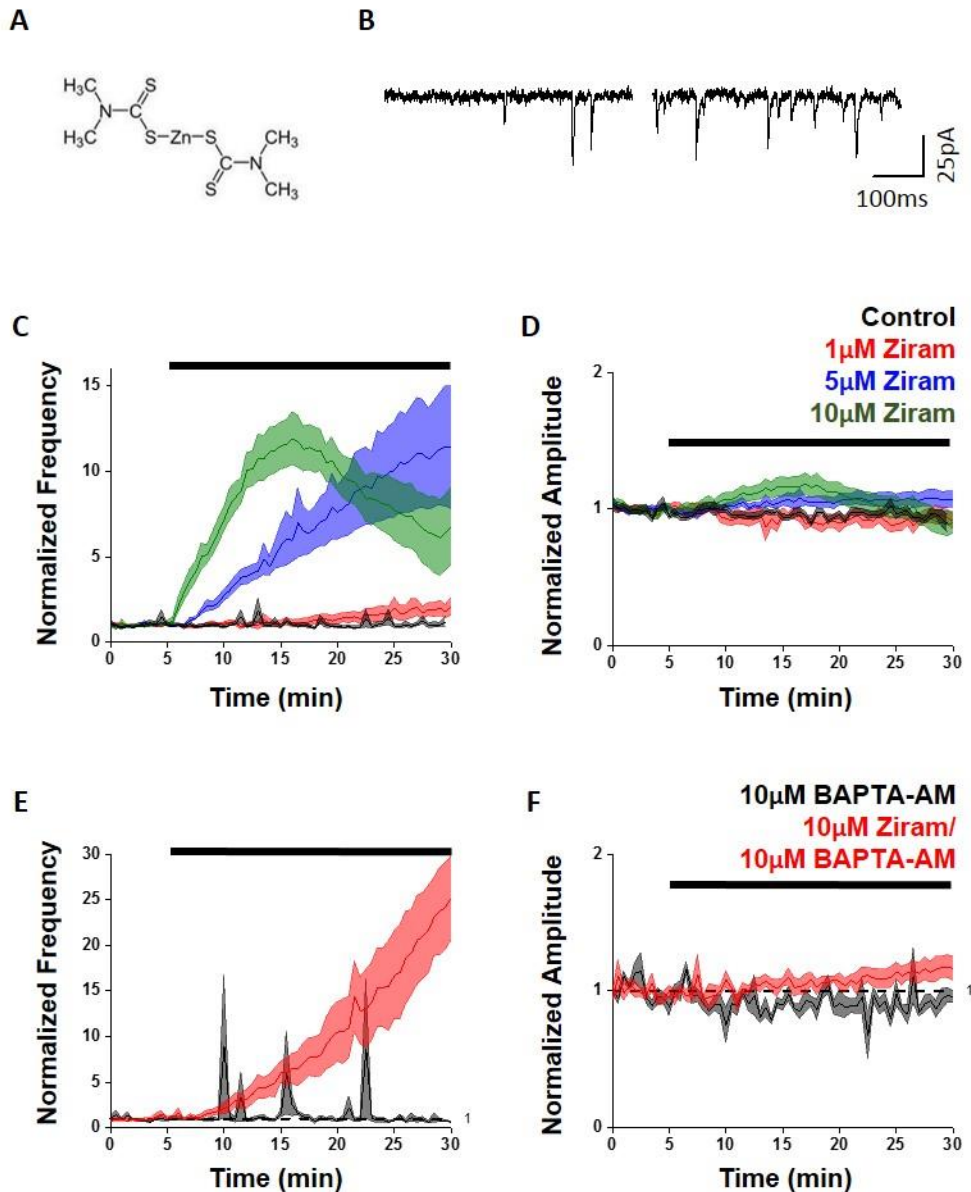
Figure 1. Ziram increases mini EPSC frequency in a dose-dependent manner. (A) Structure of ziram (B) mEPSC trace before (left) and after (right) application of 10μM ziram. (C) Normalized mEPSC frequency in increasing concentrations of ziram (D) Normalized mEPSC amplitude. In (C-D) Control trace is black, n=19; 1μM ziram is red, n=6; 5μM ziram is blue, n=7; 10μM ziram is green, n=7. (E) Normalized mEPSC frequency in the presence of 10μM BAPTA-AM (black trace, n=5) or 10μM BAPTA-AM and 10μM ziram (red trace, n=5). (F) Mini amplitude in 10μM BAPTA-AM (black trace, n=5) or 10μM BAPTA-AM and 10μM ziram. In all plots, the black bar indicates the presence of ziram. All values are mean ± SEM.

63

Whitney test, $p < 0.0001$). Following the large increase in 10μM ziram, the mini frequency declined until the end of the recording at 30 min to approximately 50% of peak. Neurons treated with 5μM ziram, on the other hand, showed a steady increase that continued to the end of the recording with a fold change of 11.44 ± 3.51 compared to controls at 1.13 ± 0.25 (Figure 1C; n = 7-19 cells per treatment; KWANOVA followed by Mann-Whitney test, $p < 0.0001$). Neurons exposed to 1μM ziram, like the 5μM condition, gradually increased and peaked at the end of the recording with a 1.81 ± 0.39 fold change (Figure 1C; n = 6-19 cells per treatment, KWANOVA followed by Mann-Whitney test, $p = 0.056$). We were intrigued by the decline in the highest concentration of ziram, which was not seen in the same time frame with the lower doses. This could be related to a desensitization, for instance as a constant influx of calcium, or alternatively there may be an additional target of ziram that is time sensitive, or reliant on effect of a primary target of ziram. Notably, the change in kinetics of 10μM on neuronal frequency in this time frame – as both increase and decline – as well as distinct changes in kinetics due to concentration could not be observed in experiments with long incubations of ziram; these may be important for understanding how different populations of neurons adapt and respond over time.

When comparing the amplitude of mini events, we observed that at the two higher concentrations of ziram tested there was a slight but significant increase in size at 15min (Figure 1D; 10μM ziram increased 1.15 ± 0.07 fold and 5μM ziram increased 1.06 ± 0.03 fold; n = 7-19 cells per treatment; KWANOVA followed by Mann-Whitney; $p = 0.008$ and $p = 0.028$) The amplitude between conditions was not different, however, at 25min recording (Figure 1D; n = 7-19 cells per condition; KWANOVA followed by Mann-Whitney, $p = 0.37$). While these changes were not as drastic as the changes in frequency, it was noted that the trend in 10μM followed a similar pattern of peak and decline, whereas 5μM gradually increased towards the end of the recording, and this could indicate a link between the two effects.

Calcium is not required for an increase in mini frequency with ziram

Calcium is intrinsically linked to the probability of synaptic vesicle release – and so mini frequency, and can also lead to sensitization at synapses. We next examined whether calcium could explain the robust changes in mini frequency, both increase and decrease, that we observed in recordings with 10μM ziram. To do so we bath applied the fast calcium chelator BAPTA-AM to our cultures, followed by ziram, and measured mini EPSC frequency as before. If calcium was necessary for the increase in minis, we would expect that applying ziram in the presence of BAPTA-AM would preclude a change in frequency. Further, if a calcium-induced effect led to the decline in frequency, this would similarly be prevented by treatment with BAPTA followed by ziram.

Cortical neurons were perfused for at least 30 minutes in 10μM BAPTA-AM prior to patch-clamp and recording of mini EPSCs. After recording a five minute baseline, the perfusion was switched to either 10μM ziram or vehicle in continued BAPTA-AM. When cortical neurons were exposed to ziram with BAPTA present, a robust increase in frequency was still observed (Figure 1E). Unlike neurons treated with 10μM ziram alone, the increase did not peak and decline but rather developed gradually and continued until the end of the recording. As before with various concentrations of ziram, we fit a curve to describe the change in mini EPSC frequency seen in both ziram and BAPTA. The kinetics were similarly fit with a 2nd degree polynomial (see Table 1). The absolute value of the β_2 coefficient for ziram/BAPTA treated neurons was 0.03 (0.028, 0.031) and this value fell between that of neurons treated with 10μM ziram and 5μM ziram. However, while the trend in 5 or 10μM ziram was to increase towards a maximum vertex, the curve fit for BAPTA/ziram increased away from a minimum vertex and there was no peak and decline observed in BAPTA/ziram during the time of recording.

Test Group	Equation	α mean	95% CI	β1 mean	95% CI	β2 mean	95% CI	Evaluated model	AIC value	Adj R²
CTR Frequency n=19	Linear $y=\alpha + \beta x$	0.93 ± 0.02	0.89, 0.97	$-5.45\text{E-}04 \pm 0.001$	-0.003, 0.002	--	--	Linear Exp Grw2 Polynomial	0.11 7.79 2.40	-0.01 -0.03 -0.01
1uM Ziram Frequency n=6	2nd degree polynomial $y=\alpha + \beta 1x + \beta 2x^2$	0.53 ± 0.16	0.14, 0.92	0.03 ± 0.02	-0.01, 0.07	$7.22\text{E-}04 \pm 4.53\text{E-}04$	-0.004, 0.001	Linear Exp Grw2 Polynomial	-89.50 -84.05 -89.65	0.93 0.93 0.94
5uM Ziram Frequency n=7	2nd degree polynomial $y=\alpha + \beta 1x + \beta 2x^2$	-2.40 ± 0.13	-2.71, -2.09	0.53 ± 0.02	0.47, 0.59	$-0.001 \pm 9.79\text{E-}04$	-0.004, 0.001	Linear Exp Grw2 Polynomial	-100.52 -94.49 -99.92	0.99 0.99 0.99
10uM Ziram Frequency n=7	2nd degree polynomial $y=\alpha + \beta 1x + \beta 2x^2$	-8.60 ± 0.48	-9.74, -7.47	2.06 ± 0.11	1.79, 2.32	-0.05 ± 0.006	-0.061, -0.033	Linear Exp Grw2 Polynomial	-10.80 -30.21 -39.65	0.99 0.98 0.99
10uM BAPTA/10uM Ziram Frequency n=5	2nd degree polynomial $y=\alpha + \beta 1x + \beta 2x^2$	0.23 ± 0.20	-0.29, 0.75	-0.12 ± 0.03	-0.20, 0.03	0.03 ± 0.001	0.028, 0.031	Linear Exp Grw2 Polynomial	-16.87 -134.91 -149.00	0.93 0.99 0.99
2uM Disulfiram Frequency n=5	2nd degree polynomial $y=\alpha + \beta 1x + \beta 2x^2$	1.04 ± 0.19	0.55, 1.52	0.01 ± 0.03	-0.06, 0.09	$0.002 \pm 9.56\text{E-}04$	-0.0002, 0.005	Linear Exp Grw2 Polynomial	-58.61 -53.89 -61.91	0.80 0.81 0.82
10uM Disulfiram Frequency n=5	2nd degree polynomial $y=\alpha + \beta 1x + \beta 2x^2$	0.12 ± 0.12	-0.20, 0.43	0.16 ± 0.02	0.10, 0.21	$0.003 \pm 7.48\text{E-}04$	0.001, 0.005	Linear Exp Grw2 Polynomial	-71.44 -75.84 -85.14	0.98 0.98 0.98

Table 1. Curve fitting of mini EPSC frequency kinetics.

Similar to ziram alone, the amplitude of minis trended towards a slight increase in ziram with

BAPTA compared to BAPTA alone that was significant at 15min (Figure 1F; n = 5 cells per treatment; Mann-

Whitney test, p = 0.016) but not at 25min (p = 0.22).

These findings indicate that calcium is not necessary for the increase in mini frequency that occurs

in neurons immediately following ziram exposure. Calcium does, however, change the kinetics of the

increase, and appears to be important for the decline in mini frequency seen within 25 minutes of ziram

exposure alone. The model fit to neurons in BAPTA/ziram suggests that the increase would continue on,

however a longer recording time would be necessary to confirm a link between calcium and the decline.

Even so, there is a relationship between the mini frequency kinetics and calcium, which may be due to

ziram acting directly on calcium channels or on intracellular calcium stores. Another possibility is that

ziram enhances excitability, and this leads to a depolarization of neurons which would affect influx of Ca^{2+}

through voltage-gated Ca^{2+} channels (VGCCs).

Ziram enhances excitability of cortical neurons

Measuring minis provides information primarily with regard to pre-synaptic and post-synaptic

changes in neurons. In the next set of experiments we wanted to determine whether ziram affected the

physiological properties, particularly the excitability of the neuron. Calcium is not altogether required for

spontaneous glutamate release, which is aptly demonstrated in the experiments described thus far, but

there is a crucially tight relationship between calcium concentration and release probability

(Schneggenburger and Rosenmund 2015). A subtle increase in calcium can lead to a precipitous change in

synaptic vesicle release probability, and this would be detected in mini frequency change. Further, calcium

can also lead to calcium-dependent inactivation of P/Q calcium channels (Lee, Wong et al. 1999, Lee,

Scheuer et al. 2000), and this which would lead to a decrease in spontaneous release possibly like that

seen in high doses of ziram. Importantly, changes in excitability of cortical neurons exposed to ziram can lead to changes in calcium flux. In order to measure excitability in our cultures we recorded the response of neurons to current injections while in a patch clamp orientation. In these recordings we patch-clamped cortical neurons, and applied a current for one second every 10 seconds to measure the properties of induced action potentials. After five minutes, ziram was added to the perfusion and the recordings continued for at least 25 min to measure any changes that occurred within an exposed neuron.

In this set of experiments we first determined whether there were changes in the baseline membrane potential, V_m, the potential prior to current injection. Control recordings and those treated with 10μM ziram came from similar populations with baseline V_m of -68.4 ± 1.3 mV and -68.9 ± 1.5 mV respectively (scatter plot in Figure 2B). In the cells treated with ziram, baseline V_m began to depolarize over time with a mean increase of 3.8 ± 1.1 mV at 25 minutes of recording. Although slightly larger than control cells, this did not differ significantly, where a mean increase of 1.6 ± 2.2 mV was measured at the same time (Figure 2B; n = 10-11 cells per treatment; Mann-Whitney test, p = 0.22). We did note that of the cells in ziram, 11 out of 12 showed a depolarization from initial baseline V_m to the end of recording while in control cells this was the case for 6 out of 11 cells. In ziram, two of the treated cells underwent a strong depolarization and the recording could not be continued to the full 25min duration. Beyond 25 min several more cells in ziram were 'lost' (could not be recorded from) and so we chose to compare action potential features at times up to 25min maximum. This may be due to the constant current injection (1s of current every 10s), the persistent nature of which is not necessarily physiological to these cells, and so while the control condition cells may adapt to constant current over time with some changes, the introduction of ziram as an additional 'stressor' to the depolarizing current may have prevented the cells from adapting properly over longer time. Thus, in the time between addition of ziram and when cells begin to reach this 'limit', we hoped to find clues to understand where ziram might be acting.
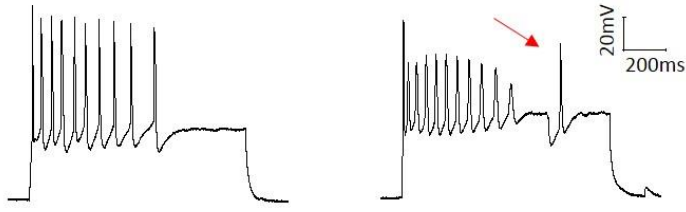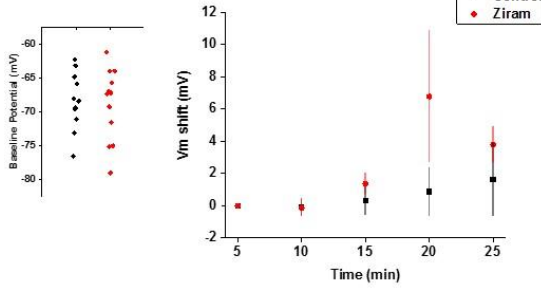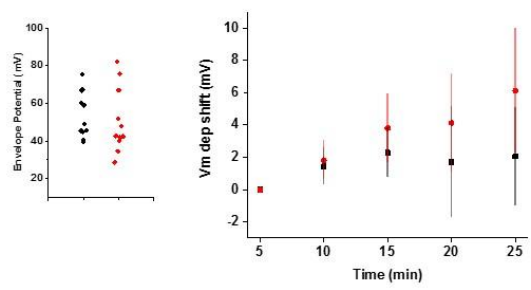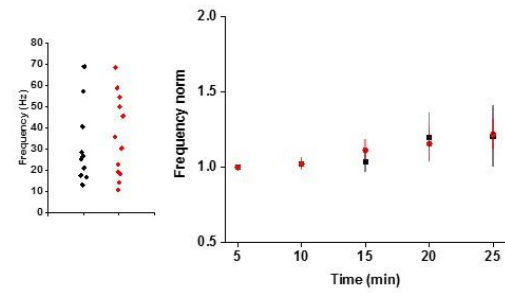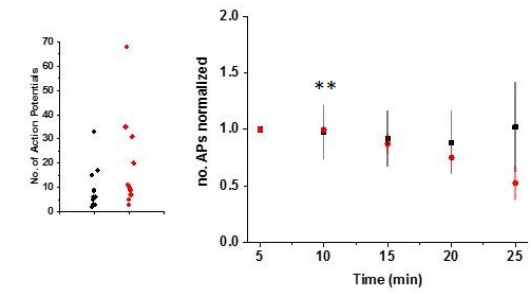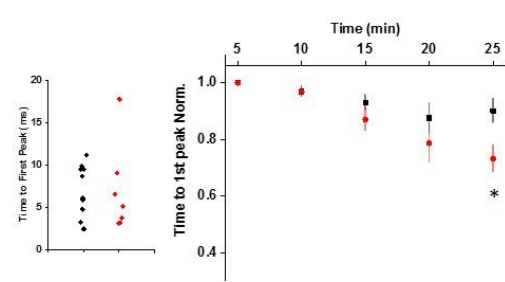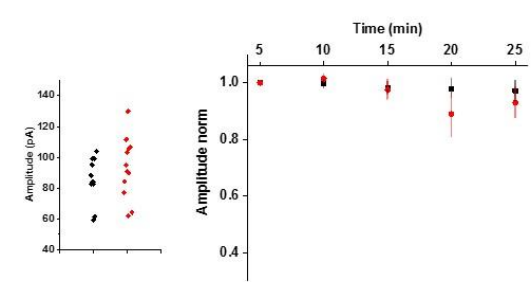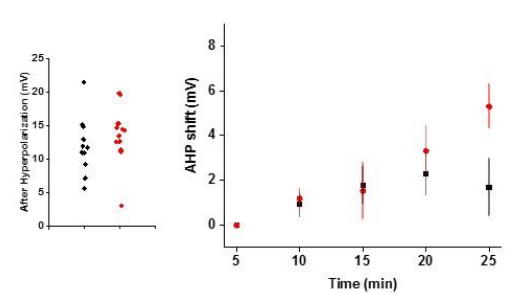
Figure 2. Ziram enhances excitability in cortical neurons. (A) Sample recording following 50pA of depolarizing current injection before (left) and after (right) 10µM ziram. Red arrow points to an action potential (AP) induced after an inhibitory potential (B-H) Properties of cortical neurons before and after addition of 10µM ziram or DMSO control. Left, scatter plot of data points for each experiment representing the median response in the first five minutes; right plot is the mean ± SEM of median values over 5 min intervals, and normalized the 5 min value. Ziram or vehicle is added at the 5 min mark. In ziram (red), n = 12 cells from separate coverslips and multiple cultures; for controls (black), n = 11 cells from separate coverslips and multiple cultures. (B) Values recorded for the baseline membrane potential, V_m (prior to current injection) indicate a depolarization in both ziram and control over time. The depolarization tended to be enhanced in ziram compared to controls, but was not significant. (C) Measurement of the depolarized envelope V_m, similar to (B) shows a trend towards greater values in ziram compared to control, but was not significant. (D) The frequency of APs due to depolarizing current increases in both control and ziram but was not different between the two. (E) The number of action potentials induced by current remains unchanged in controls; in ziram there is a small but significant enhancement at 10min, followed by a general decline. (F) The time to first action potential peak declines in controls, and significantly more so in ziram by 25 min. (G) Amplitudes of APs measured did not change between conditions over time. (H) Values of the afterhyperpolarization (AHP) decreased over time. In ziram, there was a non-significant but greater decline in AHP size.

As we noticed a trend toward a depolarized baseline V_m, we next compared the changes over time in the envelope V_m, the potential reached during the current injection. The initial values for the envelope V_m were varied, with a mean jump to 54.1 ± 3.7 mV in control cells compared to 51.8 ± 4.9 mV in cells that were subsequently exposed to ziram (Figure 2C). Similar to baseline V_m described above, we observed that ziram-treated cells trended towards a more depolarized envelope potential with time, although not significantly so when compared to control cells (Figure 2C; mean increase of 6.1 ± 3.8 mV in ziram at 25 min, 2.0 ± 3.0 mV in control at 25 min; n = 10-12 cells per condition; Mann-Whitney test, p = 0.65). We were surprised to find that the increase in membrane potential at baseline and the envelope potential after current injection did not reach significance, but we did note a large standard error in these measurements. This could be due to having sampled from a diverse neural culture, and as such this may have led to variable responses to ziram, as well as in control cells to long recording periods over which current was continuously applied.

During stimulation of neurons with depolarizing current we next measured the number and features of the elicited action potentials (APs) as indicators of excitability changes. In both control and ziram cells the instantaneous frequency varied, from approximately 10Hz to 70Hz (scatter plot in Figure 2D). There was a trend towards increased frequency over time, and this was similar in both the control and ziram condition (Figure 2D; n = 8-10 cells per treatment; Mann-Whitney test, p = 0.31). On the other hand, when examining the total number of APs this was increased at ten minutes into the recording with ziram-treated neurons (5min in ziram) (Figure 2E; n = 11-12 cells per treatment; Mann-Whitney test, p = 0.007), which corresponded to a similar time in which we observed increased mini frequency with 10µM ziram. Control cells did not vary as much in the number of APs throughout the recording while ziram-treated cells trended towards a decrease in total number by 25 min (Figure 2E; n = 8-10 cells per treatment; Mann-Whitney, p = 0.13). The decrease in AP number with ziram began at 15 min with a fold

change of 0.87 ± 0.09, and continued to decline to the end of recording to 0.53 ± 0.15 of baseline. We also note that this compares to a time at which we observe a decline in mini EPSC frequency with ziram.

In characterizing induced action potentials, we next measured the time to first peak. During the baseline of recording there was a mean time to peak of 6.7 ± 1.0ms or 6.9 ± 2.0ms initially in the controls and cells exposed to ziram, respectively (Figure 2F). After exposure to ziram, the time to peak continuously decreased, most prominently at 25min where ziram was reduced to 0.73 ± 0.05 of the baseline time compared with a slight decrease to 0.90 ± 0.04 of baseline in control (Figure 2F; n = 5-10 cells per treatment; Mann-Whitney test, p = 0.013). A faster time to peak may correspond to a smaller action potential amplitude, but this did not appear to be the case. The amplitude of induced APs was unchanged at 25min in ziram compared to control (Figure 2G; n = 7-10 cells per treatment; Mann-Whitney test, p = 0.60). As such, a shorter time to peak may be due to inhibition of a potassium current. Rapidly inactivating potassium current (IA) in part regulates the time to reach threshold, and inhibition of this current can decrease the time to peak (Turrigiano, Marder et al. 1996, Choi, Park et al. 2004). Potassium current is also critical to the after-hyperpolarization (AHP), and we next compared the AHP amplitude on the end of induced APs as a measure of excitability in our neurons. The mean size of the AHP was 12.0 ± 1.3mV in control cells and 13.5 ± 1.2mV in neurons pre-ziram (Figure 2H). In both conditions, there was a decline over 25 min in the size of the AHP, to 9.3 ± 1.3 mV in control and 8.7 ± 1.3mV in ziram. While the change was greater in overall in ziram, it was not significantly so in comparison with controls (Figure 2H; n = 7-10 cells per treatment; Mann-Whitney test, p = 0.07). Interestingly, a decline in amplitude of AHPs would also be consistent with an inhibition in potassium channels.

Although each of the physiological properties we measured varied across our cells, there was a clear trend towards baseline and envelope V_m depolarization as well as a decreased time to first peak and AHP size in those treated with ziram, all of which would suggest enhanced excitability of cortical neurons. The variability across experiments and condition may be due to diversity in the cultures, and while we did

not specifically notice distinct populations emerging in the measurements, this may suggest that ziram's effects on the physiology of neurons depended on the types and expression levels of ion channels present. Also consistently observed in cells treated with ziram were spontaneous action potentials after an induced burst, and typically following an IPSP (arrow, Figure 2A). This could be related to increased excitability in inhibitory neurons, and 'anode break excitation', wherein a brief hyperpolarization due to IPSP removes inactivation and allow neurons to elicit additional APs.

In the context of neurodegeneration and PD, these findings indicate that ziram may generally lead to enhanced excitability in neurons, and that certain subtypes are more susceptible to toxicity based on their intrinsic properties e.g., the expression and properties of ion channels.

Other dithiocarbamate pesticides rapidly increase mini EPSC frequency

In considering the relationship between PD risk and exposure to ziram, characterizing the physiological effects of the drug will be useful to gain insight on the development of pathology in the nervous system. However, ziram is typically one of many toxins that agricultural workers and others may be exposed to. Of these toxins, there is variability in chemical properties and possibly in physiological targets; as such it will be important to group these commonalities in order to properly guide usage so as to protect the health of those most at risk for exposure. A number of other pesticides have been implicated in PD, including maneb and paraquat (Wang, Costello et al. 2011), and we wanted to determine whether there was a common link between the structure or targets of these pesticides. The most robust measure of ziram's effect was a rapid increase in mini frequency, so we chose to use this as an assay. In addition to maneb and paraquat, we examined two other pesticides: dieldrin and benomyl, both of which have been shown to affect similar cellular pathways as ziram, including the ubiquitin-proteasome system

and aldehyde dehydrogenase (ALDH) enzymatic activity (Wang, Li et al. 2006, Fitzmaurice, Rhodes et al. 2014). The structures and classes of each of the chemicals tested are shown in Figure 3.

We voltage clamped cortical neurons and recorded mini EPSCs as described before in ziram. Each of the four toxins, maneb, paraquat, dieldrin and benomyl, were applied to cells after a 5 minute baseline. A concentration of 10µM was chosen to test each pesticide as ziram had the strongest effect at this dose, and as ziram, benomyl and dieldrin have been shown to inhibit the proteasome as well as ALDH at this concentration (Wang, Li et al. 2006, Fitzmaurice, Rhodes et al. 2014).

Of the four pesticides, the dithiocarbamate maneb demonstrated a rapid increase of 2.5 ± 0.4 fold in mini EPSC frequency within 15min of recording (Figure 3A; n = 5-19 cells per treatment; KWANOVA followed by Mann-Whitney, $p < 0.0001$). The increase in mini frequency in maneb was maintained throughout the recording although a slight decrease at 25 minutes (2.20 ± 0.23 fold) was suggestive of the ziram induced decrease. Paraquat, which is structurally related to MPP+ and like the other pesticides has been linked to an increased risk of PD, led to a slight but non-significant decrease in mini-frequency at the end of the recording (Figure 3B; decrease of 0.61 ± 0.13 at 25 min; n = 5-19 cells per treatment; KWANOVA followed by Mann-Whitney, $p = 0.16$). Dieldrin and benomyl on the other hand both triggered a small but significant increase in frequency only towards the end of the recording at 25 min (Figure 3C-D; dieldrin increased frequency 1.9 ± 0.2 fold; benomyl increased frequency 1.3 ± 0.1 fold; n = 6-19 cells per treatment; KWANOVA followed by Mann-Whitney, $p=0.001$ and $p=0.04$ respectively). None of the pesticides tested had a significant effect on mini amplitude compared to control at either 15min or 25min (Figure 3A-D; n = 5-19 cells per treatment; KWANOVA followed by Mann-Whitney, $p \geq 0.15$).

Of the four pesticides, all but paraquat led to an increase in mini frequency; however, the increase in dieldrin and benomyl was more subtle and appeared at the end of recording. Maneb, similar to ziram, led to a rapid increase within five minutes of exposure. Maneb and ziram are both dithiocarbamate
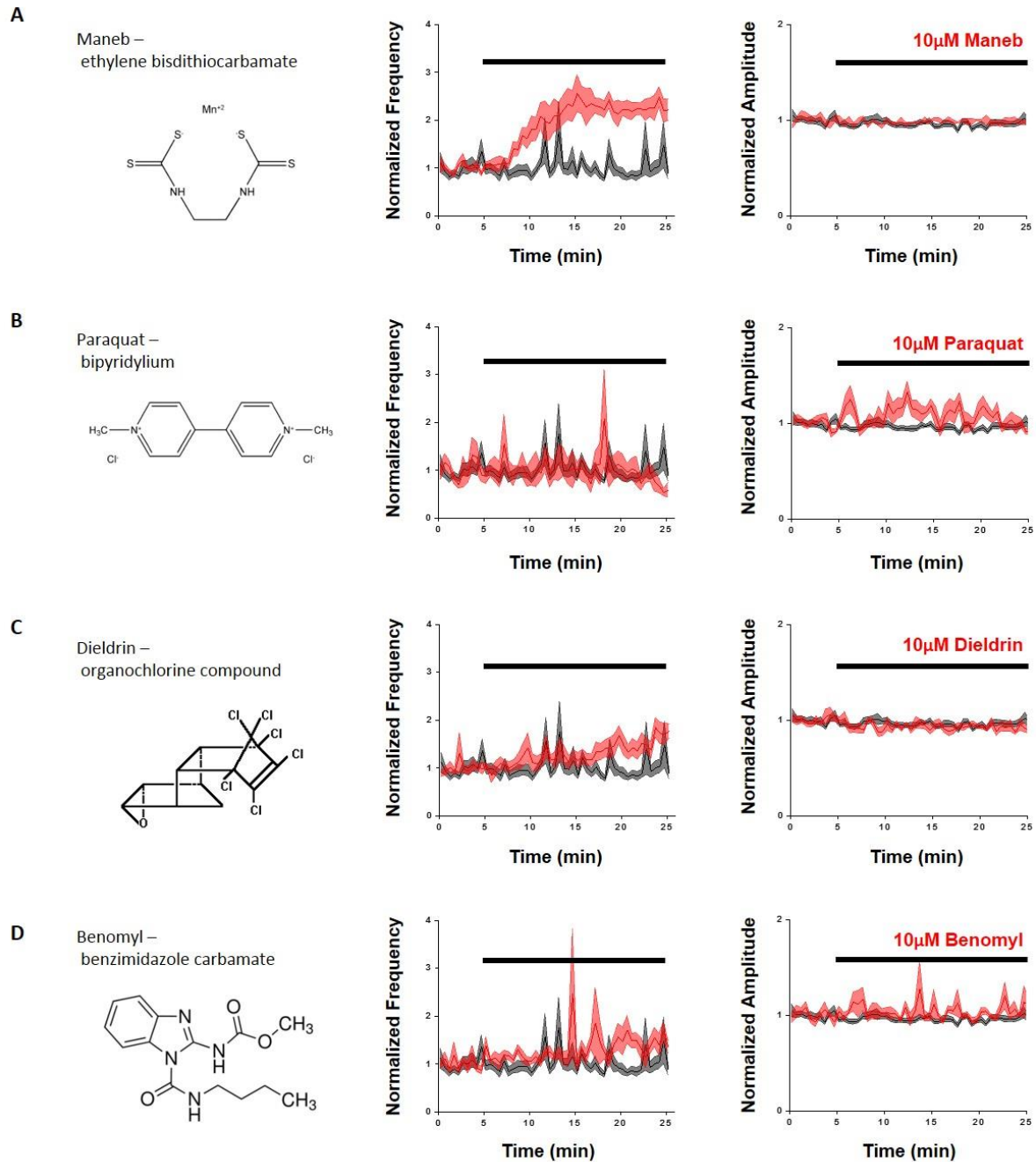
Figure 3. Pesticides linked to PD risk increase mini EPSC frequency. Cortical neurons were treated with various other pesticides in order to measure acute changes in properties of mini EPSCs. (A-D) chemical structures are on the left, in the middle is the normalized mini frequency, and on the right is the normalized mini amplitude. All plots contain the mean ± SEM from each experiment; within an experiment the medians of 30s bins was measured. For all conditions, n = 5 to 19 cells from different coverslips and

multiple cultures. The black bar above the plot represents the time in drug or vehicle; black traces are controls while red traces represent experiments with pesticide. (A) Application of 10µM maneb to cortical neurons leads to a significant increase in mini frequency, but not mini amplitude compared to controls. (B) In 10µM paraquat there is a slight but not significant decline in mini frequency at the end of recording. Although there was variability in the amplitude of mini EPSCs with paraquat, this was not significantly different from controls. (C-D) Dieldrin and benomyl (10µM) both led to a small but significant increase in mini EPSC frequency by the end of 25min recording, but no change in mini EPSC amplitude.

pesticides, which could offer a common link in their rapid physiological effects. To test whether dithiocarbamates could specifically trigger a rapid increase in minis, we performed the same experiment with the drug disulfiram (DSF). DSF is a dithiocarbamate closely related to ziram in structure (Figure 4A), and has been indicated for alcoholics due its inhibitory action against ALDH (Seneviratne and Johnson 2015). Disulfiram (DSF) is a potent ALDH inhibitor at low concentrations (IC_{50} =10nM (Vasiliou, Malamas et al. 1986, Keung and Vallee 1993)) as well as an inhibitor of the proteasome at higher concentrations (IC_{50} = 7.5μM (Wang, Zhai et al. 2011)), so we were interested to determine the effects of both low (2μM) and high (10μM) concentrations, which may distinguish the two pathways.

As with ziram and maneb, we found that application of DSF at 10μM led to a rapid increase in mini frequency, while at the lower concentration of 2μM the increase was more gradual. At 15 min of recording the increase in mini frequency was 1.41 ± 0.31 times greater than baseline for 2μM and 3.02 ± 0.76 times baseline for 10μM DSF (Figure 4A; n = 5-19 cells per treatment; KWANOVA followed by Mann-Whitney, 10μM DSF p < 0.0001, 2μM DSF p = 0.06). By 25min, both concentrations led to a significant increase in mini frequency (2.65 ± 0.95 fold for 2μM, p=0.007 and 6.10 ± 1.21 fold for 10μM, p < 0.0001). The changes appeared similar to those of ziram, and we modeled the kinetics in a similar manner to compare the two concentrations to each other and to ziram (see Table 1). In both 2μM and 10μM, the change in frequency was best fit with a 2nd degree polynomial, with β_2 values of 0.002 ± 9.56E-04 (-0.0002, 0.005) and 0.003 ± 7.48E-04 (0.001, 0.005), respectively. These are both most similar to the absolute value of β_2 in 5μM ziram, and while they appear to act on cells in a dose-dependent manner, the two concentrations of DSF overlap in 95% CI, indicating they are not significantly different from one another. In both concentrations of DSF the sign of β_2 was positive, which was in contrast with the 5 and 10μM effects in ziram. Thus, while highly similar in to ziram in structure and in the rapid onset of mini frequency increase, there were differences in the kinetics and concentration-dependent effects of the DSF on neurons. Neither 2μM nor 10μM DSF
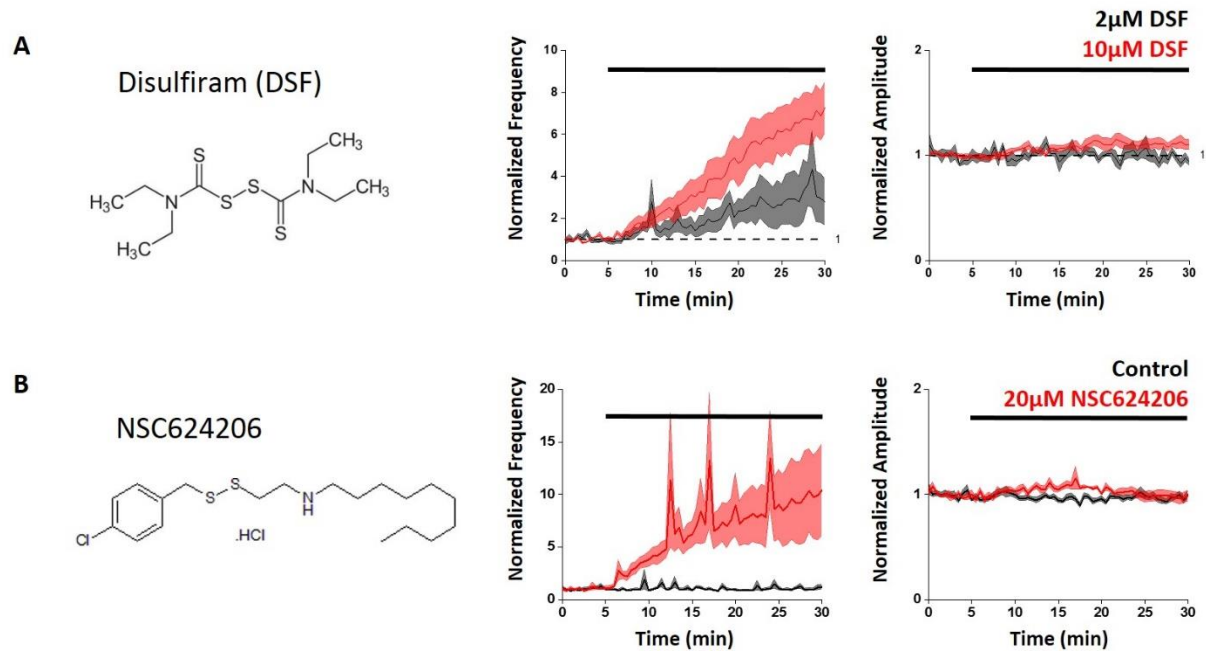
Figure 4. Disulfiram, a dithiocarbamate similar in structure to ziram, and NSC624206, an E1 inhibitor both increase mini EPSC frequency. Minis were recorded from neurons treated with disulfiram (DSF) or the E1 inhibitor NSC624206. (A-B) chemical structures are on the left, in the middle is the normalized mini frequency, and on the right is the normalized mini amplitude. All plots contain the mean ± SEM from each experiment; within an experiment the medians of 30s bins was measured. For all conditions, n = 5 to 19 cells from different coverslips and multiple cultures. The black bar above the plot represents the time in drug or vehicle. (A) Application of 2μM (black trace) or 10μM (red trace) DSF to cortical neurons leads to a significant increase in mini frequency, but not mini amplitude compared to control. (B) In 20μM NSC624206 there is a substantial increase in mini frequency during the recording, including occasional high frequency peaks. There was a significant increase in mini amplitude with NSC624206 at 15 min but not 25 min compared to controls.

led to a change in mini amplitude at either 15min or 25 min (Fig 4C; n = 5-19 cells per treatment; KWANOVA followed by Mann-Whitney, p = 0.24).

Each of the dithiocarbamates (ziram, maneb and DSF) tested led to a strong increase in mini EPSC frequency that began within five minutes of exposure, despite having differences in the precise pattern of that increase. This may indicate a common molecular target, and one which is closely related to pre-synaptic vesicle release probability. Dithiocarbamates share the property of having a carbon atom attached to an amine group and two sulfur atoms, and these two sulfur atoms are important for the reactivity of these chemicals. The two bound sulfur atoms lead to dithiocarbamates being efficient metal chelators, as well as thiol-reactive and capable of acting on exposed cysteine residues. Strong lipophilic properties allow for membrane permeability, and so it may be no surprise that dithiocarbamates would affect intracellular pathways (Hogarth 2012, Mathieu, Duval et al. 2015). We next sought to determine whether we could find a common molecular target of the dithiocarbamates we had found to have a common physiological impact.

Dithiocarbamates and E1 ubiquitin activating enzyme

Dithiocarbamates share common structural properties, and thus likely common molecular targets – at the least with respect to the effects we described on mini EPSC frequency. One common target between the toxins we have tested is ALDH. DSF has been shown to inhibit this enzyme at a critical cysteine residue in the active site (Veverka, Johnson et al. 1997), and along with benomyl these two chemicals should have the most potent effect on ALDH of those we examined (the IC_{50} for benomyl inhibition is 140nM) (Fitzmaurice, Rhodes et al. 2013, Fitzmaurice, Rhodes et al. 2014). However, we see the strongest effect in our assay for minis with 10μM ziram (and not benomyl or DSF); thus we wanted to examine another pathway of which ziram is a potent inhibitor: the ubiquitin proteasome system (UPS).

Of the pesticides we examined in this study, all but paraquat have been shown to disrupt the UPS. Ziram, dieldrin, benomyl and DSF inhibit proteasomal activity at 10μM concentration, and maneb at a higher concentration of 20μM (Wang, Li et al. 2006, Chou, Maidment et al. 2008). Ziram has been found to do so by directly inhibiting activity of E1 ubiquitin activating enzyme, the first enzyme of three required for the conjugation of ubiquitin to substrate proteins in the pathway. The inhibitory activity of ziram is due to disruption of a thioester bond between E1 and ubiquitin prior to transfer of ubiquitin to E2 enzyme (Chou, Maidment et al. 2008). Previous work has implicated a link between E1 and the proteasome in modulating mini EPSC frequency in hippocampal neurons (Rinetti and Schweizer 2010). We thus wanted to determine whether E1 enzyme could be a common target for the dithiocarbamates found here to enhance mini EPSC frequency.

One method for measuring inhibition of E1 is by western blot to detect the presence of bands corresponding to E1 enzyme as well as E1 conjugated to a single ubiquitin (Ub), 8kD larger in size (Haas, Warms et al. 1982, Chou, Maidment et al. 2008). When cells are treated with ziram, this leads to reduction of the E1-Ub thioester bond and this is seen directly as a depletion of the larger E1-Ub band with respect to the E1-only band on a western blot (Chou, Maidment et al. 2008). To test whether other dithiocarbamates could disrupt E1 in a similar manner, we treated cultured cortical neurons with one of the following: ziram, maneb, DSF or NSC624206. NSC624206 is an E1 inhibitor that was used as a control, and that we found to similarly enhance mini EPSC release (Figure 4E) (Ungermannova, Parker et al. 2012). Neurons were exposed to each drug for 15min, following which the whole cell lysate was probed with antibody against E1 enzyme. As described previously, treatment with ziram led to a depletion of the E1-Ub band relative to that of control (Figure 5). On the other hand, we were surprised to find that the published E1 inhibitor NSC624206 did not lead to a decreased level of E1-Ub band. Neither DSF nor maneb led a depletion of E1-Ub, but instead both conditions consistently led to a 'third' band of E1 which has not been described before in a western blot (arrows in Figure 5). Further, treatment with maneb, DSF or
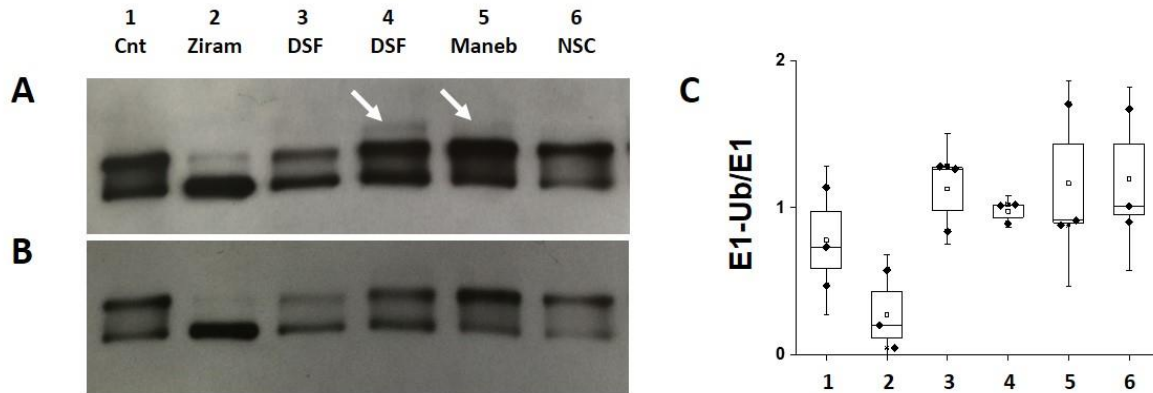
Figure 5. Dithiocarbamates modify E1 ubiquitin activating enzymes. Cortical neurons were treated with one of the following for 15 min: (1) 0.1% DMSO control, (2) 10μM ziram, (3) 2μM DSF, (4) 10μM DSF, (5) 10μM maneb, or (6) 20μM NSC624206. Cell lysates were probed via western blot for E1 enzyme, which appears as two bands under control conditions. The lower band is E1 enzyme and the higher band represents E1 bound to a single ubiquitin. (A-B) are different exposures of a representative blot where (A) is the longer exposure demonstrating the presence of a 'third' band (white arrows) in higher concentration of DSF (4) and in maneb (5); (B) shows an exposure used for quantification. (C) The ratio of single-ubiquitin conjugation (E1-Ub) to E1 is shown for the various conditions over separate experiments (n = 3 different cultures). The E1-Ub band is diminished in ziram (2) but appears to be more stable in DSF (3, 4), maneb (5) and NSC624206 (6) compared to controls. Box plots show SE and median, the whiskers represent SD, open squares are the mean values and solid diamonds show the individual data points.

NSC624206 led to a small but not significant increase in the ratio of E1-Ub to E1 band compared to control (Figure 5; n = 3 cultures per treatment; KWANOVA, p = 0.14).

The third E1 band that we observed in the presence of 10μM DSF or maneb is very close to the size that would be expected with two ubiquitins conjugated to E1 enzyme. Although a third band has not described previously using a western to probe E1, the chemical reaction between activation of ubiquitin by E1 enzyme and transfer of ubiquitin to E2 has been carefully mapped out. There is a step during which E1 is conjugated to both an adenylated ubiquitin and a thioester-ubiquitin (Haas and Rose 1982, Haas, Warms et al. 1982). Immediately following this step, the thioester-ubiquitin is transferred to E2 and adenylated ubiquitin takes its place. Compellingly, dithiocarbamates can modify cysteine residues either with a single mixed disulfide (adduction), or via stabilization between two sulfides (Mathieu, Duval et al. 2015); further, maneb and DSF have previously been shown to be able to dimerize proteins (Papaioannou, Mylonas et al. 2014, Roede and Jones 2014). Thus, it is likely that treatment of our neurons with either maneb or DSF leads to a stabilization – possibly via dimerization – of two ubiquitin molecules bound to E1. Based on our observations, we find that modification of E1 enzyme is common to dithiocarbamates, and that the nature of modification varies by structure of the chemical acting on E1.

Dithiocarbamates, but not an E1 inhibitor, induce activity in aminergic neurons

We found that E1 enzyme is a common molecular target among dithiocarbamates, and that increased spontaneous vesicle release at excitatory synapses is a common physiological phenotype. The properties of APs in neurons treated with ziram suggest that ion channels are likely to be additional targets, and further considering the reactivity of dithiocarbamates, there are likely more cellular targets yet to be described.

One effect of ziram which has recently been described is a depolarization-induced firing in aminergic neurons at the *Drosophila* larval neuromuscular junction (NMJ) (Martin, Myers et al. 2016). In these experiments, properties of release in both glutamatergic and octopaminergic neurons expressing the fluorescent calcium indicator GCaMP6 were examined. Interestingly, of the two neuronal types, the octopaminergic, but not the glutamatergic neurons, fired spontaneous calcium peaks in the presence of ziram. The calcium peaks were blocked by addition of TTX, indicating that they were depolarization-sensitive. Intriguingly, these experiments demonstrate a differential sensitivity of types of neurons which may relevant to PD. We were thus interested in whether the target(s) of ziram which leads to spontaneous calcium peaks in aminergic neurons would be common to other dithiocarbamates.

In order to test the hypothesis that dithiocarbamates lead to spontaneous firing in octopaminergic neurons, we examined the effects of DSF, as well as the E1 inhibitor NSC624206, on the *Drosophila* larval NMJ. We chose DSF, as it had a robust effect on mini frequency, and NSC624206, as it is an E1 inhibitor and has reactive properties similar to dithiocarbamates, acting on E1 via disulfide bond (Ungermannova, Parker et al. 2012). For these experiments, we used third instar larvae expressing GCaMP6 under a promoter specific to octopaminergic neurons. To image the NMJ, larvae were dissected so that the body wall muscles were exposed and the ventral ganglion was severed (Jan and Jan 1976). Following the dissection and before application of drug, an initial recording of GCaMP6 was performed in a haemolymph-like solution, HL3.1 (Feng, Ueda et al. 2004). No change in fluorescence was observed in octopaminergic nerve endings at the NMJ during baseline recordings (Figure 6, top traces). When ziram was applied to the prep, robust fluorescent peaks were observed within ten minutes, similar to previously published work (Figure 6A; 8.9 ± 2.2 peaks per min) (Martin, Myers et al. 2016). We next tested whether DSF could induce a similar spiking in terminals. The larval prep was initially imaged at ten minutes following exposure to DSF, however at this time point no change in GCaMP6 signal was seen (data not shown). The same larval prep was imaged again at 15, 20 and 25 min, and starting at 20 min and continuing
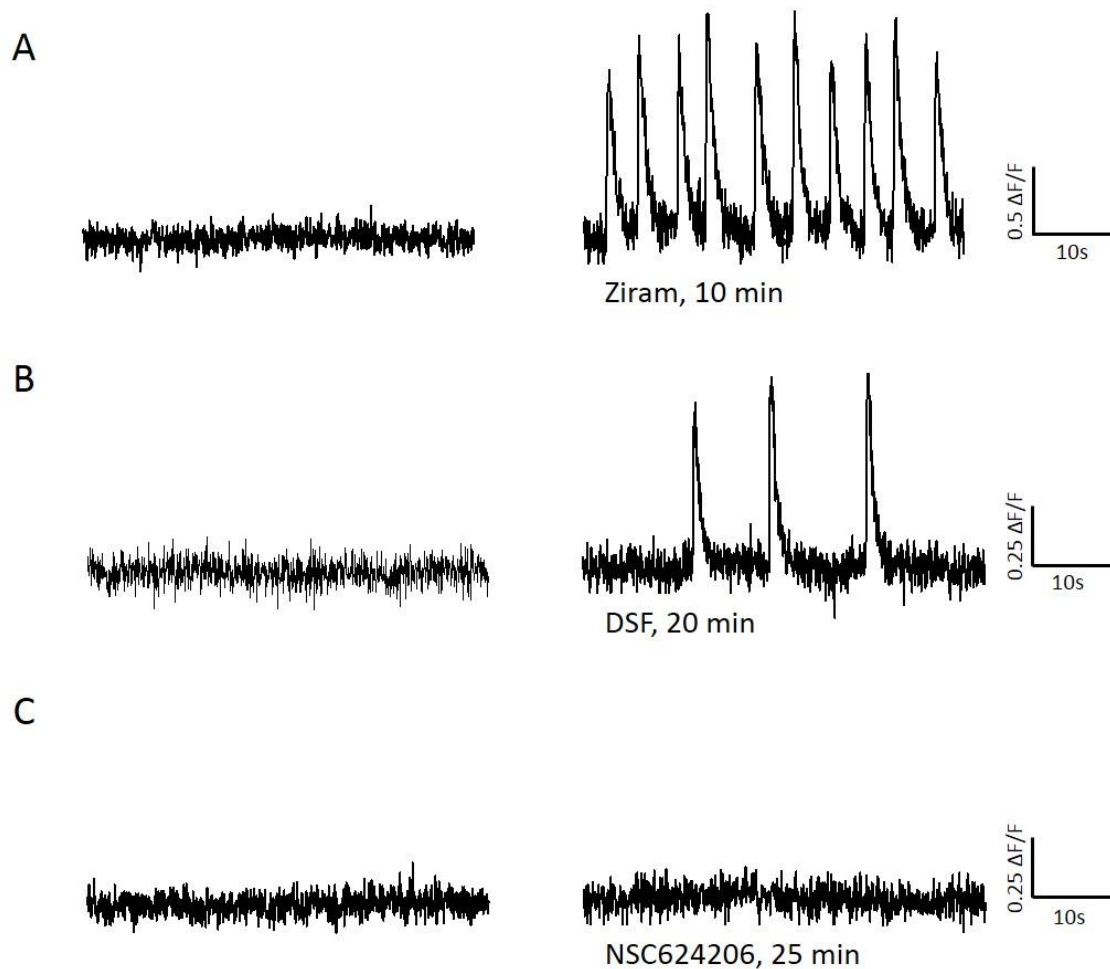
Figure 6. Dithiocarbamates ziram and DSF induce spontaneous calcium transients in octopaminergic neurons. *Drosophila* larvae expressing GCaMP6 in octopaminergic neurons were dissected to expose the body wall muscles and nerve endings; the NMJ was subsequently exposed to either 20μM ziram, 20μM DSF or 20μM NSC624206. (A-C) Representative ΔF/F traces shown on the left are imaged immediately before addition of drug. Traces on the right represent the same nerve ending at the indicated time in drug. (A) Exposure to ziram consistently led to spontaneous calcium peaks within ten minutes. (B) Preparations treated with DSF showed spontaneous peaks by 20 or 25min, although at lower frequency than that of

ziram. (C) NSC624206 did not induce peaks in octopaminergic neurons within 25 min of exposure. For all

experiments, n = 5 different preparations.

at 25, firing was observed in octopaminergic neurons exposed to DSF (Figure 6B). Interestingly, the firing not only began later than in the preps treated with ziram, but the frequency of spiking was lower as well (3.1 ± 1.5 peaks/min at 20min, 3.4 ± 0.7 peaks/min at 25min) In one instance, there was no firing at 20 min in DSF but only at 25min. We finally examined whether NSC624206 would lead to an induction of firing in the same prep, either by blocking E1 or possibly another target common with dithiocarbamates. However, in the presence of this inhibitor no spontaneous firing was observed throughout 25 min of recording (Figure 6C).

In the previous study performed by Martin et al. (2016) E1 RNAi was used to demonstrate that the effects of ziram on the NMJ were independent of this target. Our results with NSC624206 were consistent with this finding, and we also noted that the presence of sulfhydryl groups in this inhibitor did not confer similar effects as the dithiocarbamates ziram and DSF. We find it intriguing that the effect of DSF differed from ziram in the time of onset (20 minutes versus 10 minutes), as well as in the frequency of events. These data, along with the changes in minis, further support the finding that dithiocarbamates have similar physiological effects, and that there is inherent variability in these effects. Further, as indicated by the variability in E1 modification, this may be due to subtle changes in the reactivity of chemicals in the dithiocarbamates family.

Discussion

There is a robust body of evidence to support the contribution of environmental toxins to the etiology of Parkinson's disease. However, there are a number of classes and types of pesticides which are thought to be related to the increased risk, and extensive characterization of toxicity and the common properties between different chemical structures is lacking. In this study, we first examined the effects of ziram on the physiological activity of cortical neurons. We chose ziram as it is heavily used – the EPA

estimates that 2 million pounds are used annually – and as exposure has been found to lead to higher risk of PD (Wang, Costello et al. 2011, Rhodes, Fitzmaurice et al. 2013).

In experiments where we measured miniature EPSCs in cortical neurons treated acutely with ziram, we found that exposure to the toxin led to enhanced spontaneous release in a dose dependent manner, and at the highest dose tested the effect peaked and declined. The concentration-dependent changes may be an important consideration in the relationship between cumulative exposure and the onset of PD. Epidemiological studies have found that PD risk is related to frequency, duration and the cumulative time of exposure to pesticides (Brown, Rumsby et al. 2006, Hancock, Martin et al. 2008). In our measurements of minis with ziram, we found that the onset of the increase occurred within 5 minutes in 5 or 10μM doses, and nearly 25 min in the 1μM dose. It's not clear whether cells would eventually adapt to these changes, or if the rapid stressor would be enough to induce cell death. Although other studies have shown decreased viability and eventual death with long, continuous exposure to ziram (from 6hrs to 1 week) (Sook Han, Shin et al. 2003, Wang, Li et al. 2006, Chou, Maidment et al. 2008) it's not clear whether a short exposure would do the same. Most likely, those that spray pesticides or live near an area where spraying occurs are exposed in brief bursts, and over several iterations. In our hands, we found that within a rapid time-frame (5 to 25 min) there were robust changes in spontaneous activity with ziram, in a concentration dependent manner, which may be relevant to understanding early precipitating factors for PD.

The frequency of mini EPSCs is used as a proxy for spontaneous release probability, and the release probability in turn is intrinsically linked with the local Ca^{2+} concentration. We found that in cells buffered with the fast Ca^{2+} chelator BAPTA-AM, ziram still led to a frequency increase, but the kinetics were altered. We no longer observed the peak and decline with 10μM ziram, and instead the frequency was continuously enhanced. This indicated to us that the frequency increase was independent of Ca^{2+}, but the kinetics were not. One possibility is that the activity of one or more targets of ziram are dependent on

the local concentration of Ca^{2+} inside of cells, but that the Ca^{2+} levels were not altered by ziram. Alternatively, ziram may lead to an increase in calcium influx or release from calcium stores. In studies using heterologous cells treated with ziram, increases in intracellular calcium have been reported (Sook Han, Shin et al. 2003, Jin, Lao et al. 2014). Ziram has also been described to produce depolarization-dependent calcium peaks in aminergic neurons (Martin, Myers et al. 2016). In our experiments, an increase in intracellular Ca^{2+} with exposure to 10µM ziram would be expected to enhance mini frequency, and at high enough concentration subsequently lead to desensitization (e.g., Ca^{2+} dependent inactivation of Ca^{2+} channels) and a decline in frequency; this is precisely what we observed in 10µM ziram without BAPTA. This would support the hypothesis that there was an enhancement in intracellular Ca^{2+} when ziram was present, and importantly may indicate further downstream second messenger effects and excitotoxicity as a result.

In characterizing the physiology of our neurons, we also found that 10µM ziram led to a general enhancement of excitability; although these measurements were not always statistically significant, there was a consistent trend towards depolarization in membrane potential and envelope potential, as well as a decreased time to peak and AHP size. Of these, the decreased time to peak was significantly altered compared to control conditions. These results could be due to a single ion channel as a target of ziram, or multiple targets. A change in baseline V_m may be due to inhibition of a channel open at rest; e.g. inhibition of a potassium channel, or enhancement of inward current through a non-selective cation channel as suggested by Soon Han et al (2003). Inhibition of K^+ channels may cause the observed changes in envelope potential and AHP, and fast inactivating K^+ current (IA) importantly underlies the time to peak. It is also possible that ziram exposure leads to the opening or enhanced conductance of a channel with depolarizing effects that is not normally open at rest, e.g. voltage gated Na^+ or Ca^+ channels, or that it prevents repolarization of the membrane via Na^+/K^+- ATPase or the Na^+/Ca^{2+}-exchanger, the latter of which was implied by the Jin et al. study (2014). Although determination of the ion channel or channels

which may be targets of ziram would require extensive follow up, the indication that depolarization occurs is important in the context of our findings with calcium, as well as with aminergic neurons in *Drosophila*. First, if ziram does indeed to lead to depolarizing effects, this would likely explain an increase or enhancement of calcium via voltage-gated channels – either as a direct or indirect target. Second, as we describe here and was previously published (Martin, Myers et al. 2016), aminergic neurons spontaneously fire when exposed to ziram, and the effects are blocked by the Na^+ channel inhibitor TTX. It is possible that some level of depolarization occurs in most or all neurons with ziram, and that depending on the individual properties of neurons, this would result in more or less excitotoxicity. These properties are important considerations in the development of PD, in which selective cell types, including but not limited to dopaminergic, and adrenergic neurons are affected.

We demonstrated in this study that ziram leads to consistent physiological changes in neurons. Additionally, we sought to determine whether and how these effects might be grouped among other pesticides with a link to PD risk. Of the tested pesticides – maneb, paraquat, benomyl and dieldrin – only paraquat did not lead to an increase in mini frequency. Interestingly, these three chemicals, but not paraquat, have been found to indirectly inhibit proteasome activity as well as ALDH enzymatic activity (Wang, Li et al. 2006, Fitzmaurice, Rhodes et al. 2014). Of the three, maneb led to a rapid increase of in frequency of greater than two-fold within five minutes, while benomyl and dieldrin increased the frequency by less than two-fold within 20 min. As maneb and ziram both led to a similarly rapid increase, and both are dithiocarbamates, we tested the effects of another dithiocarbamate, DSF, on mini EPSCs. We found that at two concentrations (2 and 10μM), DSF also led to an acute increase in mini frequency within five minutes. DSF, a drug given to alcoholics for its inhibitory activity against ALDH, has also been found to inhibit the UPS. In comparing results among the chemicals tested, we found that those which inhibited the proteasome and ALDH increased mini frequency, and that the dithiocarbamates had the most pronounced effects (largest amplitude and shortest time of onset).

The rapid effects and common targets of dithiocarbamates may be due to their reactive chemical nature; dithiocarbamates are known to be thiol-reactive and act as metal chelators via the presence of two disulfide bonds. Interestingly, in spite of those similarities and the common targets, we found evidence that there was variability in precisely how the targets were altered; this could presumably lead to some of the differences in kinetics and amplitude of effects that we see in minis. As an example of the variability in target modification, we found that neurons treated with either ziram, maneb or DSF differentially altered E1 enzyme. With ziram, the amount of thioester-ubiquitin was greatly reduced, while maneb and DSF appeared to stabilize the thioester-ubiquitin and an additional bond which could represent adenylated-ubiquitin. Interestingly, when we examined the effects of the published E1 inhibitor NSC624206, we neither observed a decrease in thioester-ubiquitin nor a third band. In the work describing the discovery and characterization of the chemical, the authors found that NSC624206 can interfere the thioester bond as well as block the transfer of ubiquitin from E1 to E2, and that this was due to the presence of a disulfide bond in the structure (Ungermannova, Parker et al. 2012). In their experiments they used purified proteins, whereas in our cells E1 may already be pre-loaded with ubiquitin; thus we may not have seen a decrease in the E1-ubiquitin bond if the disruption was primarily in transfer of E1 and E2. Interestingly, it appears that of the thiol-reactive chemicals tested (including NSC624206) there were clear differences in the type of modification. Further support for this notion comes from a recent study with maneb demonstrating thiol reactivity against human thioredoxin-1 (Trx1); in this work the authors found that Trx1 could be modified in variable ways. Mass spectrometry was used to show that maneb adducts a single cysteine residue in Trx1, while x-ray crystallography indicated that maneb treatment led to dimers of the protein via cysteine residue. Another example of variation in thiol-reactivity is in the modification of BK channels by cysteine modifying agents. The same residue in the RCK1 domain is modified by MTSET, MTSES and NEM leading to changes in Ca^{2+} or voltage-dependent gating. When treated with MTSET, gating is shifted to more negative potentials, while in the other two it is shifted to

more positive potentials; the effects also varied depending on the amount of Ca^{2+} present and the voltage (Zhang and Horrigan 2005). Our experiments here indicate that dithiocarbamates likely have similar targets, and support that these targets are differentially modified – and this may lead to variability in the kinetics or nature of the physiological outcome.

Finally, we demonstrated in this study that dithiocarbamates, but not necessarily chemicals with thiol reactivity, can lead to spontaneous calcium transients in aminergic neurons of the *Drosophila* NMJ. Both ziram and DSF, but not NSC624206 induced these effects within 25 min of exposure in *Drosophila* larvae expressing GCaMP6 under octopaminergic promoter control. In a previous report, ziram led to firing within 10 min of exposure (Martin, Myers et al. 2016), and we replicated those findings here. With DSF, on the other hand, firing at octopaminergic neurons did not occur until 20 or 25 min following exposure. Further, while the frequency of peaks with ziram was approximately 9 per min at 10 min of exposure, with DSF the frequency was approximately 3 per min at 20 min and 25 min. Again, this could be due to differences in the nature of modification on cellular targets as seen with E1, or due to changes in the affinity or kinetics of the drugs; however, the target in this case has yet to be determined. Intriguingly, K^+ channels are important modulators of burst firing, and similarly appear as potential targets leading to enhanced excitability in cortical neurons treated with ziram. Although the specific expression of ion channels is not known in octopaminergic neurons, examples of BK channels and K-ATP channels have been described in modulating burst firing of substantia nigra dopaminergic neurons (Schiemann, Schlaudraff et al. 2012, Kimm, Khaliq et al. 2015), and these are also sensitive to cysteine-residue modification (Trapp, Tucker et al. 1998, Zhang and Horrigan 2005). These properties may offer a clue to targets present in PD-sensitive neurons, and also potential targets to look for in octopaminergic neurons which spontaneously fire in the presence of ziram or DSF.

In sum we found in this study that ziram, a dithiocarbamate fungicide, led to consistent and robust changes in synaptic release from cortical neurons. These effects were dose-dependent, and were modified

by the presence of Ca^{2+}. Further, ziram led to increased excitability in cortical neurons. Other pesticides including maneb, benomyl and dieldrin increased mini EPSC frequency, although this was most pronounced in onset with maneb, another dithiocarbamate. The rapid mini increase could also be replicated with the dithiocarbamate DSF. We found that each of these dithiocarbamates could affect E1 enzyme, an important target for modulation of synaptic transmission. Finally, we report that spontaneous activity in aminergic neurons is induced by dithiocarbamates DSF and ziram, but not NSC624206, a chemical with thiol reactivity, a property common to dithiocarbamates. These data indicate that of the pesticides and chemicals tested in this study, dithiocarbamates are most similar in their physiological effects. This may be particularly important as the EPA currently recognizes that dithiocarbamates can lead to neuropathy, but do not find indication that this occurs via common mechanisms of toxicity (EPA 2004). Our data suggests that dithiocarbamates do in fact have common properties and targets which disrupt synaptic transmission, and that these effects may be important as early indicators of neurotoxicity in the development of PD.

References

Allen, M. T. and L. S. Levy (2013). "Parkinson's disease and pesticide exposure--a new assessment." Crit Rev Toxicol **43**(6): 515-534.

Braak, H., K. Del Tredici, U. Rub, R. A. de Vos, E. N. Jansen Steur and E. Braak (2003). "Staging of brain pathology related to sporadic Parkinson's disease." Neurobiol Aging **24**(2): 197-211.

Brown, T. P., P. C. Rumsby, A. C. Capleton, L. Rushton and L. S. Levy (2006). "Pesticides and Parkinson's disease--is there a link?" Environ Health Perspect **114**(2): 156-164.

Chen, T. W., T. J. Wardill, Y. Sun, S. R. Pulver, S. L. Renninger, A. Baohan, E. R. Schreiter, R. A. Kerr, M. B. Orger, V. Jayaraman, L. L. Looger, K. Svoboda and D. S. Kim (2013). "Ultrasensitive fluorescent proteins for imaging neuronal activity." Nature **499**(7458): 295-300.

Choi, J. C., D. Park and L. C. Griffith (2004). "Electrophysiological and morphological characterization of identified motor neurons in the Drosophila third instar larva central nervous system." J Neurophysiol **91**(5): 2353-2365.

Chou, A. P., N. Maidment, R. Klintenberg, J. E. Casida, S. Li, A. G. Fitzmaurice, P. O. Fernagut, F. Mortazavi, M. F. Chesselet and J. M. Bronstein (2008). "Ziram causes dopaminergic cell damage by inhibiting E1 ligase of the proteasome." J Biol Chem **283**(50): 34696-34703.

Cole, L. M. and J. E. Casida (1986). "Polychlorocycloalkane insecticide-induced convulsions in mice in relation to disruption of the GABA-regulated chloride ionophore." Life Sci **39**(20): 1855-1862.

Cole, S. H., G. E. Carney, C. A. McClung, S. S. Willard, B. J. Taylor and J. Hirsh (2005). "Two functional but noncomplementing Drosophila tyrosine decarboxylase genes: distinct roles for neural tyramine and octopamine in female fertility." J Biol Chem **280**(15): 14948-14955.

Dauer, W. and S. Przedborski (2003). "Parkinson's disease: mechanisms and models." Neuron **39**(6): 889-909.

Domico, L. M., G. D. Zeevalk, L. P. Bernard and K. R. Cooper (2006). "Acute neurotoxic effects of mancozeb and maneb in mesencephalic neuronal cultures are associated with mitochondrial dysfunction." Neurotoxicology **27**(5): 816-825.

EPA. (2004). "Registration Eligibility Decision for Ziram." 2016, from https://www3.epa.gov/pesticides/chem_search/reg_actions/reregistration/red_PC-034805_12-Jul-04.pdf.

Feng, Y., A. Ueda and C. F. Wu (2004). "A modified minimal hemolymph-like solution, HL3.1, for physiological recordings at the neuromuscular junctions of normal and mutant Drosophila larvae." J Neurogenet **18**(2): 377-402.

Fitzmaurice, A. G., S. L. Rhodes, M. Cockburn, B. Ritz and J. M. Bronstein (2014). "Aldehyde dehydrogenase variation enhances effect of pesticides associated with Parkinson disease." Neurology **82**(5): 419-426.

Fitzmaurice, A. G., S. L. Rhodes, A. Lulla, N. P. Murphy, H. A. Lam, K. C. O'Donnell, L. Barnhill, J. E. Casida, M. Cockburn, A. Sagasti, M. C. Stahl, N. T. Maidment, B. Ritz and J. M. Bronstein (2013). "Aldehyde

dehydrogenase inhibition as a pathogenic mechanism in Parkinson disease." Proc Natl Acad Sci U S A **110**(2): 636-641.

Fleming, L., J. B. Mann, J. Bean, T. Briggle and J. R. Sanchez-Ramos (1994). "Parkinson's disease and brain levels of organochlorine pesticides." Ann Neurol **36**(1): 100-103.

Haas, A. L. and I. A. Rose (1982). "The mechanism of ubiquitin activating enzyme. A kinetic and equilibrium analysis." J Biol Chem **257**(17): 10329-10337.

Haas, A. L., J. V. Warms, A. Hershko and I. A. Rose (1982). "Ubiquitin-activating enzyme. Mechanism and role in protein-ubiquitin conjugation." J Biol Chem **257**(5): 2543-2548.

Hancock, D. B., E. R. Martin, G. M. Mayhew, J. M. Stajich, R. Jewett, M. A. Stacy, B. L. Scott, J. M. Vance and W. K. Scott (2008). "Pesticide exposure and risk of Parkinson's disease: a family-based case-control study." BMC Neurol **8**: 6.

Hatcher, J. M., K. D. Pennell and G. W. Miller (2008). "Parkinson's disease and pesticides: a toxicological perspective." Trends Pharmacol Sci **29**(6): 322-329.

Hertzman, C., M. Wiens, D. Bowering, B. Snow and D. Calne (1990). "Parkinson's disease: a case-control study of occupational and environmental risk factors." Am J Ind Med **17**(3): 349-355.

Hogarth, G. (2012). "Metal-dithiocarbamate complexes: chemistry and biological activity." Mini Rev Med Chem **12**(12): 1202-1215.

Jan, L. Y. and Y. N. Jan (1976). "Properties of the larval neuromuscular junction in Drosophila melanogaster." J Physiol **262**(1): 189-214.

Jin, J., A. J. Lao, M. Katsura, A. Caputo, F. E. Schweizer and S. Sokolow (2014). "Involvement of the sodium-calcium exchanger 3 (NCX3) in ziram-induced calcium dysregulation and toxicity." Neurotoxicology **45**: 56-66.

Keung, W. M. and B. L. Vallee (1993). "Daidzin: a potent, selective inhibitor of human mitochondrial aldehyde dehydrogenase." Proc Natl Acad Sci U S A **90**(4): 1247-1251.

Kimm, T., Z. M. Khaliq and B. P. Bean (2015). "Differential Regulation of Action Potential Shape and Burst-Frequency Firing by BK and Kv2 Channels in Substantia Nigra Dopaminergic Neurons." J Neurosci **35**(50): 16404-16417.

Langston, J. W., P. Ballard, J. W. Tetrud and I. Irwin (1983). "Chronic Parkinsonism in humans due to a product of meperidine-analog synthesis." Science **219**(4587): 979-980.

Lee, A., T. Scheuer and W. A. Catterall (2000). "Ca2+/calmodulin-dependent facilitation and inactivation of P/Q-type Ca2+ channels." J Neurosci **20**(18): 6830-6838.

Lee, A., S. T. Wong, D. Gallagher, B. Li, D. R. Storm, T. Scheuer and W. A. Catterall (1999). "Ca2+/calmodulin binds to and modulates P/Q-type calcium channels." Nature **399**(6732): 155-159.

Li, Q., M. Kobayashi and T. Kawada (2012). "Mechanism of ziram-induced apoptosis in human T lymphocytes." Arch Toxicol **86**(4): 615-623.

Liou, H. H., M. C. Tsai, C. J. Chen, J. S. Jeng, Y. C. Chang, S. Y. Chen and R. C. Chen (1997). "Environmental risk factors and Parkinson's disease: a case-control study in Taiwan." Neurology **48**(6): 1583-1588.

Martin, C. A., K. M. Myers, A. Chen, N. T. Martin, A. Barajas, F. E. Schweizer and D. E. Krantz (2016). "Ziram, a pesticide associated with increased risk for Parkinson's disease, differentially affects the presynaptic function of aminergic and glutamatergic nerve terminals at the Drosophila neuromuscular junction." Exp Neurol **275 Pt 1**: 232-241.

Mathieu, C., R. Duval, X. Xu, F. Rodrigues-Lima and J. M. Dupret (2015). "Effects of pesticide chemicals on the activity of metabolic enzymes: focus on thiocarbamates." Expert Opin Drug Metab Toxicol **11**(1): 81-94.

Meco, G., V. Bonifati, N. Vanacore and E. Fabrizio (1994). "Parkinsonism after chronic exposure to the fungicide maneb (manganese ethylene-bis-dithiocarbamate)." Scand J Work Environ Health **20**(4): 301-305.

Papaioannou, M., I. Mylonas, R. E. Kast and A. Brüning (2014). "Disulfiram/copper causes redox-related proteotoxicity and concomitant heat shock response in ovarian cancer cells that is augmented by auranofin-mediated thioredoxin inhibition." Oncoscience **1**(1): 21-29.

Priyadarshi, A., S. A. Khuder, E. A. Schaub and S. Shrivastava (2000). "A meta-analysis of Parkinson's disease and exposure to pesticides." Neurotoxicology **21**(4): 435-440.

Rhodes, S. L., A. G. Fitzmaurice, M. Cockburn, J. M. Bronstein, J. S. Sinsheimer and B. Ritz (2013). "Pesticides that inhibit the ubiquitin-proteasome system: effect measure modification by genetic variation in SKP1 in Parkinsons disease." Environ Res **126**: 1-8.

Rinetti, G. V. and F. E. Schweizer (2010). "Ubiquitination acutely regulates presynaptic neurotransmitter release in mammalian neurons." J Neurosci **30**(9): 3157-3166.

Roede, J. R. and D. P. Jones (2014). "Thiol-reactivity of the fungicide maneb." Redox Biol **2**: 651-655.

Schiemann, J., F. Schlaudraff, V. Klose, M. Bingmer, S. Seino, P. J. Magill, K. A. Zaghloul, G. Schneider, B. Liss and J. Roeper (2012). "K-ATP channels in dopamine substantia nigra neurons control bursting and novelty-induced exploration." Nat Neurosci **15**(9): 1272-1280.

Schneggenburger, R. and C. Rosenmund (2015). "Molecular mechanisms governing Ca(2+) regulation of evoked and spontaneous release." Nat Neurosci **18**(7): 935-941.

Seneviratne, C. and B. A. Johnson (2015). "Advances in Medications and Tailoring Treatment for Alcohol Use Disorder." Alcohol Research : Current Reviews **37**(1): 15-28.

Sook Han, M., K. J. Shin, Y. H. Kim, S. H. Kim, T. Lee, E. Kim, S. Ho Ryu and P. G. Suh (2003). "Thiram and ziram stimulate non-selective cation channel and induce apoptosis in PC12 cells." Neurotoxicology **24**(3): 425-434.

Trapp, S., S. J. Tucker and F. M. Ashcroft (1998). "Mechanism of ATP-sensitive K channel inhibition by sulfhydryl modification." J Gen Physiol **112**(3): 325-332.

Turrigiano, G. G., E. Marder and L. F. Abbott (1996). "Cellular short-term memory from a slow potassium conductance." J Neurophysiol **75**(2): 963-966.

Ungermannova, D., S. J. Parker, C. G. Nasveschuk, D. A. Chapnick, A. J. Phillips, R. D. Kuchta and X. Liu (2012). "Identification and mechanistic studies of a novel ubiquitin E1 inhibitor." J Biomol Screen **17**(4): 421-434.

Vasiliou, V., M. Malamas and M. Marselos (1986). "The Mechanism of Alcohol Intolerance Produced by Various Therapeutic Agents." Acta Pharmacologica et Toxicologica **58**(5): 305-310.

Veverka, K. A., K. L. Johnson, D. C. Mays, J. J. Lipsky and S. Naylor (1997). "Inhibition of aldehyde dehydrogenase by disulfiram and its metabolite methyl diethylthiocarbamoyl-sulfoxide." Biochem Pharmacol **53**(4): 511-518.

Wang, A., S. Costello, M. Cockburn, X. Zhang, J. Bronstein and B. Ritz (2011). "Parkinson's disease risk from ambient exposure to pesticides." Eur J Epidemiol **26**(7): 547-555.

Wang, F., S. Zhai, X. Liu, L. Li, S. Wu, Q. P. Dou and B. Yan (2011). "A novel dithiocarbamate analogue with potentially decreased ALDH inhibition has copper-dependent proteasome-inhibitory and apoptosis-inducing activity in human breast cancer cells." Cancer Lett **300**(1): 87-95.

Wang, X.-F., S. Li, A. P. Chou and J. M. Bronstein (2006). "Inhibitory effects of pesticides on proteasome activity: Implication in Parkinson's disease." Neurobiology of Disease **23**(1): 198-205.

Zhang, G. and F. T. Horrigan (2005). "Cysteine modification alters voltage- and Ca(2+)-dependent gating of large conductance (BK) potassium channels." J Gen Physiol **125**(2): 213-236.

Zhang, J., V. A. Fitsanakis, G. Gu, D. Jing, M. Ao, V. Amarnath and T. J. Montine (2003). "Manganese ethylene-bis-dithiocarbamate and selective dopaminergic neurodegeneration in rat: a link through mitochondrial dysfunction." J Neurochem **84**(2): 336-346.

Chapter 4: Ziram, a pesticide associated with increased risk for Parkinson's disease, differentially affects the presynaptic function of aminergic and glutamatergic nerve terminals at the *Drosophila* neuromuscular junction

Abstract

Multiple populations of aminergic neurons are affected in Parkinson's disease (PD), with serotonergic and noradrenergic loci responsible for some non-motor symptoms. Environmental toxins, such as the dithiocarbamate fungicide ziram, significantly increase the risk of developing PD and the attendant spectrum of both motor and non-motor symptoms. The mechanisms by which ziram and other environmental toxins increase the risk of PD, and the potential effects of these toxins on aminergic neurons, remain unclear. To determine the relative effects of ziram on the synaptic function of aminergic versus non-aminergic neurons, we used live-imaging at the *Drosophila melanogaster* larval neuromuscular junction (NMJ). In contrast to nearly all other studies of this model synapse, we imaged presynaptic function at both glutamatergic Type Ib and aminergic Type II boutons, the latter responsible for storage and release of octopamine, the invertebrate equivalent of noradrenalin. To quantify the kinetics of exo- and endo- cytosis, we employed an acid-sensitive form of GFP fused to the *Drosophila* vesicular monoamine transporter (DVMAT-pHluorin). Additional genetic probes were used to visualize intracellular calcium flux (GCaMP) and voltage changes (ArcLight). We find that at glutamatergic Type Ib terminals, exposure to ziram increases exocytosis and inhibits endocytosis. By contrast, at octopaminergic Type II terminals, ziram has no detectable effect on exocytosis and dramatically inhibits endocytosis. In contrast to other reports on the neuronal effects of ziram, these effects do not appear to result from perturbation of the UPS or calcium homeostasis. Unexpectedly, ziram also caused spontaneous and synchronized bursts of calcium influx (measured by GCaMP) and electrical activity (measured by ArcLight) at aminergic Type II, but not glutamatergic Type Ib, nerve terminals. These events are sensitive to both tetrodotoxin and cadmium chloride, and thus appear to represent spontaneous depolarizations followed by calcium

influx into Type II terminals. We speculate that the differential effects of ziram on Type II versus Type Ib terminals may be relevant to the specific sensitivity of aminergic neurons in PD, and suggest that changes neuronal excitability could contribute to the increased risk for PD caused by exposure to ziram.

Introduction

Parkinson's disease (PD) is a prevalent neurodegenerative disease best known for movement deficits and dopamine (DA) neuron loss in the substantia nigra (Corti et al., 2011). However, other populations of aminergic neurons are also affected in PD and are responsible for many non-motor symptoms of PD such as depression, insomnia and gastrointestinal dysfunction (Kuhn et al., 2011; Politis et al., 2012; Taylor et al., 2009). It remains unclear why aminergic neurons are particularly susceptible to the pathogenic mechanisms of PD, but several recent studies highlight the potential importance of alterations in neuronal excitability (Dragicevic et al., 2015).

While several heritable forms of PD have been identified, the vast majority of cases are sporadic, suggesting the possibility that environmental exposures play a role in disease etiology. Recent epidemiological data demonstrate that exposure to the fungicide ziram increases the risk of PD two-fold (Fitzmaurice et al., 2014; Rhodes et al., 2013; Wang et al., 2011). Risk is further increased to three-fold in individuals exposed to ziram in addition to the herbicide paraquat and the fungicide maneb (Wang et al., 2011). Ziram, maneb and paraquat can each selectively kill aminergic neurons *in vitro* and *in vivo* (Chou et al., 2008; Cicchetti et al., 2005; McCormack et al., 2002; Meco, 1994). It remains unclear why these environmental toxins show relatively selective neurotoxic effects in aminergic cells.

There are several proposed mechanisms by which ziram might exert its neurotoxic effects. Ziram directly inhibits the enzyme aldehyde dehydrogenase (ALDH) which is responsible for the detoxification of multiple oxidative species including dopamine metabolites (Fitzmaurice, 2012). Ziram also directly

inhibits E1 ligase (Chou et al., 2008; Rinetti and Schweizer, 2010), the first enzyme in the biochemical cascade responsible for protein ubiquitination (Ciechanover, 1994; Kleiger and Mayor, 2014). Although the precise protein targets are not known, ziram impairs mitochondrial function (Li et al., 2012; Yamano and Morita, 1995) depletes cellular sulfhydryls (Yamano and Morita, 1995) and disrupts calcium homeostasis in some cell types, possibly through effects on the Sodium Calcium Exchanger NCX3 or a non-specific cation channel (Jin et al., 2014b; Sook Han et al., 2003). More specifically neuronal effects of ziram include an increase in spontaneous synaptic events (miniature Excitatory Post-Synaptic Currents and Inhibitory Post-Synaptic Currents, mEPSCs and mIPSCs) recorded in postsynaptic hippocampal neurons, consistent with an increased probability of presynaptic vesicle fusion (Rinetti and Schweizer, 2010). Inhibition of E1 ligase activity by other drugs (MG1-32, lactacystin) also increases spontaneous vesicle fusion (Rinetti and Schweizer, 2010) but the mechanism remains incompletely understood. It is possible that ziram has additional synaptic effects relevant to either its neurotoxic potential and/or its ability to increase the risk for PD.

The disruption of presynaptic activity in hippocampal neurons prompted us to explore the presynaptic effects of ziram on another well-characterized model synapse, the *Drosophila* larval neuromuscular junction (NMJ) (Gramates and Budnik, 1999). Unlike mammals, which release acetylcholine as a fast-acting acting excitatory neurotransmitter at the NMJ, flies release glutamate, similar to excitatory synapses in the mammalian CNS. Glutamatergic synapses at the fly NMJ include Type Ib (big) and Is (small) (Atwood et al., 1993; Jan and Jan, 1976; Jia et al., 1993). Importantly, the larval NMJ contains two other types of synapses that are not glutamatergic: Type II terminals that store and release the aminergic neurotransmitter octopamine and Type III terminals that release peptide neurotransmitters (Atwood et al., 1993; Jia et al., 1993; Monastirioti et al., 1995). Since octopamine is structurally and functionally similar to mammalian noradrenaline (Roeder, 2004), Type II boutons provide a model for

neurons that store and release amines other than dopamine that are sensitive to the pathophysiology of PD (Kuhn et al., 2011; Politis et al., 2012; Taylor et al., 2009).

Despite their potential use to model PD and synaptic function in general, relatively few studies of the fly NMJ have focused on Type II terminals because octopamine, like most mammalian amines, does not activate ionotropic receptors and cannot be followed via postsynaptic electrophysiological recordings. Other methods to quantify presynaptic function such as FM dyes or genetic probes can be used to study the activity of aminergic Type II terminals, but surprisingly, to our knowledge this has not yet been reported.

Here we have used genetic probes for vesicle recycling, voltage changes and calcium to compare the effects of ziram on aminergic Type II versus glutamatergic Type Ib nerve terminals. We report unexpected differences in their respective responses to toxin exposure including an increase in the spontaneous depolarization of aminergic, but not glutamatergic, processes. These differences may be relevant to the selective neurotoxic effects of ziram on mammalian aminergic neurons *in vitro* (Chou et al., 2008) and the observed increased risk for PD associated with ziram exposure in humans (Fitzmaurice et al., 2014; Rhodes et al., 2013; Wang et al., 2011).

Materials and Methods

Fly husbandry

Flies were reared on standard molasses yeast agar at room temperature. Flies expressing E1 RNAi and DVMAT-pHluorin were generated as described in (Martin et al., 2014) and (Grygoruk et al., 2014), respectively, and are available on request. Other lines including *elav-GAL4(X)* (Robinow and White, 1991), *Tdc2-GAL4* (Cole et al., 2005), *DVGLUT-GAL4* (Daniels et al., 2004), *UAS-Arclight* (Cao et al., 2013) and *UAS-GCaMP6m(III)* (Chen et al., 2013) are available from the Bloomington Stock Center. For pHluorin imaging

100

experiments, *UAS-DVMAT-pHluorin(III) was expressed using elav-GAL4(X).* For pHluorin imaging experiments involving E1 RNAi, F_1 progeny were collected from *elav-GAL4;+;UAS-DVMAT-pHluorin* females crossed to *+;+;UAS-E1-RNAi* males. Controls for these experiments included F_1 progeny from e*lav-GAL4;+;UAS-DVMAT-pHluorin* females crossed to Canton S (wild type) males. F_1 progeny used for calcium imaging were derived from *elav-GAL4* females crossed to *UAS-GCaMP6m (III)* males. For experiments using *UAS-ArcLight*, F_1 progeny were derived from *DVGLUT-GAL4* or *Tdc2-GAL4* females crossed to *UAS-ArcLight* males.

pHluorin imaging

To visualize DVMAT-pHluorin, fillets of third instar larvae were prepared in chilled HL3.1 Ca^{2+}-free media (final mM concentration: NaCl 70, KCl 5, $MgCl_2$ 4, $NaHCO_3$ 10, trehalose 5, sucrose 115, HEPES 5) adjusted to pH 7.32 (Feng et al., 2004). Stock solutions of 10 mM ziram were made in Dimethyl Sulfoxide (DMSO, Sigma, St. Louis, MO), aliquoted, stored at -20ºC and discarded after one freeze-thaw cycle; stocks of 10 mM lactacystin (Sigma, St. Louis, MO) were made in ddH_2O and treated as for ziram. Fresh stocks of L-glutamic acid (LGA) (Sigma, St. Louis, MO) were made weekly, and fresh stocks of HL3.1 were made monthly. LGA, $CaCl_2$, ziram, lactacystin or vehicle (DMSO) were added to HL3.1 on the day of the experiment. For ziram preincubation in Figures 1-3, fillets were incubated for 45 minutes at 18ºC in 'recording solution' (HL3.1 supplemented with 2 mM calcium and 700 µM L-glutamic acid to suppress muscle contractions) and containing either 20 µM ziram (Chem Services, West Chester, PA) or DMSO as a control (final DMSO concentration 0.2%). After incubation, the fillets were washed 3x in chilled recording solution prior to imaging. Experiments involving lactacystin were conducted the same as the ziram preincubation experiments, but with the addition of 100 µM lactacystin or vehicle alone (ddH_2O) as indicated.

Nerve terminals were imaged using a Zeiss Axio Examiner Z1 microscope and Zeiss Achroplan water-immersion objective (100x, 1.0 N.A.) fitted with a cooled back-illuminated electron-multiplying CCD camera (Andor iXon 897, South Windsor, CT) and a capture rate of 20 frames/second using Andor IQ2 software. A DG4 light source (Sutter, Novato, CA) with a GFP Brightline® Filter Set (Semrock, Rochester, NY) was used for illumination. Segment A4 muscle 13 was visualized for all experiments. To stimulate exocytosis, a suction electrode was used to stimulate a single nerve root (10 V, 40 Hz for 2 seconds). Exocytosis was quantified as maximal $\Delta F/F = [(F_{peak} - F_{baseline})/F_{baseline}]*100$, where F_{peak} is the average fluorescence for the ten frames (0.5s) after the end of the 2 sec stimulus period and $F_{baseline}$ is the average of the ten frames immediately preceding stimulus. We observed minimal decay in many of the endocytic curves for Type II terminals, prohibiting the calculation of tau by fitting a non-linear exponential curve. Therefore, to directly compare Type Ib and Type II terminals, we quantified endocytosis for all curves as the decrease in fluorescence due to endocytosis as % of F_{peak} at t = 10 sec post stimulus as described (Grygoruk et al., 2014).

Calcium imaging

To monitor intracellular calcium concentrations, a calcium sensitive form of GFP, *UAS-GCaMP6* (Chen et al., 2013) was expressed pan-neuronally using *elav-GAL4(X)* (Robinow and White, 1991). Larvae were dissected as for pHluorin experiments and either 1) preincubated in 20 µM ziram (0.2 % DMSO) or DMSO alone for 45 minutes (18°C) followed by washing in recording solution (Figure 4) or 2) imaged during continuous incubation in recording solution containing either 20 µM ziram (0.2 % DMSO) or DMSO alone at ambient temperature (Figure 5). For evoked response recordings, nerve roots were stimulated (10 V, 40 Hz for 2 seconds) and imaged as for DVMAT-pHluorin. Due to differences in the kinetics of the pH (pHluorin) versus calcium- sensitive (GCaMP) GFP-based probes, $\Delta F/F$ was calculated for GCaMP as $[(F_{peak} - F_{baseline})/F_{baseline}]*100$, with F_{peak} representing the average of four frames right before and four frames right

after the end of stimulus (0.4 sec total) (Macleod, 2012) with $F_{baseline}$ representing the average of the ten frames prior to stimulus (0.5 seconds total).

For experiments involving the channel inhibitors tetrodotoxin (TTX) and Cadmium Chloride ($CdCl_2$), larval fillets were imaged in recording solution (HL3.1 with 2 mM calcium and 700 μM L-glutamic acid) plus 0.2% DMSO +/- 20 μM ziram without channel inhibitor, then washed 3x with recording solution containing either 20 μM ziram or 20 μM ziram plus 1 μM TTX or 100 μM $CdCl_2$. After incubation in this solution for an additional 5 minutes, the preparations were imaged for $\geq$ 1.2 minutes.

ArcLight Recordings

To monitor intracellular voltage changes, a voltage sensitive form of GFP, *UAS-ArcLight* was expressed in either octopaminergic neurons using the *Tdc2-GAL4* driver or glutamatergic using the *DVGLUT-GAL4* driver. Larvae were dissected as for pHluorin experiments and imaged during continuous incubation in recording solution containing either 20 μM ziram (0.2 % DMSO) or DMSO alone at ambient temperature. (Note that in Figure 6 the fluorescence signal from ArcLight decreases in response to depolarizations in contrast to the increase in fluorescence seen with GCaMP in Figures 5.)

Data Analysis

Averaged data in the figures are presented as mean ± SEM. The number of recordings (max 2 per fillet) was used as the statistical n throughout. For each recording, 1-7 boutons were imaged and averaged as a single n. Boutons that moved out of the z plane during or after a stimulus were not analyzed. Statistical analysis was carried out in Graphpad Prism. To avoid assumptions about the nature of the data (e.g. whether it was normally distributed) a non-parametric Mann-Whitney test was used throughout. An effect was judged statistically significant if $p < 0.05$. A custom script written in the R programming language (Gnu Operating System) was used to quantify the average amplitude and frequency of some

spontaneous events. An additional custom script in R was used to perform resampling statistical analysis ("bootstrapping") of the E1 RNAi data.

Results

Ziram exposure at glutamatergic terminals results in aberrant exo- and endocytosis

To further explore the presynaptic effects of ziram (Rinetti and Schweizer, 2010), we used the well-characterized neuromuscular junction (NMJ) of the *Drosophila* 3rd instar larva (Jan and Jan, 1976). Standard fillet preparations were used and the exposed abdominal musculature and NMJ was pre-incubated in ziram. To induce exocytosis, a nerve root innervating a selected muscle was stimulated (see Methods). We first recorded evoked DVMAT-pHluorin exo- and endocytosis at the canonical Type Ib excitatory nerve terminals (Figure 1A-D). Ziram exposure at Type Ib terminals caused a significant increase in exocytosis relative to preparations incubated in vehicle alone, with ΔF/F values of 21.9% ± 1.7 of baseline for control versus 30.6% ± 2.8 for ziram-treated preps (Mean ± SEM) (Figure 1C; n= 23-25 fillets per treatment; Mann-Whitney test, p < 0.01). We also observed a modest decrease in obligate endocytosis that occurs following cessation of the stimulus, with % of F_{peak} at t = 10 sec post stimulus 6.2% ± 5.6 for control versus 14.7% ± 7.5 for ziram-treated preps (Figure 1D; n = 23-25 fillets per treatment; Mann-Whitney test, p < 0.01). In sum, at glutamatergic, Type Ib terminals, ziram increases evoked exocytosis and modestly retards endocytosis.

Ziram exposure at aminergic terminals disrupts endocytosis but not exocytosis

To determine how ziram exposure might affect synaptic function at aminergic Type II terminals (Figure 2A-D), we again exposed larval fillets to ziram followed by stimulation of the nerve root in the
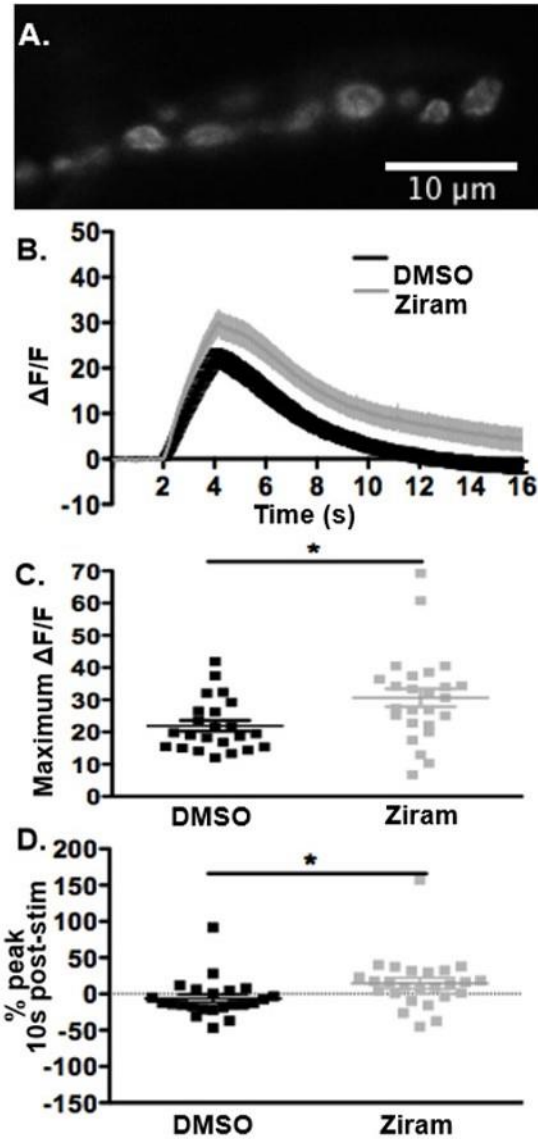
Figure 1. Exposure to ziram at excitatory glutamatergic terminals results in aberrant exo- and endo-cytosis. A) Representative image of DVMAT-pHluorin signal at Type Ib boutons. Scale bar: 10 microns. B) Averaged trace (mean+/-SEM, n = 23-25 fillets) of Type Ib boutons exposed to ziram (20 μM, 45 min, light grey trace) or vehicle (dark grey), washed, and electrically stimulated (40 Hz, 2 sec) to induce exocytosis. C) Maximum ΔF/F was determined for control and ziram-treated preparations as a measure of exocytosis (Mann-Whitney test; n = 23-25 represented by each symbol; p < 0.01; mean+/-SEM also shown). D) To compare endocytic rates, the % peak fluorescence 10 seconds after stimulus was determined (Mann-Whitney test; n = 23-25; p < 0.01).
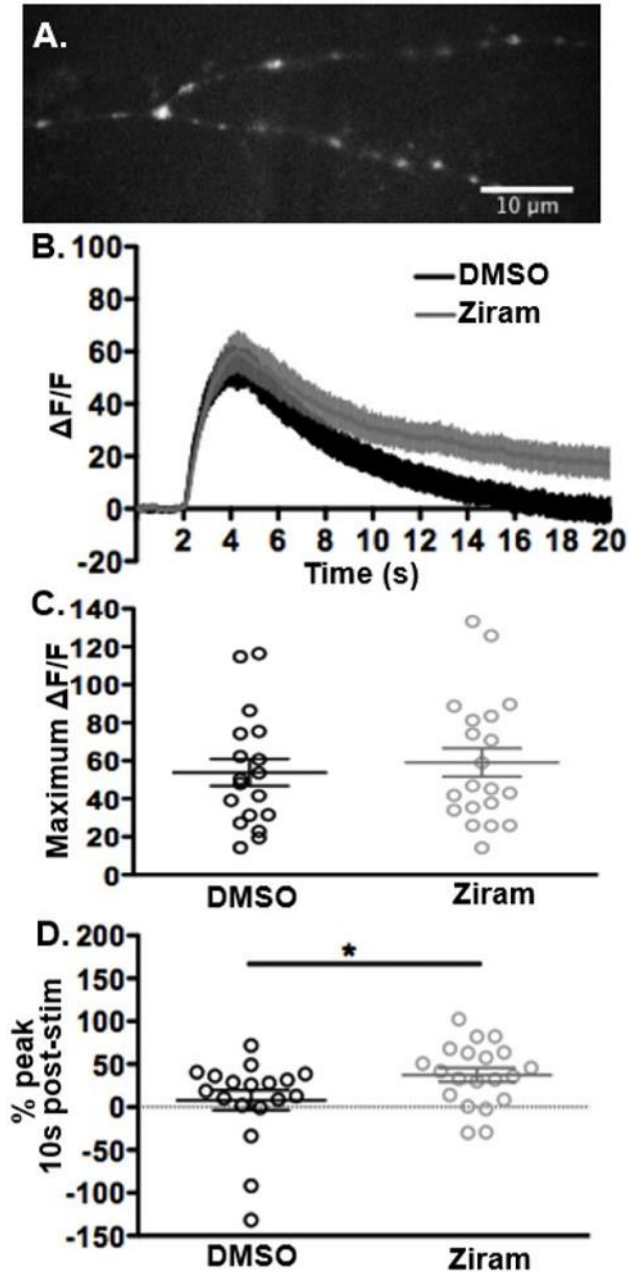
Figure 2. Exposure to ziram at aminergic terminals results in aberrant endocytosis. A) Representative image of DVMAT-pHluorin signal in Type II boutons. Scale bar= 10 microns. B) Averaged traces from Type II boutons exposed to ziram (20 µM, 45 min, light grey trace) or vehicle (dark grey), washed, and electrically stimulated (40 Hz, 2 sec) to induce exocytosis. C) Maximum $\Delta F/F$ did not differ between Type II boutons treated with ziram versus vehicle alone (n = 18-20; Mann-Whitney test; $p > 0.05$). D) The %

peak fluorescence at 10 seconds post stimulus was significantly higher in Type II boutons (n = 18-20; Mann-Whitney test; p < 0.05) suggesting a slower rate of endocytosis.

absence of ziram and imaged as described for Type Ib terminals. Under control conditions, exocytosis was higher in Type II terminals compared to Type Ib with an average maximal ΔF/F of 53% versus 22% at Type Ib terminals (compare Figure 1C, 2C). However, in contrast to Type Ib terminals, exocytosis at Type II terminals exposed to ziram did not significantly differ from DMSO controls, with ΔF/F values of 52.9% ± 7.1 for control versus 59.1% ± 10.4 for treated preps (Figure 2C; n = 18-20 per treatment; Mann-Whitney test, $p > 0.05$). Endocytosis at Type II terminals was generally slower than Type Ib in control conditions, with the average return to baseline occurring at 17s versus 12s (compare Figures 1D, 2D). Endocytosis was further slowed at Type II terminals following exposure to ziram, with ziram-treated fillets showing a decay at t = 10 seconds post-stimulus to 37.5% ± 8.0 of peak versus 8.1% ± 11.7 in controls (Figure 2D; n = 18-20 per treatment; Mann-Whitney test, $p < 0.05$). In sum, Type II terminals exhibit a clear slowing of in endocytosis without a detectable change in exocytosis following ziram exposure, a pattern different from that observed in Type Ib terminals.

Inhibition of components of the Ubiquitin Proteasome System does not mimic ziram's effect at Type Ib or Type II terminals

Ziram inhibits the ubiquitin activating E1 ligase and inhibition of the Ubiquitin Proteasome System (UPS) may underlie some of the effects of ziram at mammalian nerve terminals (Chou et al., 2008; Rinetti and Schweizer, 2010). Exposure to proteasome inhibitors has also been suggested to increase the evoked response at the fly NMJ (Speese et al., 2003). By contrast, we did not observe any change in exocytosis using the proteasome inhibitor lactacystin (100 μm) at Type Ib terminals (Figure 3A; n = 18-21 per treatment; Mann-Whitney test, $p > 0.05$). Similarly, lactacystin exposure did not appear to affect endocytosis, as measured by % peak at 10s post-stimulus, at Type Ib terminals (Figure 3B; n = 18-21 per treatment, Mann-Whitney test, $p > 0.05$). A previously described degron transgene (Pandey et al., 2007)
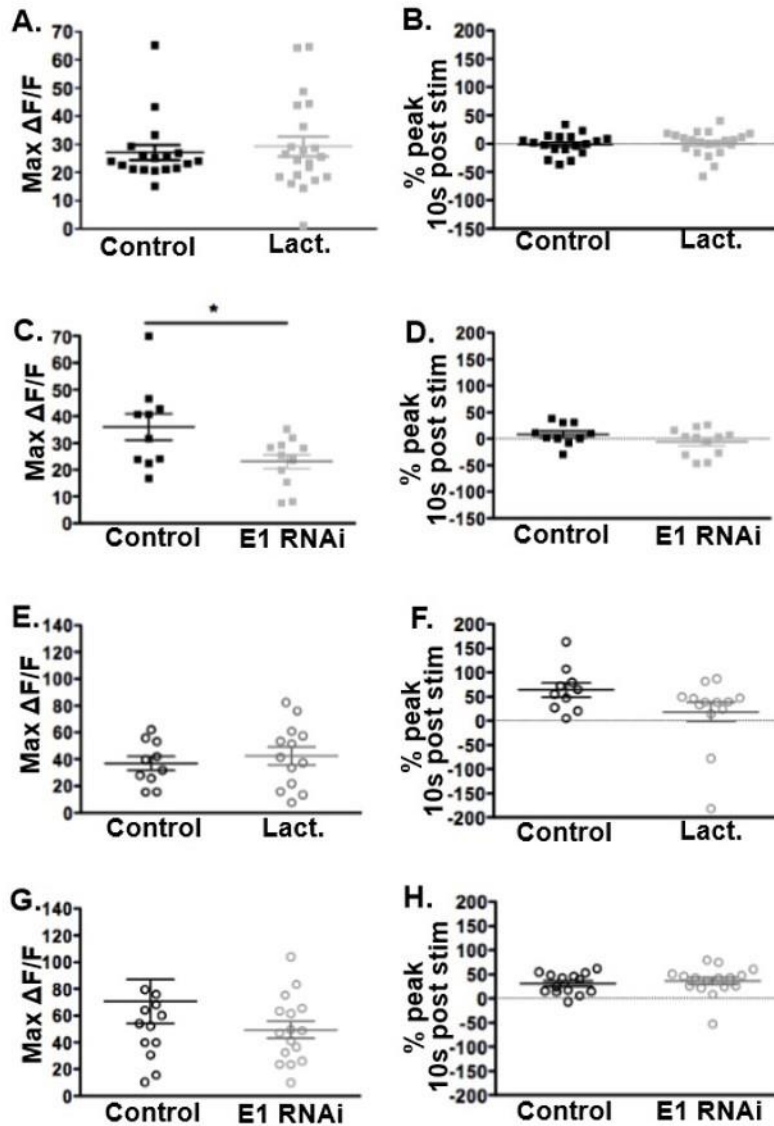
Figure 3. Inhibition of the Ubiquitin Proteasome System does not mimic ziram's action at the fly NMJ. A-B) Type Ib terminals were exposed to lactacystin (100 µM, 45 min) or vehicle, washed and imaged before and after stimulation (40 Hz, 2 sec). Neither the maximum Δ F/F (A) nor the % peak fluorescence at 10 seconds (B) differed between terminals exposed to lactacystin (light grey) versus vehicle alone (dark grey) (n = 18-21 per treatment, Mann-Whitney test, $p > 0.05$). C-D) Type Ib terminals expressing E1 RNAi (light grey) versus controls (dark grey). C) Maximum ΔF/F in Type Ib boutons expressing E1 RNAi (light grey) and the % of peak fluorescence at 10 seconds post stimulus (D) did not significantly differ (n = 10-12 per treatment, Mann-Whitney test, $p > 0.05$). E-H) Type II terminals exposed to lactacystin or expressing E1 RNAi were treated and analyzed identically to Type Ib terminals. Neither Maximum ΔF/F (E,G) nor % peak

fluorescence 10 seconds post stimulus (F,H) differed significantly in Type II boutons treated with lactacystin (E, F, n = 10-13 per treatment, Mann-Whitney test, p > 0.05) or expressing E1 RNAi (G, H; n = 14-16 per treatment, Mann-Whitney test, p > 0.05).

was used to confirm that UPS function was indeed disrupted by incubation in ziram (Supplemental Figure 1). Taken together, these data suggest that inhibition of the proteasome may not be responsible for the increase in exocytosis or the slight decrease in endocytosis we observe in ziram-treated Type Ib terminals.

To further evaluate the potential effects of ubiquitin E1 ligase inhibition, we used a genetic approach. RNAi representing *Drosophila* E1 ligase was expressed at Type Ib terminals (see Methods) and DVMAT-pHluorin was imaged as in Figures 1 and 2. As in our experiments using lactacystin, a degron transgene was used as a positive control to demonstrate the disruption of UPS function by E1 RNAi (Supplemental Figures 2 and 3). Metrics for exo- nor endo- cytosis did not significantly differ from controls (Figure 3C, D, n = 10-12; Mann-Whitney test, p > 0.05). We noted a trend toward a decreased maximum $\Delta F/F$ in lines expressing RNAi for E1 ligase (Mann-Whitney, p = 0.08). Using resampling statistics instead of a non-parametric approach yielded p = 0.04 for the difference of the medians. We conclude that there is a weak trend towards *decreased* exocytosis but note that the direction of this trend is the *opposite* of the effect seen in Type Ib terminals treated with ziram. It thus is highly unlikely that the ziram-induced *increase* in exocytosis at Type Ib terminals is due to an inhibition of E1 ligase activity.

We next tested the effects of E1 ligase RNAi and lactacystin at Type II terminals. Neither treatment altered exo- or endocytosis at Type II terminals (Figure 3E-H). The differences between the effects of ziram and those of either lactacystin or E1 RNAi suggest that ziram may influence the exocytotic cycle in Type Ib and II terminals via mechanisms that do not involve the UPS.

Ziram exposure does not alter baseline calcium levels or calcium influx during exocytosis at Type Ib or Type II terminals

Ziram exposure has been shown to increase levels of intracellular calcium in PC12 (Sook Han et al., 2003) and in BHK cells (Jin et al., 2014a) and calcium is tightly coupled with the release of secretory vesicles. We therefore examined whether the ziram-induced increase in exocytosis we observed in Type Ib terminals might be due to higher baseline calcium concentrations and/or an increase in calcium influx during stimulation. To address this question, we expressed the genetically encoded calcium indicator GCaMP6 and imaged the Type Ib (Figure 4A-C) and Type II boutons (Figure 4D-F) after exposure to ziram (20 µM ziram for 45 minutes followed by recording in the absence of ziram). Exocytosis was initiated as for pHluorin imaging via electrical stimulation of a nerve root (10 V, 40 Hz for 2 seconds). Exposure to ziram did not result in a detectable increase in calcium influx during stimulus-evoked exocytosis at Type Ib boutons (Figure 4B; n=11 per treatment; Mann-Whitney test, $p > 0.05$), or detectably alter baseline calcium levels (Figure 4C; n = 11 per treatment; Mann-Whitney test, $p > 0.05$). These data suggest that neither an increase in calcium influx during exocytosis nor changes in baseline calcium levels are responsible for the increase in exocytosis we observe at ziram-treated Type Ib terminals.

For completeness, we similarly tested the potential effects of ziram exposure on calcium dynamics at Type II terminals. As expected, we did not detect a statistically significant difference in either baseline calcium levels or evoked calcium influx in ziram-exposed fillets versus controls (Figure 4D-G n = 7-21 per treatment; Mann-Whitney test, $p > 0.05$).

We note that the evoked calcium response for Type Ib and Type II terminals show a distinctly different time course under baseline conditions. Type II terminals exhibit an immediate increase in GCaMP fluorescence, followed by a plateau during stimulus and a gradual decay. By contrast, Type Ib terminals exhibit a more gradual increase in fluorescence that peaks near the end of stimulus and then immediately declines. These differences reinforce the notion that baseline synaptic function in Type Ib and Type II terminals is likely divergent, consistent with the differences we observe in their response to ziram.
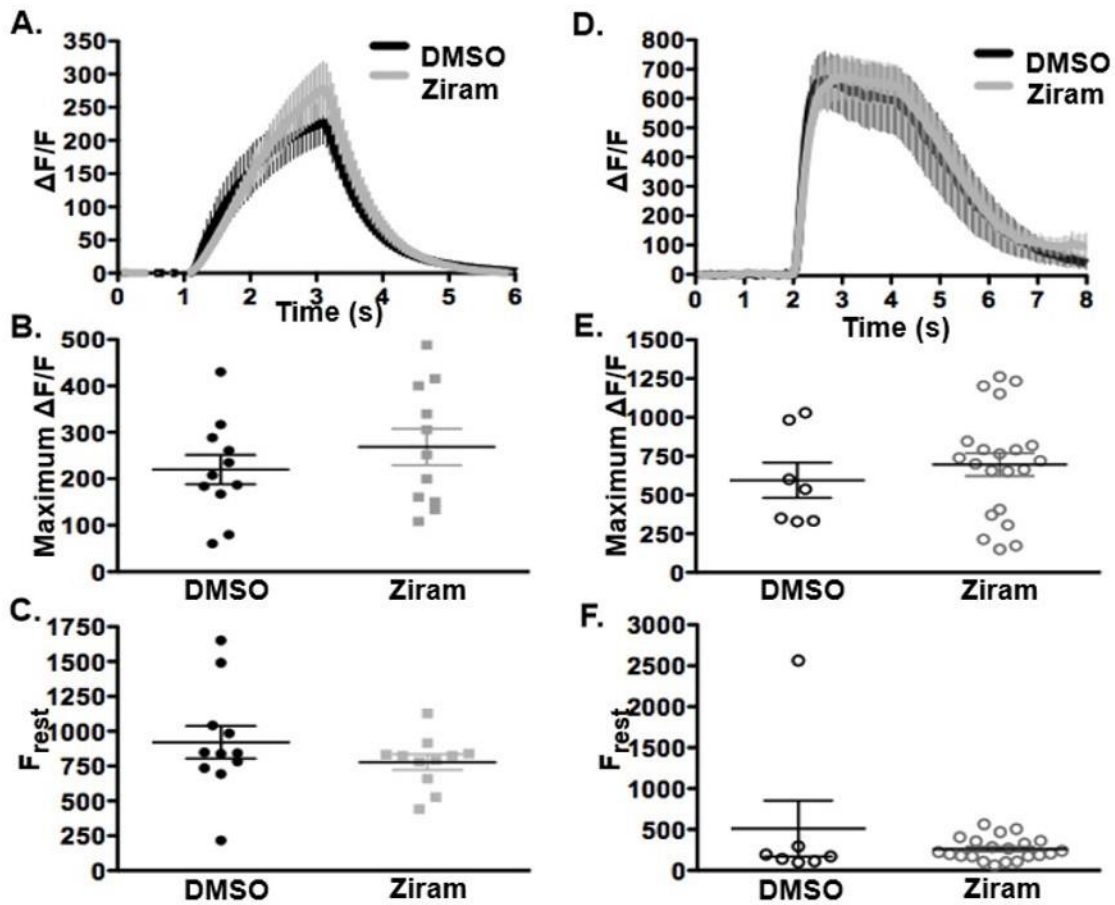
Figure 4. Ziram exposure does not alter calcium influx or baseline calcium levels at Type Ib or Type II synapses. Type Ib (A-C, n = 11 per treatment) or Type II boutons (D-F, n = 7-21 per treatment) expressing GCaMP were exposed to ziram (light grey, 100 μM, 45 min) or vehicle alone (DMSO, dark grey), washed and stimulated to induce calcium influx (40 Hz, 2 sec). Neither maximum ΔF/F (B, E) nor baseline fluorescence (C, F) showed statistically significant differences between preparations treated with ziram versus vehicle alone (Mann-Whitney test, p > 0.05).

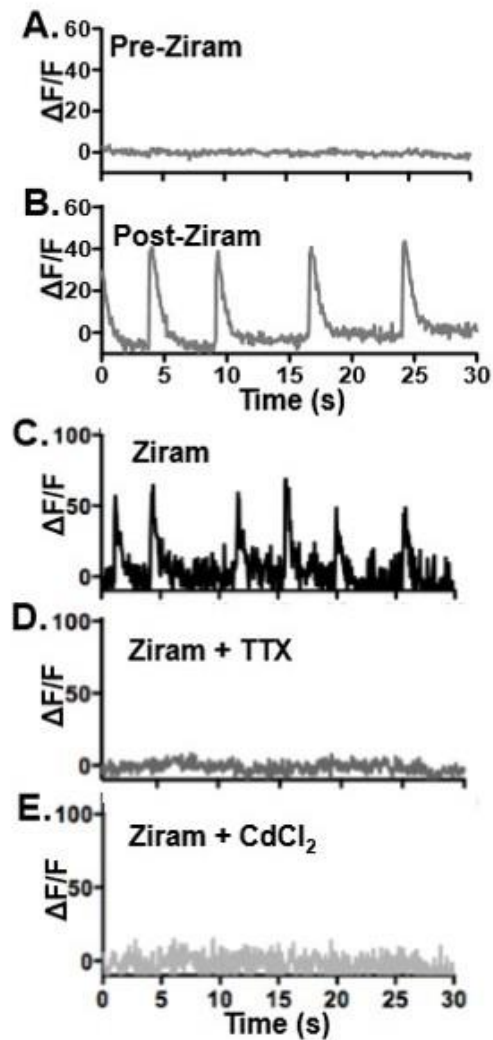**Figure 5. Ziram exposure causes coordinated and spontaneous calcium events in aminergic terminals.** GCaMP fluorescence was quantified in Type II terminals exposed to vehicle (DMSO) alone (not shown) or 20μM ziram (A, B). Traces show repetitive calcium spikes after 10 minutes exposure to ziram (B, n=6) but not at the onset of exposure (A) or in the presence of vehicle either at the onset of treatment or after 10 minute exposure (n=8). C-D) Tetrodotoxin and $CdCl_2$ block ziram-induced spontaneous calcium events at aminergic terminals. Representative traces of Type II terminal from larval fillets treated with ziram (C, 20 μM, 10 min) followed by 5 min incubation in the same concentration of ziram plus either 1μM tetrodotoxin (D, n = 3) or 100 μM $CdCl_2$ (E, n = 3) to inhibit sodium and calcium channels respectively.

Ziram exposure causes spontaneous calcium events in Type II aminergic, but not Type Ib glutamatergic, terminals

While conducting baseline and evoked calcium recordings following pre-incubation in ziram at 18ºC, we observed spontaneous and synchronized spikes of GCaMP6 fluorescence in aminergic Type II terminals but not in Type Ib terminals. To explore this phenomenon, larval fillets expressing GCaMP6 pan-neuronally were incubated in 20 µM ziram at ambient temperature while continuously imaging the NMJ. Repetitive, spontaneous calcium events were observed in Type II terminals within 5-10 minutes of ziram exposure in all experiments (Figure 5B, n = 6, one representative trace is shown) but not following incubation in vehicle alone (not shown, n = 8). Spontaneous calcium events were never observed in Type Ib terminals or the slightly smaller and glutamatergic Type Is terminals (data not shown). Quantification of spontaneous calcium events in Type II terminals after 10 minutes of incubation in ziram indicated an average frequency of 8.0 ± 1.0 events/minute, with an average amplitude of 25.8 ± 5.6 ⯑F/F (n = 6). We did not detect a change in either baseline calcium levels or in evoked calcium influx under these conditions (data not shown) consistent with the notion that global changes in calcium homeostasis are unlikely to be responsible for the transient events we observe. Importantly, cytosolic calcium is highly buffered, and actively transported into intracellular stores and the extracellular milieu (Brini et al., 2014; Gleichmann and Mattson, 2011; Matthews and Dietrich, 2015). Thus, an increase in calcium transients can occur in the absence of elevated cytosolic levels.

Ziram induced spontaneous calcium events are sensitive to TTX and CdCl$_2$

We hypothesized that the calcium spikes observed in the presence of ziram might result from depolarization and/or propagation of an action potential in the observed axon. Since neuronal

depolarization most often requires activation of sodium channels, we tested the effects of the sodium channel inhibitor tetrodotoxin (TTX). Co-incubation of TTX with ziram (Figure 5D, n=3, a representative trace is shown) blocked the spontaneous calcium events observed at aminergic terminals incubated with ziram alone (Figure 5C).

The calcium transients we observed at Type II terminals could represent intracellular calcium release, e.g. from the endoplasmic reticulum or calcium influx from the extracellular milieu, most likely mediated by voltage gated calcium channels as seen in a variety of other neurons (Simms and Zamponi, 2014). To test the latter hypothesis, we applied a broad inhibitor of voltage gated calcium channels, $CdCl_2$, to larval fillets exposed to ziram. Similar to TTX, $CdCl_2$ co-application with ziram ablated the spontaneous calcium transients of Type II terminals (Figure 5E; n= 3). Together, the effects of TTX and CdCl2 suggest that the calcium spikes we observe at Type II terminals in response to ziram are likely due to depolarization of the axon followed by influx of Ca through voltage gated calcium channels.

Incubation with lactacystin did not induce any detectable calcium spikes in Type II (or Type I) terminals (data not shown). Furthermore, co-incubation with lactascystin did not affect the ability of ziram to induce calcium spikes in Type II terminals (data not shown). These observations suggest that ziram-induced calcium spikes occur independently of the UPS, similar to the effects of ziram on the exocytotic cycle at the fly NMJ.

Ziram induces spontaneous depolarization of aminergic, but not glutamatergic, terminals

To further confirm that the ziram-induced synchronized calcium transients we observed at Type II terminals were mediated by axon depolarization, we conducted recordings using the voltage sensitive fluorescent reagent ArcLight. *UAS-ArcLight* was expressed in Type II octopaminergic neurons of the NMJ
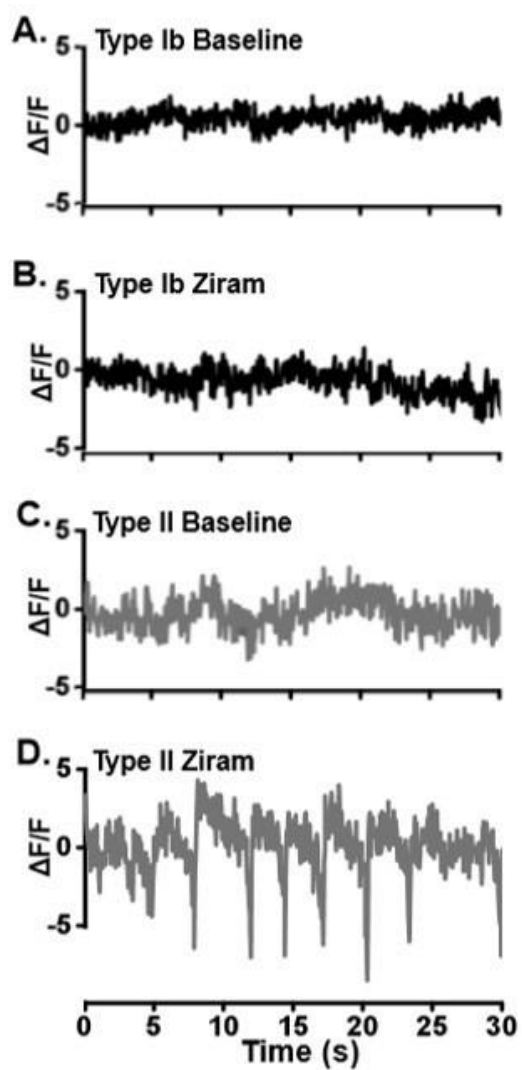
Figure 6. Ziram induces spontaneous voltage mediated events at aminergic terminals. Representative traces ArcLight recordings at a Type Ib terminal (A,B, n = 3 per treatment) and Type II terminal (C,D, n = 7 per treatment) before (A,C) and after (B,D) 10 min treatment with 20 μM ziram.

using the *Tdc2-GAL4* driver or in Type Ib glutamatergic neurons using the *DVGLUT-GAL4* driver (Figure 6A,B). Recordings were taken at baseline (Figure 6A), and following 10 min of continuous 20 µM ziram incubation while simultaneously imaging the nerve terminals (Figure 6B). No events were observed in Type Ib glutamatergic terminals at baseline or after exposure to ziram (Figure 6A,B; n = 3). By contrast, spontaneous voltage driven events (average frequency 10.6 ± 1.4 events/minute) synchronized across all boutons, were consistently observed in Type II terminals to ziram (Figure 6D; n = 7) but not vehicle alone (data not shown). These data confirm that ziram induces spontaneous depolarizations in processes containing Type II terminals, consistent with an increase in excitability, but does not cause parallel excitatory changes in glutamatergic, Type Ib terminals.

Discussion

Epidemiological studies have demonstrated an increase in Parkinson's disease (PD) in human populations exposed to ziram and other pesticides (Fitzmaurice et al., 2014; Rhodes et al., 2013; Wang et al., 2011), but the underlying mechanisms remain unclear. More fundamentally, the range of these pesticides effects on neurons and their influence on specific neuronal subtypes are not known. To investigate these questions, and more specifically explore the potential presynaptic effects of ziram, we have used the *Drosophila* neuromuscular junction (NMJ) as a model. To our knowledge, the fly NMJ has not been used previously to examine the effects of putative neurotoxins associated with PD. Importantly, our studies also differ from previous experiments using the fly NMJ because we have directly compared the synaptic physiology of two distinct types of nerve terminals: aminergic Type II and glutamatergic Type Ib terminals. We suggest that this comparison is relevant to the pathophysiology of PD since multiple subtypes of mammalian aminergic neurons are sensitive to the neurodegenerative processes that characterize this disease, including noradrenergic neurons of the locus coeruleus and serotonergic neurons in the raphe nuclei (Kuhn et al., 2011; Politis and Loane, 2011; Politis et al., 2012; Szot, 2012;

Taylor et al., 2009). Using the fly NMJ, we observed striking differences in the effect of ziram on Type Ib glutamatergic versus Type II aminergic and suggest that these differences may be relevant to neurotoxic effects of ziram in mammals and perhaps PD patients. We anticipate that this system will be useful to explore the synaptic effects of other pesticides associated with an increased risk of PD.

In contrast to glutamatergic Type I terminals which have been extensively studied (Menon et al., 2013; Olsen and Keshishian, 2012), there is a striking paucity of data on the synaptic physiology of Type II aminergic terminals, in large part due to their lack of postsynaptic electrophysiological accessibility. We have circumvented this issue by taking advantage of genetically expressed fluorescent indicators of presynaptic activity. Using a *DVMAT-pHluorin* transgene and live-imaging techniques, we have shown that ziram treatment delays endocytosis in Type II and, to a lesser extent, Type Ib terminals. By contrast, we observe an increase in exocytosis in Type Ib, but no detectable change in exocytosis in Type II in response to ziram exposure. Using the additional transgenic probe GCaMP to image calcium dynamics, we did not detect an increase in baseline or evoked calcium levels suggesting that the disruption of exo- and endo-cytosis was not due to increased calcium influx. However, we observed a striking occurrence of spontaneous calcium transients in Type II, but not Type Ib, terminals. These events were blocked by tetrodotoxin and by $CdCl_2$, suggesting that ziram promotes spontaneous sodium-channel driven depolarizations that elicit calcium influx in Type II processes. We further confirmed this hypothesis using the voltage sensitive fluorescent transgene, ArcLight, and directly demonstrated spontaneous depolarizations in processes containing Type II, but not Type Ib, boutons. It remains unclear whether the effects of ziram on membrane trafficking and neuronal excitability are caused by the same or different underlying mechanisms, and further experiments will be needed to address this issue.

The increase in spontaneous depolarizations in Type II terminals demonstrates that ziram can cause an increase in excitability in a subset of aminergic neurons in the fly and perhaps other systems.

These data are similar to the increase in aminergic excitability seen in several models of neurodegeneration and PD (Reviewed in (Dragicevic et al., 2015)). These include the increase in firing frequency of dopaminergic neurons over-expressing alpha-synuclein (Subramaniam et al., 2014) or subjected to oxidative stress (Avshalumov et al., 2005). The effects of ziram-induced changes in exo- and endocytosis are more difficult to predict. However, an increase in evoked exocytosis seen in Type I terminals would be expected to cause an increase in glutamate release, and similar effects in the CNS could also lead to an increase in the excitation of downstream circuits. Future experiments to directly test these hypotheses and the effects of ziram exposure in fly as a whole may require parenteral administration; but it has proven difficult to administer neurotoxic doses of ziram through feeding (Martin et al., 2014).

It remains unclear how the proposed molecular targets of ziram could account for the effects on exocytosis and excitability that we observe. Ziram has been shown to inhibit E1 ligase, the enzyme responsible for ubiquitin activation prior to protein conjugation (Chou et al., 2008). Ubiquitin conjugation to proteins can result in a myriad of downstream effects in the neuron, including proteasomal degradation and regulation of endocytosis (DiAntonio and Hicke, 2004). Ziram-exposed primary hippocampal neurons exhibit an increase in mEPSCs that is mimicked by pharmacologic inhibition of ubiquitin E1 ligase (Rinetti and Schweizer, 2010). By contrast, we find that neither genetic inhibition of E1 ligase nor chemical inhibition of downstream proteasome activity induced spontaneous depolarizarion of Type II terminals or recapitulated the effect of ziram on exocytosis or endocytosis (as measured by pHluorin imaging). Also, in contrast to some other studies in mammalian cultured cells (Sook Han et al., 2003), we did not observe an effect of ziram on baseline calcium levels despite the occurrence of spontaneous calcium transients.

It remains possible that some of the effects of ziram at the fly NMJ result from disruption of mitochondrial activity (Yamano and Morita, 1995) or ALDH inhibition (Fitzmaurice et al., 2014). Alternatively, it is possible that other targets are responsible for the effects we observe (Stoytcheva,

2011). The activity of ziram as a thiol and its ability to deplete protein thiols in non-neuronal cells may be relevant to these effects (Shen, 2001). It interesting to note that other thiol-based toxins and the related drug disulfiram conjugate to a sulfur group in ALDH (Fitzmaurice et al., 2014; Shen, 2001, 2000) and the active site of E1 ligase also contains a critical cysteine residue (Ciechanover, 1994). We speculate that additional targets may be sensitive to the effects of ziram via conjugation to protein thiols and that these additional targets may be responsible for the effects of ziram we observe at the fly NMJ.

The spontaneous firing in Type II terminals seen with ziram exposure could result from a direct modification of channel activity. A number of mammalian channel subunits contain thiol groups that are sensitive to either nitrous oxide or exogenous thiol reagents (Ooi et al., 2013; Yang et al., 2013; Zhang and Horrigan, 2005). In addition, the dithiocarbamate pesticide mancozeb has been shown to activate the voltage-gated KCNQ2 potassium channel in CHO cells (Li et al., 2013). It is also possible that the relatively specific effects of ziram on Type II, but not Type Ib, terminals reflect the preferential activity of select channels in octopaminergic cells. Transcriptional analyses may help to identify channels potentially enriched in *Drosophila* aminergic neurons (Henry et al., 2012). In addition, electrophysiological studies in other insects have implicated several channels potentially involved in regulating the firing rates of octopaminergic neurons in *Drosophila* (Dugravot et al., 2003; Gautier et al., 2008; Grolleau and Lapied, 2000; Heidel and Pflüger, 2006). One or more of these could be a target for ziram.

In mammals, a growing body of literature implicates altered channel activity in the pathogenesis of PD (Dragicevic et al., 2015). These include studies implicating the ATP gated potassium channels Kir6.2 in dopamine cell bursting and the neurodegenerative effects of MPTP (Liss et al., 2005; Schiemann et al., 2012), the oxidative effects of alpha-synuclein on A type potassium channels (Subramaniam et al., 2014), the loss of pacemaking activity in medium spiny neurons caused by disruption of a cyclic nucleotide-gated (HCN) potassium channel (Chan et al., 2011), and the contribution of calcium channels to mitochondrial

dysfunction (Guzman et al., 2010). Investigating the contribution of these or other channels to our findings will be facilitated by the availability of mutations in most, if not all, channel genes in *Drosophila*. Although many of these mutations are lethal in the adult, nearly all survive as larvae, thus allowing a broad screen for mutations that mimic or block the effects of ziram.

At present, we cannot rule out the possibility that some of our data are idiosyncratic or specific to the larval NMJ, and further experiments using other neuronal subtypes in both flies and mammals are needed. We speculate, however, that the differences we observe between Type Ib and Type II boutons may represent a generalizable paradigm for the behavior of aminergic versus non-aminergic cells in response to ziram and perhaps other pesticides. If so, it is possible that the differential effects of ziram on Type Ib vs Type II are relevant to the sensitivity of aminergic pathways to the pathophysiologic processes that cause PD, and the effects of PD-related insults on neuronal excitability.
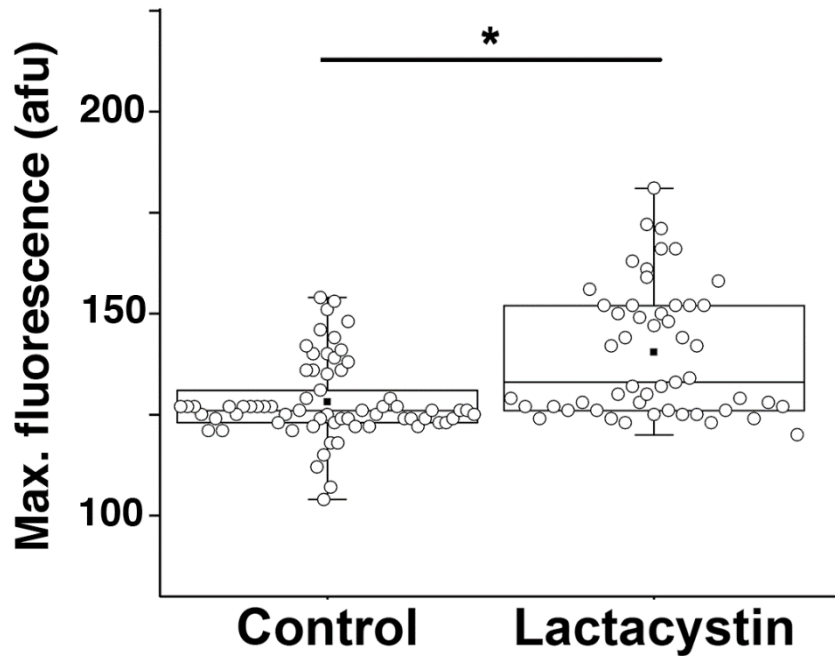
Supplemental Figure 1. Lactacystin inhibits proteasome activity in octopaminergic neurons. Octopaminergic neurons expressing the GFP-labeled *UAS-degron* and incubated in 100⬜M lactacystin (45 min) show higher levels of fluorescence than cells treated in parallel with vehicle (DMSO) alone. Maximum fluorescence was recorded from individual cells in each nerve cord (Mann-Whitney, $p < 0.05$, 6 animals per treatment, 3 separate experiments, 1 to 14 cells per animal). Box and whiskers represent minimum, first quartile, median (line), mean (solid grey circle), third quartile and maximum.
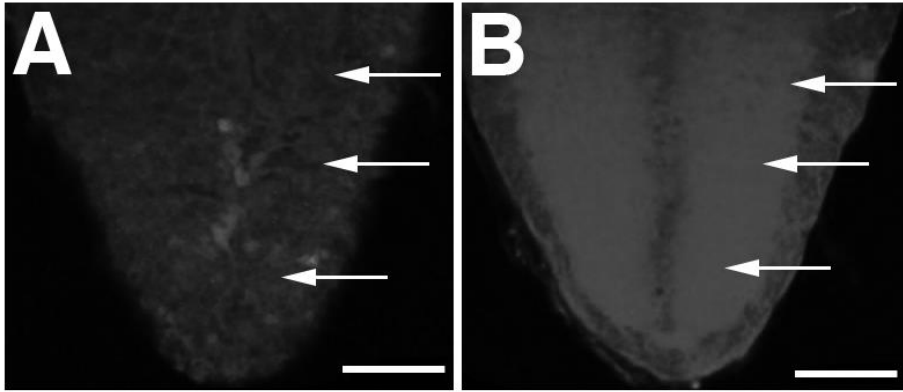
Supplemental Figure 2. Pan-neuronal E1 RNAi expression decreases proteasome activity in the larval nerve cord. A) Flies pan-neuronally expressing the GFP-tagged *UAS-degron* construct show minimal labeling of the neuropil in the ventral nerve cord (representative image for 6 of 7 animals from 3 experiments; 1 additional sample showed weak labeling of the neuropil). B) Larvae co-expressing *UAS-E1-RNAi* and the *UAS-degron* show widespread fluorescent labeling in the neuropil (representative image for 5 of 6 animals from 3 experiments; 1 other sample showed weaker labeling of the neuropil). Posterior segments are shown in both images, with the terminus of the nerve cord oriented downward in each panel. Arrows in A and B indicate comparable areas. Scale bars: 50 microns.
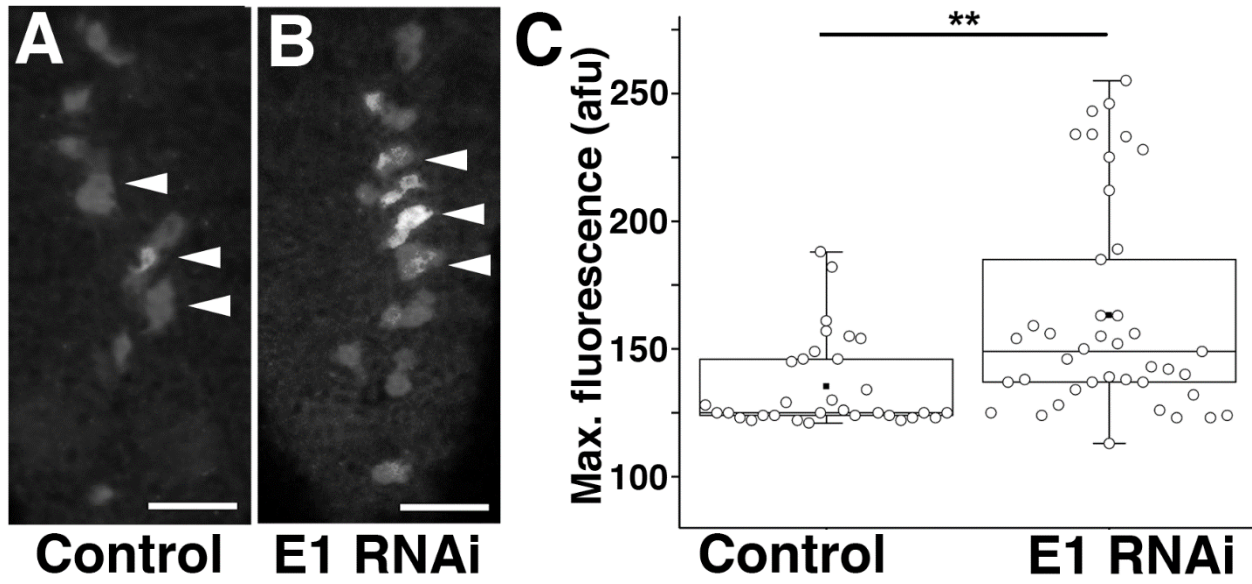
Supplemental Figure 3. E1 RNAi expression in octopaminergic neurons inhibits proteasome activity.

Octopaminergic neurons expressing a GFP labeled *UAS-degron* alone (A) show lower levels of fluorescence than those co-expressing the *UAS-degron* plus a *UAS-E1 RNAi* transgene (B). The midline of the nerve cord terminus is shown in each panel. Arrowheads indicate cell clusters. Scale bars: 25 microns. C) Maximum fluorescence (arbitrary units or afu) was quantified from individual cells in each nerve cord (Mann-Whitney, $p < 0.005$, ≥ 3 animals per treatment, 7 to 18 cells per animal, 3 separate experiments). Box and whiskers represent minimum, first quartile, median (line), mean (solid grey circle), third quartile and maximum.

Supplemental Methods. For all Supplemental Experiments, flies expressing the degron transgene *UAS-GFP CLI* alone, or both *UAS-GFP CLI* and *UAS-E1 RNAi* were crossed to driver lines expressing either *elav-GAL4* (Supplemental Figure 1) or *Tdc2-GAL4* (Supplemental Figures 2 and 3). F_1 progeny were collected as third instar larvae and larval fillets dissected in chilled HL3.1. For Supplemental Figure 1, the fillet was then pre treated in either 100⃞M lactacystin (45 min, 18°C) or vehicle alone (DMSO) prior to fixation. For all experiments, tissue was fixed in 4% paraformaldehyde (25 min) washed 3x in PBS and immersed in 70%

glycerol for mounting. Confocal stacks (1024 x 1024 pixels) were collected on a Zeiss Pascal LSM 5 confocal microscope using a 20x/0.8 Plan-Apochromat objective and a pinhole size of 1 Airy unit. Identical laser intensity and gain settings were used for all samples and conditions in each experiment To quantify fluorescence intensity, Regions of Interest (ROIs) were traced around individual cells using Image J, and the maximum level of fluorescence (arbitrary units or "afu") within each ROI was plotted.

References

Atwood, H.L., Govind, C.K., and Wu, C.F. (1993). Differential ultrastructure of synaptic terminals on ventral longitudinal abdominal muscles in Drosophila larvae. Journal of Neurobiology *24*, 1008-1024.

Avshalumov, M.V., Chen, B.T., Koos, T., Tepper, J.M., and Rice, M.E. (2005). Endogenous hydrogen peroxide regulates the excitability of midbrain dopamine neurons via ATP-sensitive potassium channels. J Neurosci *25*, 4222-4231.

Brini, M., Cali, T., Ottolini, D., and Carafoli, E. (2014). Neuronal calcium signaling: function and dysfunction. Cell Mol Life Sci *71*, 2787-2814.

Cao, G., Platisa, J., Pieribone, V.A., Raccuglia, D., Kunst, M., and Nitabach, M.N. (2013). Genetically Targeted Optical Electrophysiology in Intact Neural Circuits. Cell *154*, 10.1016/j.cell.2013.1007.1027.

Chan, C.S., Glajch, K.E., Gertler, T.S., Guzman, J.N., Mercer, J.N., Lewis, A.S., Goldberg, A.B., Tkatch, T., Shigemoto, R., Fleming, S.M.*, et al.* (2011). HCN channelopathy in external globus pallidus neurons in models of Parkinson's disease. Nat Neurosci *14*, 85092.

Chen, T.W., Wardill, T., Sun, Y., Pulver, S.R., Renninger, S.L., Baohan, A., Schreiter, E., Kerr, R.A., Orger, M.B., Jayaraman, V.*, et al.* (2013). Ultrasensitive fluorescent proteins for imaging neuronal activity. Nature *499*, 295-300.

Chou, A.P., Maidment, N., Klintenberg, R., Casida, J.E., Li, S., Fitzmaurice, A.G., Fernagut, P.-O., Mortazavi, F., Chesselet, M.-F., and Bronstein, J.M. (2008). Ziram Causes Dopaminergic Cell Damage by Inhibiting E1 Ligase of the Proteasome. Journal of Biological Chemistry *283*, 34696-34703.

Cicchetti, F., Lapointe, N., Roberge-Tremblay, A., Saint-Pierre, M., Jimenez, L., Ficke, B.W., and Gross, R.E. (2005). Systemic exposure to paraquat and maneb models early Parkinson's disease in young adult rats. Neurobiol Dis *20*, 360-371.

Ciechanover, A. (1994). The ubiquitin-proteasome proteolytic pathway. Cell *79*, 13-21.

Cole, S.H., Carney, G.E., McClung, C.A., Willard, S.S., Taylor, B.J., and Hirsh, J. (2005). Two Functional but Noncomplementing Drosophila Tyrosine Decarboxylase Genes: Distinct role for neuronal tyramine and octopamine in female fertility. J Biol Chem *280*, 14948-14955.

Corti, O., Lesage, S., and Brice, A. (2011). What Genetics Tells us About the Causes and Mechanisms of Parkinson's Disease. Physiol Rev *91*, 1161-1218.

Daniels, R.W., Collins, C.A., Gelfand, M.V., Dant, J., Brooks, E.S., Krantz, D.E., and DiAntonio, A. (2004). Increased expression of the Drosophila vesicular glutamate transporter leads to excess glutamate release and a compensatory decrease in quantal content. J Neurosci *24*, 10466-10474.

DiAntonio, A., and Hicke, L. (2004). Ubiquitin-dependent regulation of the synapse Annual Review of Neuroscience *27*, 223-246.

Dragicevic, E., Schiemann, J., and Liss, B. (2015). Dopamine midbrain neurons in health and Parkinson's disease: Emerging roles of voltage-gated calcium channels and ATP-sensitive potassium channels. Neuroscience *284*, 798-814.

Dugravot, S., Grolleau, F., Macherel, D., Rochetaing, A., Hue, B., Stankiewicz, M., Huignard, J., and Lapied, B. (2003). Dimethyl disulfide exerts insecticidal neurotoxicity through mitochondrial dysfunction and activation of insect K_ATP channels Journal of Neurophysiology *90*, 259-270.

Feng, Y., Ueda, A., and Wu, C.-F. (2004). A MODIFIED MINIMAL HEMOLYMPH-LIKE SOLUTION, HL3.1, FOR PHYSIOLOGICAL RECORDINGS AT THE NEUROMUSCULAR JUNCTIONS OF NORMAL AND MUTANT DROSOPHILA LARVAE. Journal of Neurogenetics *18*, 377-402.

Fitzmaurice, A.G. (2012). The role of pesticide-induced aldehyde dehydrogenase inhibition in the pathogenesis of Parkinson's disease. Dissertation, In Engineering and Applied Aciences (California Institute of Technology).

Fitzmaurice, A.G., Rhodes, S.L., Cockburn, M., Ritz, B., and Bronstein, J.M. (2014). Aldehyde dehydrogenase variation enhances effect of pesticides associated with Parkinson disease. Neurology *82*, 419-426.

Gautier, H., Auger, J., Legros, C., and Lapied, B. (2008). Calcium-activated potassium channels in insect pacemaker neurons as unexpected target site for the novel fumigant dimethyl disulfide. J Pharmacol Exp Ther *324*, 149-159.

Gleichmann, M., and Mattson, M.P. (2011). Neuronal calcium homeostasis and dysregulation. Antioxid Redox Signal *14*, 1261-1273.

Gramates, L.S., and Budnik, V. (1999). Assembly and Maturation of the Drosophila Larval Neuromuscular Junction. In Int Rev Neurobiol, R.A.H. Ronald J. Bradley, and J. Peter, eds. (Academic Press), pp. 93-117.

Grolleau, F., and Lapied, B. (2000). Dorsal unpaired median neurones in the insect central nervous system: towards a better understanding of the ionic mechanisms underlying spontaneous electrical activity. The Journal of Experimental Biology.

Grygoruk, A., Chen, A., Martin, C.A., Lawal, H.O., Fei, H., Gutierrez, G., Biedermann, T., Najibi, R., Hadi, R., Chouhan, A.K.*, et al.* (2014). The redistribution of Drosophila vesicular monoamine transporter mutants from synaptic vesicles to large dense-core vesicles impairs amine-dependent behaviors. J Neurosci *34*, 6924-6937.

Guzman, J.N., Sanchez-Padilla, J., Wokosin, D., Kondapalli, J., Ilijic, E., Schumacker, P.T., and Surmeier, D.J. (2010). Oxidant stress evoked by pacemaking in dopaminergic neurons is attenuated by DJ-1. Nature *468*, 696-700.

Heidel, E., and Pflüger, H.J. (2006). Ion currents and spiking properties of identified subtypes of locust octopaminergic dorsal unpaired median neurons. Eur J Neurosci *23*, 1189-1206.

Henry, G.L., Davis, F.P., Picard, S., and Eddy, S.R. (2012). Cell type–specific genomics of Drosophila neurons. Nucleic Acids Res *40*, 9691-9704.

Jan, L.Y., and Jan, Y.N. (1976). L-glutamate as an excitatory transmitter at the Drosophila larval neuromuscular junction. The Journal of Physiology *262*, 215-236.

Jia, X.-X., Gorczyca, M., and Budnik, V. (1993). Ultrastructure of neuromuscular junctions in Drosophilal: Comparison of wild type and mutants with increased excitability. Journal of Neurobiology *24*, 1025-1044.

Jin, J., Lao, A.J., Katsura, M., Caputo, A., Schweizer, F.E., and Sokolow, S. (2014a). Involvement of the sodium-calcium exchanger 3 (NCX3) in ziram-induced calcium dysregulation and toxicity. Neurotoxicology.

Jin, J., Lao, A.J., Katsura, M., Caputo, A., Schweizer, F.E., and Sokolow, S. (2014b). Involvement of the sodium–calcium exchanger 3 (NCX3) in ziram-induced calcium dysregulation and toxicity. Neurotoxicology *45*, 56-66.

Kleiger, G., and Mayor, T. (2014). Perilous journey: a tour of the ubiquitin–proteasome system. Trends in Cell Biology.

Kuhn, D.M., Sykes, C.E., Geddes, T.J., Jaunarajs, K.L.E., and Bishop, C. (2011). Tryptophan hydroxylase 2 aggregates through disulfide cross-linking upon oxidation: possible link to serotonin deficits and non-motor symptoms in Parkinson's disease. J Neurochem *116*, 426-437.

Li, P., Zhu, J., Kong, Q., Jiang, B., Wan, X., Yue, J., Li, M., Jiang, H., Li, J., and Gao, Z. (2013). The ethylene bis-dithiocarbamate fungicide Mancozeb activates voltage-gated KCNQ2 potassium channel. Toxicol Lett *219*, 211-217.

Li, Q., Kobayashi, M., and Kawada, T. (2012). Mechanism of ziram-induced apoptosis in human T lymphocytes. Arch Toxicol *86*, 615-623.

Liss, B., Haeckel, O., Wildmann, J., Miki, T., Seino, S., and Roeper, J. (2005). K-ATP channels promote the differential degeneration of dopaminergic midbrain neurons. Nat Neurosci *8*, 1742-1751.

Macleod, G.T. (2012). Calcium Imaging at the Drosophila Larval Neuromuscular Junction. Cold Spring Harb Protoc *2012*, pdb.top070078.

Martin, C.A., Barajas, A., Lawless, G., Lawal, H.O., Assani, K., Lumintang, Y.P., Nunez, V., and Krantz, D.E. (2014). Synergistic effects on dopamine cell death in a Drosophila model of chronic toxin exposure. Neurotoxicology.

Matthews, E.A., and Dietrich, D. (2015). Buffer mobility and the regulation of neuronal calcium domains. Front Cell Neurosci *9*, 48.

McCormack, A.L., Thiruchelvam, M., Manning-Bog, A.B., Thiffault, C., Langston, J.W., Cory-Slechta, D.A., and Di Monte, D.A. (2002). Environmental Risk Factors and Parkinson's Disease: Selective Degeneration of Nigral Dopaminergic Neurons Caused by the Herbicide Paraquat. Neurobiol Dis *10*, 119-127.

Meco, G., Bonifati, V., Vanacore, N., Fabrizio, E. (1994). Parkinsonism after chronic exposure to the fungicide maneb (manganese ethylene-bis-dithiocarbamate). Scand J Work Environ Health *20*, 301-305.

Menon, K.P., Carrillo, R.A., and Zinn, K. (2013). Development and plasticity of the Drosophila larval neuromuscular junction. Wiley interdisciplinary reviews Developmental biology *2*, 647-670.

Monastirioti, M., Gorczyca, M., Rapus, J., Eckert, M., White, K., and Budnik, V. (1995). Octopamine immunoreactivity in the fruit fly Drosophila melanogaster. J Comp Neurol *356*, 275-287.

Olsen, D.P., and Keshishian, H. (2012). Experimental Methods for Examining Synaptic Plasticity in Drosophila. Cold Spring Harb Protoc *2012*, pdb.top067785.

Ooi, L., Gigout, S., Pettinger, L., and Gamper, N. (2013). Triple cysteine module within M-type K+ channels mediates reciprocal channel modulation by nitric oxide and reactive oxygen species. J Neurosci *33*, 6041-6046.

Pandey, U.B., Nie, Z., Batlevi, Y., McCray, B.A., Ritson, G.P., Nedelsky, N.B., Schwartz, S.L., DiProspero, N.A., Knight, M.A., Schuldiner, O.*, et al.* (2007). HDAC6 rescues neurodegeneration and provides an essential link between autophagy and the UPS. Nature *447*, 859-863.

Politis, M., and Loane, C. (2011). Serotonergic Dysfunction in Parkinson's Disease and Its Relevance to Disability. The Scientific World Journal *11*, 9.

Politis, M., Wu, K., Loane, C., Quinn, N.P., Brooks, D.J., Oertel, W.H., Björklund, A., Lindvall, O., and Piccini, P. (2012). Serotonin Neuron Loss and Nonmotor Symptoms Continue in Parkinson's Patients Treated with Dopamine Grafts. Sci Transl Med *4*, 128ra141.

Rhodes, S.L., Fitzmaurice, A.G., Cockburn, M., Bronstein, J.M., Sinsheimer, J.S., and Ritz, B. (2013). Pesticides that inhibit the ubiquitin-proteasome system: effect measure modification by genetic variation in SKP1 in Parkinsons disease. Environ Res *126*, 1-8.

Rinetti, G.V., and Schweizer, F.E. (2010). Ubiquitination Acutely Regulates Presynaptic Neurotransmitter Release in Mammalian Neurons. The Journal of Neuroscience *30*, 3157-3166.

Robinow, S., and White, K. (1991). Characterization and spatial distribution of the ELAV protein during Drosophila melanogaster development. Journal of Neurobiology *22*, 443-461.

Roeder, T. (2004). TYRAMINE AND OCTOPAMINE: Ruling Behavior and Metabolism. Annu Rev Entomol *50*, 447-477.

Schiemann, J., Schlaudraff, F., Klose, V., Bingmer, M., Seino, S., Magill, P.J., Zaghloul, K.A., Schneider, G., Liss, B., and Roeper, J. (2012). K-ATP channels in dopamine substantia nigra neurons control bursting and novelty-induced exploration. Nat Neurosci *15*, 1272-1280.

Shen, M., Benson, L., Johnson, K., Lipsky, J., Naylor, S. (2001). Effect of Enzyme Inhibitors on Protein Quaternary Structure Determined by On-line Size Exclusion Chromatography- Microelectrospray Ionization Mass Spectrometry. J Am Soc Mass Spectrom *12*, 97-104.

Shen, M., Lipsky, J., Naylor, S. (2000). Role of disulfiram in the in vitro inhibition of rat liver mitochondrial aldehyde dehydrogenase. Biochem Pharmacol *60*, 947-953.

Simms, Brett A., and Zamponi, Gerald W. (2014). Neuronal Voltage-Gated Calcium Channels: Structure, Function, and Dysfunction. Neuron *82*, 24-45.

Sook Han, M., Shin, K.-J., Kim, Y.-H., Kim, S.-H., Lee, T., Kim, E., Ho Ryu, S., and Suh, P.-G. (2003). Thiram and Ziram Stimulate Non-Selective Cation Channel and Induce Apoptosis in PC12 Cells. Neurotoxicology *24*, 425-434.

Speese, S.D., Trotta, N., Rodesch, C.K., Aravamudan, B., and Broadie, K. (2003). The Ubiquitin Proteasome System Acutely Regulates Presynaptic Protein Turnover and Synaptic Efficacy. Current biology *13*, 899-910.

Stoytcheva, M. (2011). Pesticides in the Modern World - Effects of Pesticides Exposure (Rijeka, Croatia: InTech).

Subramaniam, M., Althof, D., Gispert, S., Schwenk, J., Auburger, G., Kulik, A., Fakler, B., and Roeper, J. (2014). Mutant alpha-synuclein enhances firing frequencies in dopamine substantia nigra neurons by oxidative impairment of A-type potassium channels. J Neurosci *34*, 13586-13599.

Szot, P. (2012). Common factors among Alzheimer's disease, Parkinson's disease, and epilepsy: Possible role of the noradrenergic nervous system. Epilepsia *53*, 61-66.

Taylor, T.N., Caudle, W.M., Shepherd, K.R., Noorian, A., Jackson, C.R., Iuvone, P.M., Weinshenker, D., Greene, J.G., and Miller, G.W. (2009). Nonmotor symptoms of Parkinson's disease revealed in an animal model with reduced monoamine storage capacity. J Neurosci *29*, 8103-8113.

Wang, A., Costello, S., Cockburn, M., Zhang, X., Bronstein, J., and Ritz, B. (2011). Parkinson's disease risk from ambient exposure to pesticides. Eur J Epidemiol *26*, 547-555.

Yamano, T., and Morita, S. (1995). Effects of pesticides on isolated rat hepatocytes, mitochondria, and microsomes II. Arch Environ Contam Toxicol *28*, 1-7.

Yang, Y., Jin, X., and Jiang, C. (2013). S-Glutathionylation of Ion Channels: Insights into the Regulation of Channel Functions, Thiol Modification Crosstalk, and Mechanosensing. Antioxidants & Redox Signaling *20*, 937-951.

Zhang, G., and Horrigan, F.T. (2005). Cysteine Modification Alters Voltage- and Ca2+-dependent Gating of Large Conductance (BK) Potassium Channels. The Journal of General Physiology *125*, 213-236.

Chapter 5: Conclusions and Future Studies

In my doctoral dissertation I aimed to identify and characterize modifications of pre-synaptic release, including the role of synaptic protein ubiquitination (Chapter 2) and the effects of pesticides (Chapters 3 and 4). I found, using a combination of pharmacology, electrophysiology, and imaging, that disruption of ubiquitination alters both spontaneous synaptic release and evoked release. Inhibitors of the E1 ubiquitin activating enzyme, as well as inhibitors of deubiquitinase (DUBs) similarly enhanced spontaneous release and reduced evoked release. This may be due to the disruption of the ubiquitin pathway as 'cycle,' where negative or positive feedback loops are disrupted at any point in the pathway. Our lab previously found that blocking the proteasome leads to a similar outcome of increased spontaneous fusion. Thus, further experiments to test the prediction that ubiquitination acts as a biological oscillator may include altering the pool of free ubiquitin to determine if this leads to the same outcome; additionally blocking two steps of the pathway, E1 and DUBs, simultaneously to determine if this cancels the effect of 'disrupting the cycle.'

The results of experiments on evoked, synchronous release indicate a strong reduction in the amount of exocytosis in the presence of ubiquitin inhibitors; however, it remains unclear as to whether there was always an inability of synaptic vesicles to properly fuse upon stimulus, an inability to properly retrieve and recycle vesicles, or all of the above. E1 inhibitors clearly disrupted the ability to release, but this was not as obvious with DUB inhibition. Additionally, there was evidence that recycling was inadequate, but this may have been confounded by the enhancement of spontaneous fusion. One possible way to test this would be to do a dose-response curve for the effects of ubiquitin inhibitors. In Chapter 3, I found that ziram (which inhibits E1), enhanced spontaneous release in a dose-dependent manner. Using lower concentrations of each drug and monitoring evoked release by pHluorins may allow a more clear measurement and delineation of whether endocytosis and recycling are disrupted. With the concentration of NSC624206 used, for instance, endocytosis could not be measured because exocytosis

was immediately abolished. Further, it would be interesting to examine the properties of exo and endocytosis with vGlut1-pHluorin in the presence of more or less free ubiquitin. One caveat of pharmacology is the possibility of off-target effects. In my experiments, I attempted to control for this by the use of multiple chemically distinct inhibitors of the same pathway, however, addition or removal of free ubiquitin should in theory be far more specific to the pathway.

Perhaps the most obvious next step will be to identify the specific synaptic targets of ubiquitination, and what the outcome of the modification is for each at synapses. I began these studies by developing a mutant form of VAMP2 that can no longer be ubiquitinated. The mutant form of the protein has a differential distribution between the plasma membrane and the synaptic vesicle. In order to follow up with these findings, work is ongoing to develop a CRISPR-based knockout system in mammalian neurons to study the alteration of VAMP2 in isolation (e.g., no endogenous and thus ubiquitinated VAMP2 present). A number of other synaptic targets have been uncovered, however, and these may require a more high-throughput system for examining the effects of ubiquitination on synaptic release. The use of the model organism *Drosophila melanogaster* may provide just such a solution. *Drosophila* are genetically tractable, and express fewer isoforms of synaptic proteins that are homologous to their mammalian counterparts. Additionally, *Drosophila* add the advantage and convenience of an *in vivo* preparation to examine the effects of ubiquitination on neural circuitry. Importantly, our lab has recently discovered that inhibitors of ubiquitination lead to enhanced mini EJPs at the *Drosophila* NMJ (unpublished), making this an ideal assay to test the effects of mutations in ubiquitinated proteins.

While I was examining the effects of protein ubiquitination via pharmacology, I was also examining the effects of pharmacology on both a mammalian and invertebrate preparations. Ziram is a pesticide with widespread use, and those that handle the chemical have been found to be at increased risk of Parkinson's disease (PD) and particularly early onset PD. In addition to ziram, a number of other pesticides have been suggested to have a link to PD, and the challenges facing this field include not only

uncovering the targets of these drugs, but how to classify the different toxins and their effects. In Chapters 3 and 4 of this dissertation, I characterized the effects of ziram on the nervous system and determined whether these effects were be shared by similar toxins.

In both the mammalian and invertebrate preparations, ziram induced changes in the properties of neural excitability. In mammalian cortical neurons, the changes in spontaneous fusion were Ca^{2+} dependent, and measurements of excitability at the cell body indicated that ziram exposure generally led to membrane depolarization, a reduction in the time to peak and in the size of the afterhyperpolarization. At *Drosophila* NMJ, ziram lead to spontaneous activity at aminergic synapses, and this effect was abolished in the presence of TTX. These combined data indicate that ziram can have depolarizing effects on neurons, for instance at the cell body in cortical neurons and along the axon in aminergic neurons., The next step is to identify the ion channel or channels that are likely targets of ziram. The most obvious candidates are K^+ channels, which are crucial in setting the baseline membrane potential, repolarizing the membrane following activity, and modulating excitability to allow for burst firing or other specific patterns of activity. In order to identify the targets, *Drosophila* again offers genetic tractability as well as a simplified circuit for testing mutations and pharmacological inhibitors of ion channels. Additionally, uncovering unique ion channels at aminergic neurons may offer critical insight into the differential sensitivity of neurons in PD. Once a target or targets are identified, it will be important to determine whether they are common among aminergic (particularly dopaminergic) neurons in the mammalian system.

Finally, I found that of several pesticides which are linked to PD, chemicals of the dithiocarbamate family share synaptic phenotypes common to ziram including enhanced spontaneous release at mammalian neurons and spontaneous induction of activity at *Drosophila* aminergic neurons. Not only do maneb and disulfiram (both dithiocarbamates) lead to similar synaptic dysfunction, they likely share molecular targets. This was demonstrated with E1 enzyme, where the disulfide reactivity of these drugs apparently leads to variable modification. This appears to include stabilization versus reduction of the

thioester bond between E1 and ubiquitin. Once additional targets of ziram (e.g. ion channels) are uncovered, it will be important to identify the nature of modification and whether these modifications or similar cysteine-based modifications occur via other dithiocarbamates. In examining the other pesticides, benomyl and dieldrin, but not paraquat, led to a small and graded, but significant increase in mini EPSC frequency in cortical neurons. My hypothesis is that pesticides which are linked to PD risk alter the excitability of neurons. Further examination of the properties of these pesticides at aminergic neurons in *Drosophila*, and in cellular recordings from dopaminergic neurons in mammalian (or *Drosophila*) preparations would provide evidence to test this specific hypothesis. If common targets of excitability can be found, this would allow both an understanding of the early stages leading to PD and possible therapeutic interventions.

In conclusion, in this dissertation I have uncovered a number of changes in synaptic release properties via ubiquitination or pesticide application that have not been described before. While the specific targets and mechanisms for these synaptic phenotypes remain to be uncovered, the experimental techniques and data presented here highlight unique targets and methods for follow up. This work offers a crucial starting point to a more complete understanding of presynaptic modification in synaptic transmission and how disruption may lead to neurodegeneration in PD.